V.V. GOLOVENSKYY, T.F. SHMELEVA,
Y.M. SHMELEV, I.O. SINCHUK,
S.M. BOIKO, L.V. SMENOVA

ASPECTS OF TECHNICAL DIAGNOSTICS OF ELECTRICAL EQUIPMENT IN MODERN ELECTRIC POWER SYSTEMS

MULTI-AUTHORED MONOGRAPH
Science Editor DSc. (Engineering), Prof. T. F. Shmeleva

⚛ **iScience**
Warsaw-2018

V. V. GOLOVENSKYY, T. F. SHMELEVA,
Yu. M. SHMELEV, I. O. SINCHUK,
S. M. BOIKO, L. V. SMENOVA

ASPECTS OF TECHNICAL DIAGNOSTICS OF ELECTRICAL EQUIPMENT IN MODERN ELECTRIC POWER SYSTEMS

MULTI-AUTHORED MONOGRAPH

Science Editor DSc. (Engineering), Prof. T. F. Shmeleva

Warsaw-2018

Authors:
V. V. Golovenskyy, T. F. Shmeleva, Yu. M. Shmelev,
I. O. Sinchuk, S. M. Boiko, L. V. Smenova

Reviewers:
*V. M. Synyehlazov, DSc. (Engineering), Prof., (National Aviation
University, Kiev)*
*O. M.Sinchuk, DSc. (Engineering), Prof., (the SIHE "Kryvyi Rih National
University", Kryvyi Rih)*
*O. M. Yurchenko, DSc. (Engineering), Prof., (The Institute of
Electrodynamics of the National Academy of Sciences of Ukraine, Kiev)*

T 38 Aspects of technical diagnostics of electrical equipment in
modern electric power systems. Multi-Authored Monograph / Science
Editor DSc. (Engineering), Prof. T. F. Shmeleva −2018. – 133 pp.

The basic concepts of present-day aspects, prospects and techniques of
electric power systems diagnostics are reviewed in the monograph. The
paper explores general provisions on electric power equipment diagnostics
and tools, procedural and organisational issues of its realization.
Recommended for specialists, post-graduate students and students
specialising in 141 – «Power engineering, electrical engineering,
electromechanics» and in other related professions.

TABLE CONTENTS

Introduction

Operational reliability of power supply systems electrical equipment is one of the key factors having a significant impact on economic performances of Ukraine's power supply systems. From this perspective, enhancement of electrical equipment operating procedures in the electric power systems of various levels presents particular interest.

It should be noted that reliability indexes enable evaluating an average object state. This results in obtaining overestimated values in some cases and underestimated values in other cases. Technical diagnostics allows evaluating a state of a particular object.

Electric power units are considered as the diagnosis object; the electric power units refer to the totality of machines, devises, power transmission lines, designed for electric power generation, transformation, transmission, distribution and conversion into other kind of energy. The electric power units comprise: generators, power transformers, autotransformers, reactors, voltage and current transformers, power transmission lines, switchgear, package transformer substations, distribution networks, electric motors, capacitors, automatic control and protection devices, various electric users.

Squirrel-cage induction motors are widely used in electromechanical systems nowadays. They have a number of advantages, namely: high reliability of an induction motor due to the absence of a commutator-and-brush unit; high reliability due to the absence of energized operating contactor devices; minimized maintenance of a converter and a near absence of maintenance required for induction motors; a lean operation of an induction motor due to the absence of starting resistors and individual control; high anti stalling properties due to the rigid speed/torque ratio of an induction motor M=f(n). However, induction motor drives posses the following drawbacks: considerable size and high, as compared to DC systems, cost of electric equipment (generally converting and data equipment). Nevertheless, high initial capital expenditures are compensated in a short time by really low operation cost.

The existing maintenance and preventive control system for electric power units is generally based on periodic scheduled maintenance operations, in other words, it is based on the maintenance upon the completion of the specified operation period. Such a system is not optimal though for high voltage devices that results in unjustified scheduled outages of operable equipment.

It is desirable to know the actual condition of an object; it can be achieved by its control. Completing the tasks of technical diagnostics it is possible to sustain the electric power units' reliability while adopting the

maintenance system, where time and scope of works are defined by the equipment condition. It requires creation of an efficient technical diagnostic system. The implemented diagnostics system keeps electric power units condition within certain limits.

The development of diagnostic support system calls for a study of electric power units operating conditions, identification of their key influencing factors, evaluation of electrical equipment reliability indexes, compiling the mathematical description of the object and obtaining a diagnostic model on its basis, its analysis and selection of diagnostic features, assessment of the selected features probability, selection of diagnostic tools, control points, communication and processing means.

This multi-authored monograph successively examines the diagnosis methods used for electric power units components, the issues of designing diagnostic systems for electric power units; electrical engineers' familiarization with these subjects will facilitate the decision-making in design and operation of the power supply systems electrical equipment.

CHAPTER 1

GENERAL PROVISIONS ON TECHNICAL DIAGNOSTICS
(Boiko S. M., Golovenskiy V. V.)

1.1 Features and trends of modern power industry development

Specifying SmartGrid notion with regards to electric power systems of various technical level gave rise to the emergence of such terms as StrongSmartGrid (SSG) – electric grids with the voltage over 110 kV, RegionalSmartGrid (RSG) – the voltage from 3 to 110 kV, and MicroSmartGrid (MSG) – the voltage 0.4–3 kV, typical directly for the systems themselves and arising at their integration,which determines the features of equipment construction in their connection points and in the nodes of loads connecting. The practical solution of these tasks can be performed on the basis of power electronic means and, in particular, on the basis of the wide implementation of electrical energy parameters' converters. Power electronic means are natural elements of the systems under consideration, without them there is no question of the Smart Grid construction.

Selection of the type and structure of semiconductor converters, which are suggested for the connection of different systems, should be carried out with account for the nature of the variation of electrical energy parameters typical for one or another system. The major feature of SSG, RSG and MSG systems is an essential distinction in the their electrical energy parameters variation in time. SSG systems are characterized by a relatively high stability of energy parameters [1].

In RSG systems, as a rule, some variations of the electric energy parameters take place; these variations depend on the type of connected load and the capacity of transformer substations.

Basic issues of the Smart Grid concept development in Ukraine [2]**:**

1. Development of strategic vision of the future power industry in Ukraine based on the concept of Smart Grid.

2. Redistribution of the basic requirements and operational properties of the domestic power engineering on the basis of the Smart Grid concept and their implementation principles.

3. Defining the major development trends for all parts of power system: generation, transmission and distribution, sales, consumption and dispatching.

4. Redistribution of the basic components, technologies, information and management solutions in all the above-mentioned spheres.

5. Ensuring coordination of modernization (aimed at overcoming the technological gap) and innovation development in the Ukrainian power industry.

Trends of electric power industry development that enjoy the priority progress [3]:

− Optimal integration of generating and storage capacities of diverse physical nature in an electric power system.

− Countering of negative impacts.

− Motivating active behaviour of the end-user. Providing access for an 'active consumer' and the distributed generation on the electric power markets.

− Ensuring the energy supply reliability and electric power quality in various price ranges.

− Transformation of the system-centric approach into customer-centric one.

− Self-healing in case of disturbances, including emergency ones.

− Asset management optimization.

Development trends for smart electric grids of the Ukraine's Unified Power System:

− Transition to the distributed generation.

− The transition from rigid dispatch scheduling and regulation to arranging coordinated operation of all network objects.

− Implementation of new technologies and power facilities that ensure manoeuvrability and controllability of an electric power system and its objects.

− Constructing of smart metering, monitoring, diagnosis and control systems covering the distributed generation as well as the electricity transmission, distribution and consumption.

− Development of a new generation of operational applications (SCADA\EMS\NMS) targeted at new power devices.

− Formation of a highly efficient integrated information and computing structure being a core of the electric power system.

Prospects for Smart Grid implementation in the Unified Power System of Ukraine

Major benefits of renewable energy sources [4]:

− cost reduction of traditional fossil fuel resources;

− reduction of Ukraine's dependence on fossil fuels importation;

− environmental compliance due to reduction of the negative impact on the environment.

Problematic aspects of the renewable energy implementation in the Unified Power System of Ukraine:

‒ inadequacy of Ukraine's legal framework;

‒ insufficient technical standards base and state standards for renewable energy power plants' design and connection to electric grids of the Ukrainian Unified Power System;

‒ extremely high tariffs for the electricity generated by renewable energy power plants (for solar power farms ‒ over 7 UAH/kWh);

‒ the need to include capacities of renewable energy power plants in the daily dispatch load schedule of load on mandatory basis.

Problematic aspects of the renewable energy implementation in the Unified Power System of Ukraine:

‒ rapid and uncontrolled capacities increase of renewable energy power plants;

‒ the state-owned enterprise national electric company "UKRENERGO" does not posses a tool to restrict technical specifications issue and construction ofrenewable energy power plants; consequently, technical specifications for the connection of wind power farms accounting for 2062 MWe have already been issued and approved; solar power farms - 570 MWe; applications to obtain technical specifications account for about 14000 MWe, that comprises 40% of the Ukrainian Unified Power System consumption;

‒ reduction of cycling capacities alongside with the increase of basic capacities in the general balance of the Unified Power System of Ukraine:. The need for extra spare capacity in the event of power fluctuations on solar power farms and wind power plants;

‒ deterioration of the quality of electricity in the power supply regions with functioning solar power plants;

‒ the need for extra measures aimed at reactive power neutralization and voltage regulation.

European countries experience:

1) implementation of significant capacities at renewable energy power plants (Denmark, Germany, Spain, etc.);

2) the UCTE system accident in 2006 was partially caused by significant power flows from regions with renewable energy power plants functioning;

3) the need to maintain appropriate spare capacity in the event of the power variation occurring on renewable energy power plants;

4) implementation of modern complexes to forecast the operation of renewable energy power plants, SMART GRID implementation.

1.2 Diagnostics in the life cycle of electrical equipment components

Any technical object have the following typical stages of its life cycle: design, manufacturing, operation [5].

Design – it's the process of analysis and planning of costs, lead-time, setting the requirements for electric power supply systems, product development, on the basis of which systems are created, and the operation and maintenance documentation to assure proper running of these systems.

Manufacturing – is the process of technical requirements' realization "in steel", including testing as a stage of the integrated verification of the equipment performance; the equipment being assembled from components.

Operation – is the set of technical and organizational measures that ensure technically correct application of electrical supply systems, constant availability, assuring equipment performance and their service life extension. Operation includes transportation, storage, maintenance, repair, and intended application.

Diagnostics is possible at all stages of the electric power units' life cycle (Fig. 1.1).
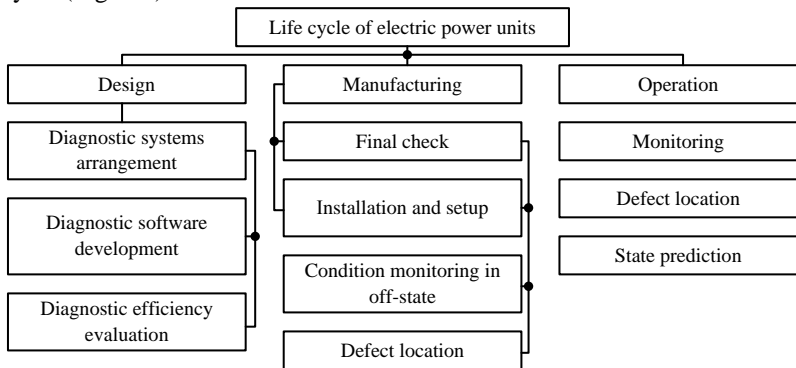
Figure 1.1 – Diagnosis in the life cycle of electric power units

At the initial stage of an electric power unit' design you need to figure out the parameters of the diagnostic system to be applied (to determine the frequency and duration of operation and diagnostics, reliability criteria, monitoring factors and components' maintainability factors). To evaluate the condition of components of the power supply units you need: firstly, to design an object adjusted for evaluation of its condition with required precision and reliability; secondly, to create technical diagnostic tools that would allow you to evaluate the object's state in the required conditions; thirdly, to determine the role and functions of the

human operator involved in the diagnosis process. To make the electric power supply unit adjusted for diagnostics, while designing it you need to compile a list of evaluated diagnostic features, methods of their evaluation, conditions of performance ability and defects signs, diagnostic algorithms. In the course of designing, you determine the achievable efficiency of the diagnostic system.

While manufacturing of the electric power unit components we need to evaluate their condition. Thus, in the course of the final check the accuracy of assembly and installation are tested. In case the power supply unit' component does not comply with the given requirements, fault location is carried out.

In the course of equipment operation continuous or periodic diagnostics is performed. If necessary, fault forecasting or fault location is carried out to apply preventive maintenance or recovery work. The diagnostics at this stage can justify the further use of power supply unit components. The diagnostics is carried out on the power supply unit in storage or the one put in diagnostic mode for this purpose.

Tasks arising from the need to perform diagnostics of power supply units on different stages can vary, which should be taken into account while developing a diagnostic system. The diversity of tasks being solved when diagnosing an object on different stages requires the development of diagnostic tools designed for use at specific stages, for example, technical means, designed for diagnosis during manufacturing or operation. The diagnostic system is efficient only in those cases when the power supply unit components condition is evaluated at all stages of its life cycle. This will increase the efficiency of the power supply unit use, while its reliability can be maintained at level provided by design.

1.3 Features of electrical equipment components' diagnostics

When developing the diagnostic systems for the electrical equipment for substations and power lines of 10-220 kV and above, you need to consider the following [6]:

1. The available power transformers are characterized by a wide variety (different cooling systems, switching devices and means of lightning overvoltage protection as well as different manufacturing technologies).

2. Different level of power transformers' reliability, the complicated collection of statistical data on the reliability of large power transformers.

3. Difference in load conditions during operation.

4. Limited self-healing properties of power transformers out of factory environment.

5. Available oil circuit-breakers are not suitable for diagnostics (absence of operation counters, sensors to estimate the value of the short-circuit current the state of insulation etc.).

6. Configuration of certain instrument transformers being produced currently does not provide for their diagnosing on operating voltage.

7. The electrical switchgear equipment of substations 35-220 kV vary considerably package enclosed-type distribution substation KRPZ-10 (outdoor switchgear KRUN series KRN-3, K-6, KRN-10, switchgears series K-6, K-12, K-13, K-37, K-47, K-57), various operational lifetime and are equipped with diverse types of circuit-breakers (VMG-133, VMG-10, VK-10, VMPP-10, VMM-10), which makes difficult to carry out their diagnostics.

8. A substation use may be various: unmanned operation, house duty, duty in special room, duty cycle manning in the control room. Thus, the "human operator" link is not included in the structural scheme in the first three types of a substation use.

9. Severe difficulties occur while diagnosing the insulation of a live power line 10-220 kV on operating voltage with the help of a measuring rods or an electro optical defect detector, since the first method is laborious, and as the second one, it is difficult to carry out measurements in clear sunny weather. According to the service conditions of an overhead power line, the breakdown of insulator string leads to the line cut-off. Thus, the task of diagnostics is to determine the initial stage of the fault and to predict the occurrence of 'zero' insulators in strings.

10. Intense environmental impact on the state of insulation.

1.4 Characteristic of the electrical equipment components' diagnostic methods

The serviceable condition of electrical equipment can be evaluated while it is functioning, observing its state (an operational diagnostics), or when it is subject to an external action, so we can observe its response (a test diagnostics) [7].

The benefit of operational diagnostics lies in the fact that its realization does not require special external sources of energy, while data is recorded and processed during its operation. Figure 1.2 shows the description of operational diagnostic methods.
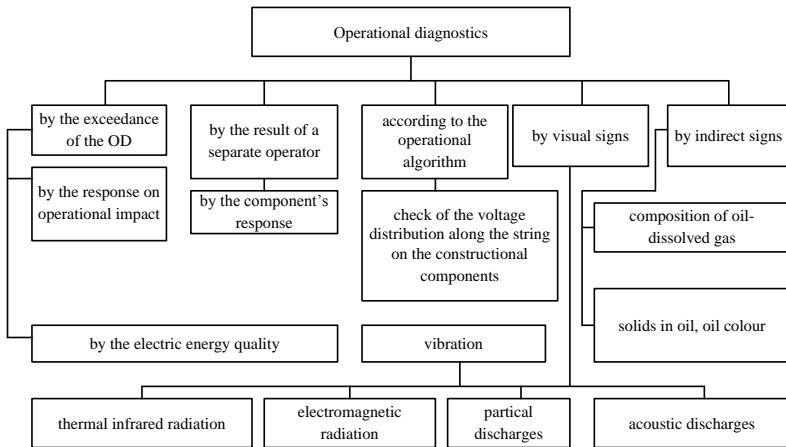
Figure 1.2 – Description of operational diagnostic methods

The state of objects in the process of their operation is evaluated by various external signs: heating of particular parts or the common thermal field, the electromagnetic field, partial and acoustic discharges, high-frequency radiation, vibrations, and so forth, produced by the functioning object. Variation of the above mentioned parameters may indicate a variation of the condition of power supply unit components. To evaluate the condition of oil-filled equipment (transformers, reactors) during their operation, the results of oil-dissolved gas analysis are applied.

Performing a test diagnostics requires special generators that produce test actions that are applied to the electric power supply unit and stimulate its response. Figure 1.3 shows the description of test diagnostic methods [8].

Test diagnostics is performed both in active and standby state. For the test diagnostics, both working inputs (i.e. inputs for operational actions) as well as the purpose-designed inputs for diagnostics (for example, measuring leads of bushing insulators) are used.

13

Figure 1.3 – Test diagnostic methods

This postulate also holds for recording the formation of the object response to the test action when it is diagnosed.
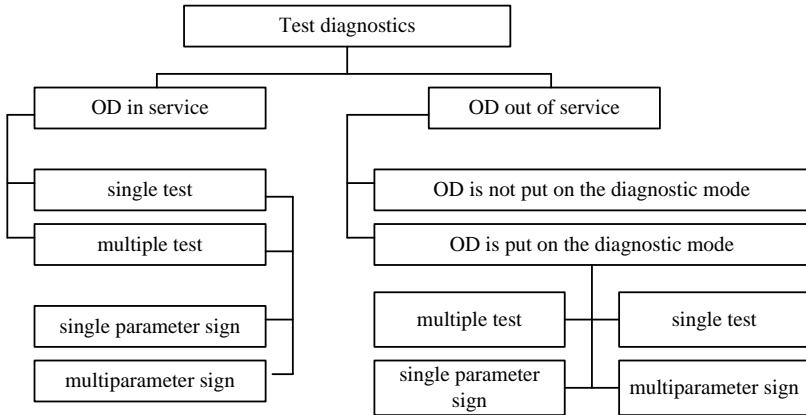
The test diagnostics is carried out by a single action, for example, a single pulse or a multiple action (a series of pulses), in other words, the test diagnostics is based on the results of the sum of elementary checks. In the test diagnosis, a single parameter case is possible when one index is evaluated or multiparameter one when more than one index is evaluated. The event, when one signal of an object output is evaluated by several parameters (for example, by amplitude and frequency), belongs to multiparameter cases.

For complex electric power supply units consisting of several interconnected components, a combination of various methods is applied when diagnosing various components. In this respect, operational as well as test diagnostics is allowed to be performed on the same electric power supply unit [9].

1.5 Defect symptoms and their detection methods

A defect presence indicates that undesirable changes occurred in the functioning of the object of diagnostics; these changes led to its performance impairment or a reduction of the degree of its performance ability. The object's failure is the simplest type of defect symptom. Failure of the object of diagnostics means that either the entire object or its part does not function and, consequently, does not show 'vital signs'. Thus, the absence of voltage on a switchboard of an electric power plant signifies its complete failure.

Mathematically, the sign of a defect occurrence can be represented as follows [10]:

− performance impairment according to parameters $\left|\xi_{i\,rt} - \xi_i\right| \geq \Delta_i$; according to characteristics $\left|f(x) - \varphi(x)\right| \geq \Delta$;

− drop of the degree of its performance ability, that is transition from the state s_i in the state s_j in the field of performance S_p: $s_i \rightarrow s_j \in S_p$;

− failure of one of the structural units of the complex object that involves transition of the object under diagnostics from serviceable conditions $S_p = (1,1,..., 1)$ to nonserviceable ones $S_n = (0,1,1,... 1)$;

All methods of defects detection can be divided into three groups: inspection, detection and location. If it is known that the object of diagnostics failed, you first need to carry out a visual inspection of the power supply unit' electrical elements. Thus, you can detect contact couplings fault, wire breakages, insulators destruction, etc.

Automated detection is now being used for various objects of diagnostics. In this case, a number of sensors are placed in the object depending on the required precision of fault location, which alarm the fault occurrence. Such sensors may include thermocouples, temperature responsive switches, short circuit currents recorders and other elements responsive to overvoltage and overcurrents.

In objects that may be represented as systems with sequential data processing (Fig. 1.1), an occurred defect can be found by detection of the signal transmission.

The fault location is carried out by developing the conclusions, which lay in the continuous narrowing of the search area of a defect location, making logical decisions and performing rational verifications. Such an approach reduces the number of verifications, which not only saves time, but also minimizes the probability of errors. To select the sequence of inspections, you need to know how certain defects affect the state of the object under diagnostics. There are two ways to achieve this goal:

1) simulation of faults;
2) analysis of the diagnostic model of the object under diagnostics.

The fault simulation is widely used for various diagnostic objects. The outcome of the experiment are summarized in the table (Table 1.1):

Table 1.1 – Table of faults

Fault	Transient characteristic type $h(t)$
Short circuit R_i	
Discontinuity C_i	
Reduction of the amplification factor	

As a result of the diagnostic model analysis, one can develop recommendations concerning fault location by ranging the diagnostic features in accordance with their effect on the condition of the object under diagnostics; for example, by calculating the sensitivity of the transmission function T_{ijk} to the variation of the analysed diagnostic parameters r_k, provided the object assumed by the model in the form of a graph or a diagram of the type (Fig. 1.4) signals transmission [11].
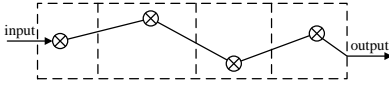
Figure 1.4 – Indicating circuit of signal
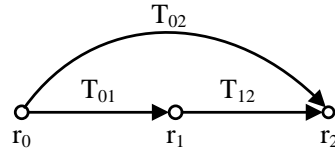transmission in the object

Figure 1.5 – Signal transmission
diagram

The transmission function sensitivity can be determined with the help of the expression:

$$S_{r_\alpha}^{T_{ij}} = \frac{\partial T_{ij}}{\partial r_\alpha},\qquad(1.1)$$

where T_{ij} – transmission functions from i-th input to j-th output; r_a – variable parameter, $\alpha = \overline{1,l}$ ($a = 0$ – input parameter, it should be constant).

1.6 Defect location algorithm

The task of the occurred fault location in contrast to the task of performance monitoring typically requires a longer analysis of the object under diagnostics or its model. In this respect, the level of detail is determined by the specified precision of fault location, that is, indicating the part of the object (structural unit) that defines the precision of the search of the fault area. Thus, if the precision of fault location is specified, the object of diagnostics can be represented by the multitude having N interrelated parts – structural units (SU) [11].

The location of a fault or a condition of the object is performed by an algorithm that includes a certain set of verifications. *A verification* is called an evaluation of the structural unit condition according to its or the entire object's output parameters. Thereby, the multitude of conditions in general case is bigger than the number of verifications, since during a single verification more that one fault can be located. Each verification requires some expenses. While developing the fault location algorithm, we try to select such a sequence of verifications that allows us to locate a fault at the lowest cost.

Function (structure) charts can be used to develop fault location algorithms. The term "function" here means that the block performs a certain function. Blocks are interconnected in the way that particular

functions are performed in a certain sequence, realizing the task designated to this particular equipment unit or the system according to its destination.

A function chart is a graphical representation of blocks it comprises and corresponding signal paths. We should bear in mind that the arrangement of function blocks on the chart doesn't correspond to their actual physical location in the equipment configuration.

In the electric circuit diagrams signals pass through signal circuits of two types: series and branched ones. A series circuit scheme (fig. 1.6) includes the group of circuits (cascades) connected in such a manner that the output of one circuit is connected to the input of another one.

As a result, the signal passes directly through the group of circuits without being transmitted in the reverse direction and without branching.

A branched circuit scheme can be of two types: divergent and convergent. In the divergent circuit scheme (Fig. 1.7, a) two or more signal circuits are connected to the output end of an element. If two or more signal circuits are connected to the input end of the element, it is called a convergent circuit scheme (Fig. 1.7, b). In this case, during the first verification you should try to determine the circuit where the fault has occurred. It allows you to exclude one of the signal circuits that is in good operating condition [12].
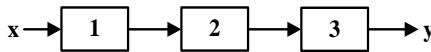
Figure 1.6 – Series signal circuit
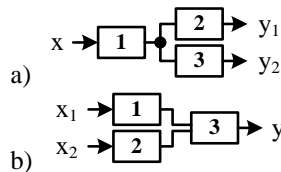
Figure 1.7 – Branched signal circuit
a) divergent; b) convergent

In view of the fact that present-day electrical automation systems comprise hundreds of components, testing each component in order to locate a defect is significantly time-consuming. The scope of search can be reduced several times, provided that not every component is tested, only the output signal of each circuit (cascade). However, to carry out this number of checks is also quite laborious. Having split the analyzed schemes into structural units (they can amount to several dozens), we can reduce the number of verifications, bringing them to the acceptable level.

Since each verification divide the space of states in two parts (that includes and does not include the target state), the performance of a verifications sequence results in the location of a certain state that

corresponds to the detection of a failed SU. A sequence of checks performed to locate a fault can be represented as a graph (a tree), where the treetops signify checks, the branches indicate the direction of transition based on the test result, and the end tops are detected faults.

The first check being completed, the question arises: 'What to do next?'. The answer depends on the results of the first check. The only two outcomes are possible: adequate (+) and inadequate (–) performance of the structural unit under test. In the latter case the SU is either completely out of order or operates with degraded performance. In any case, the result will show what kind of the following verification is required.

Fault search algorithms can be of three types: sequential, parallel and combined.

In *the sequential search* each verification points out one defect in the search space. This condition can be met for an object of diagnostics represented in the form of a series circuit of structural units, when it is known that the signal is applied to the input, and we can determine the fault presence in the object of diagnostics by the output signal in two ways: from the beginning to the end and from the end to the beginning. Let's exemplify the fault location algorithm with the help of the object of diagnostics (Fig.1.8, a).

In the first case, we need to perform a check at A point, since it will allow us to immediately exclude from consideration one element SU – 1. If the signal is within the allowable limits, the verification should be performed at B point, which will enable us to determine the state of SU – 2. If the result of the check is negative, it means that the defect is in this element. If it is positive, we need to carry out the check at C point [13].
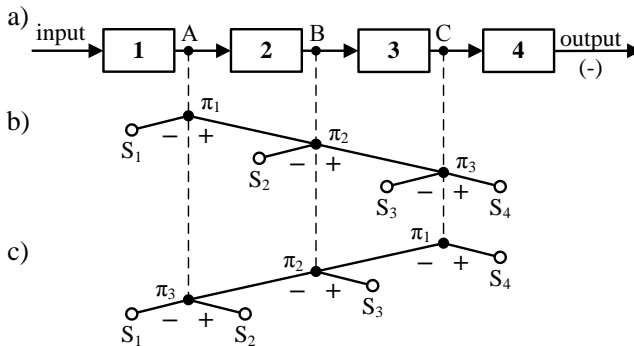

Figure 1.8 – Fault location algorithm

If the result of the check is positive, the defect is in SU 4, otherwise – he defect is in SU 3. The location (search) algorithm is shown on the Fig. 1.8, b.

In other case (from the end to the beginning), if the result of the check in C point is negative, this check is to be performed in B point. If the check result is positive – in SU 3; if the result is negative, the check is performed. According to this check' results we located the defect either in SU1 or SU 2 (Fig.1.8, c) [14].

The number of checks N to detect all defects in the object of diagnostics (OD) is determined by the relation $N = n - 1$; n – the number of the object SU.

In *parallel search* each check splits the OD in two equal or nearly equal parts, if the OD consists of even or odd number of SUs respectively.

Thus, in case of the parallel search performed for the OD comprising four SUs (Fig.1.9, a), the first check is carried out in B point. If the result is negative, the following check is carried out in A point, thus determining the location of the defect (SU 1 or SU 2). Otherwise, the check is performed in C point, that allows us to determine the defect in SU 3 or SU 4. The search algorithm is shown on the Fig. 1.9, b.
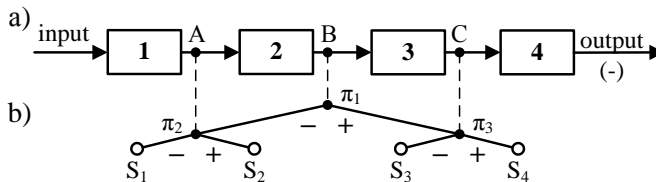
Figure 1.9 – Defect location algorithm

The number of checks N, required to locate all defects by the number of SU can be calculated using the formula:

$N = [\log_2 n]$ – integral part.

For $n = 4$ two checks are required, for $n = 8$ – three checks.

In *combined search* involves a combination of sequential and parallel algorithms.

Applying the tree-type fault location algorithm, we can determine the total length of the branches to reach the sought defect [15].

$$L_i = \sum_{j=1}^{p} l_{ij} , \tag{1.2}$$

where l_{ij} – the length of i-th branch, p – the number of branches from the beginning of search till the sought defect is reached. For example, for the graph presented in Fig. 1, 9, b:

$$L_1 = \sum_{j=1}^{2} l_{ij} \; .$$

If l_{ij} is considered as time, than, using the formula for L_i, we can define the time being spent for location of i-th defect.

$$\tau_{ni} = \sum_{j=1}^{p} \tau_{ij} \; . \tag{1.3}$$

Defect/fault location algorithms can be developed on the basis of the analysis of the object structure or use of indexes that characterise the reliability of SU.

1.7 Diagnostic parameters forecasting
Analytical prediction

Extrapolation methods applied to determine the value of a predicted variable are called *analytical* or *analytical prediction methods*.

When choosing a mathematical apparatus to solve the problem of analytical prediction, we need to pre-determine the diagnostic parameters. From the technical point of view it is complicated to estimate the parameters of each component constituting the object due to their large number, therefore, we try to select a minimum number (one to two) of the diagnostic parameters that ensure the required predictability of the object state variation [16].

The chosen parameters should be sensitive to variations occurring in the components composing the object of diagnostics, that is, any trend of condition of the constituent elements should be reflected in the behaviour of the selected diagnostic parameter. Particularly, such parameters can be transmission factor, amplification factor (gain), feedback parameters, etc.

Let's consider setting up a prediction problem. For the sake of simplicity we will assume, that the performance ability of the object is determined by one parameter ξ. In this case the forecasting of the object performance is considered as a prediction of a variation of the function $\xi(t)$, the value of which varies discretely or continuously in the time interval $T_1 = [t_o, t_n]$. This results in this function values $\xi_0, \xi_1, ..., \xi_i, ... \xi_n$ on the interval T_1 (Fig.1.10) [17].
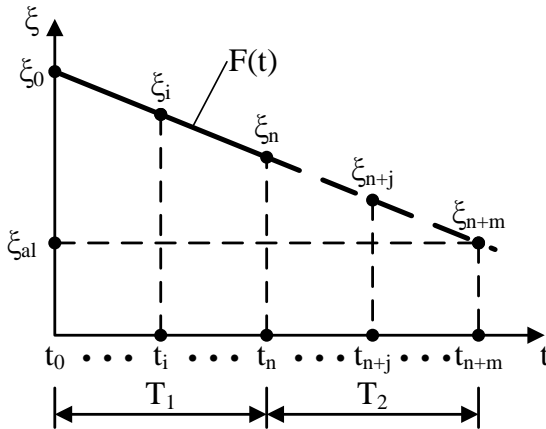
Figure 1.10 – Diagnostic parameter variation

We need to use the known values ξ_i to determine the value of the function $\xi(t)$: $\xi_{n+1}, \xi_{n+i}, \dots, \xi_i, \dots, \xi_{n+m}$ in the future points of time $t_{n+1}, \dots, t_{n+i}, \dots, t_{n+m} \in T_2$ or to find out in how much time the values ξ_{n+i}, $t_{n+i} \in T_2$ attain the acceptable level $\xi_{\partial on}$. The problem can be solved by the polynomial extrapolation method and the regression analysis.

Polynomial extrapolation method. The ideal case of the solution to this problem is an adequate description of a variation of the function $\xi(t)$ with a certain analytic expression. Since it's quite complicated to find such expressions by discrete points ξ_i it is worthwhile to determine the best structure of the analytic expression, and when predicting a specific function $\xi(t)$ – to change basic elements constituting this expression [18].

In the interval T_1 by known values ξ_i we need to find such a function $F(t)$, which would describe the variation of the state of the object of diagnostics with the given accuracy, that is to perform interpolation. In general case, we can use the polynomial of the form:

$$F(t) = \sum_{l=0}^{r} a_l \varphi_l(t), \qquad (1.4)$$

where a_l – unknown coefficients; $\varphi_l(t)$ – known simplest functions.

Obtaining polynomial $F(t)$ is to determine the coefficients a_l. It is worthwhile to use as functions $\varphi_l(t)$ the functions with the simplest structure, for example:

$$\varphi_0(t) = 1; \ \varphi_1(t) = t; \ \varphi_2(t) = t^2; \dots; \ \varphi_r(t) = t_r.$$

22

Therefore, we have a basic polynomial in the form:

$$F(t)=a_o+a_1t+a_2t^2+...+a_rt_r, \qquad (1.5)$$

A graphic illustration of its certain parts is shown in Fig. 1.12.

Many power expressions may that vary in the way of calculating a_l can be converted in this form.

For example, as a result of measuring the parameter ξ in the points of time t_o and t_1 its values obtained are ξ_0 and ξ_1 (fig.1.12).
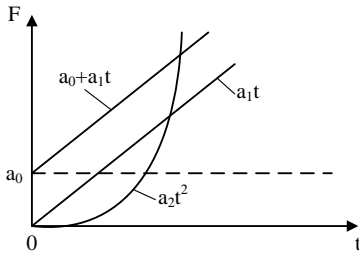
Figure 1.11 – Simple polynomials
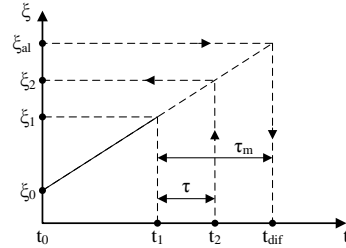
Figure 1.12 – Diagnostic parameter variation

Interrelation $(\xi_1 - \xi_0)/(t_1 - t_0) = \dot{\xi}$ will be referred to as a mean rate of the parameter variation in the interval $[t_o,t_1]$. We can describe the character of the parameter variation in this time interval using the expression:

$$F(t)=a_o+a_1t, \text{ where } a_o = \xi_0; a_1 = \dot{\xi}.$$

Assuming that the parameter variation rate is kept, you can predict the value of the parameter in time τ.

In practice, for small intervals τ such a forecast is quite acceptable. If the acceptable value of the diagnostic parameter is known $\xi_{\partial on}$, then using this formula we can define *the residual operation time*, that is the time of possible equipment operation till failure:

$$\tau_{r.o.} = (\xi_{al} - \xi_1)/\dot{\xi}. \qquad (1.6)$$

Knowing the residual operation time of equipment for each parameter, we can determine the overall time of its good performance that equals to the smallest residual operation time for all diagnostic parameters.

To make the precise prediction we should apply more complex extrapolation formula and use the results of more that two measurements.

While forecasting the state variation by one generalized parameter, Lagrange and Newton polynomials can be used for extrapolation [18].

The general form of the Lagrange polynomial can be represented in the following way:

$$F_L(t) = \sum_{l=0}^{r} L_l \xi_i \,, \tag{1.7}$$

where ξ_i – the value of the diagnostic parameter in the points of time t_i; L_l – Lagrange coefficients.

In the simplest cases:

$$l{=}1{:}\ \ F_L(t) = \frac{(t - t_1)}{(t_0 - t_1)} \xi_0 + \frac{(t - t_0)}{(t_1 - t_0)} \xi_1;$$

$$l{=}2{:}\ \ F_L(t) = \frac{(t - t_1)(t - t_2)}{(t_0 - t_1)(t_0 - t_2)} \xi_0 + \frac{(t - t_0)(t - t_1)}{(t_1 - t_0)(t_1 - t_2)} \xi_1 + \frac{(t - t_0)(t - t_1)}{(t_2 - t_0)(t_2 - t_1)} \xi_2.$$

Taking into consideration, that the coefficients of polynomials applied for extrapolation are independent of the value of the predicted parameter, that can be calculated in advance and summarized in the special tables that simplifies the process of forecasting.

The Newton polynomial is widely applied in forecasting.

$$F_N(t) = \xi_n + \Delta\xi_{n-1}(t - t_n) + \frac{\Delta^2\xi_{n-2}}{2!}(t - t_n)(t - t_{n-1}) + ... + \frac{\Delta^r\xi_0}{n!}(t - t_n)(t - t_1), \tag{1.8}$$

where $\Delta\xi$ – is the first difference between the measured values; $\Delta^2\xi$ – the second difference (difference of the differences) etc.

The polynomial of the first order $r = 1$, applied for extrapolation, is as follows:

$$F_N(t) = \xi_n + \Delta\xi_{n-1}(t - t_n), \tag{1.9}$$

and the polynomial of the second degree $r = 2$, respectively:

$$F_N(t) = \xi_n + \Delta\xi_{n-1}(t - t_n) + \frac{\Delta^2\xi_{n-2}}{2!}(t - t_n)(t - t_{n-1}), \tag{1.10}$$

where t is obtained form the area T_2 (the differences $t\text{-}t_n$ and $t\text{-}t_{n-1}$ can be expressed by the number of prediction steps $m = \Delta t$ respectively *m+1 and m*).

Since, in this case, the coefficients at the finite differences do not depend on the predicted function, they can be calculated in advance and summarized in the table. The tables of coefficients of polynomials applied for extrapolation considerably simplifies the process of forecasting, since they reduce the amount of computation required and facilitate forecasting automation.

In actual practice we confine ourselves to first and second order polynomials, since the rate of state variation does not exceed the rate of response of polynomials. The actual processes progress quite slowly. In this case the parameters variation curves, which characterize the state of the object under diagnostics, are fit between the lines that represent the polynomials of the first (AB) and the second (AC) degree (Fig.1.13).
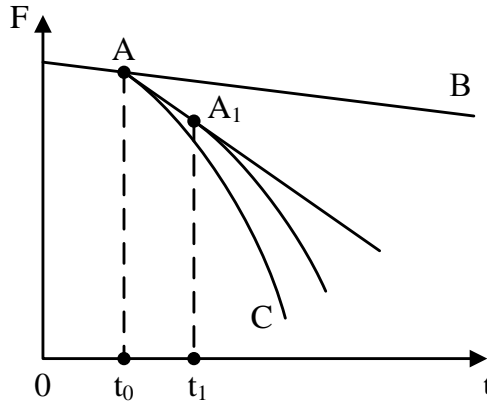
Figure 1.13 – Forecast accuracy improvement

The forecasting accuracy can be improved, if the prediction is carried out at one step only with subsequent inclusion of the obtained value (point A_1) in the area of the known values T_1. By doing so each prediction (at one step) starts with a new point A_1, obtained by the process shift at one step (t_o, t_1).

The number of measurements and forecasting time have an impact on the forecast accuracy: the more n is, the more accurate will be the forecast, since we manage to describe with greater precision (to interpolate) the process of a parameter variation in the area T_1. The longer the time period of forecast T_{mean} is, the less will be its accuracy, since not all the factors can be taken into consideration in the area T_2. The minimum number of required measurements is related to the degree r of polynomial in the following way:

$$n = r+1.$$

In real case scenario, in order to obtain an acceptable forecasting accuracy n is 3–5 times multiplied [18].

Thus, the use polynomials for extrapolation while performing analytical (deterministic) prediction involves:

1) selection of the optimal expression $F(t)$ taking into consideration the trend of parameter variation in the area T_1;

2) defining coefficients α_l to obtain the accurate forecast;

3) extrapolation of $F(t)$ on the area T_2 and determining the parameter value in the required (prognosticated) point of time;

4) evaluation of the forecast accuracy.

Regression analysis method. It is based on the application of the regression equation (Lat. regressio – backward motion) that has the form:

$$y = \beta_0 + \sum_{i=1}^{k} \beta_i x_i + \varepsilon , \qquad (1.11)$$

where y – the value, whose nature of variation is to be determined; β_0 – constant value; β_i – coefficients; x_i – parameters, influencing the predicted value; Σ – weighted sum; ε – random error.

It is a linear dependence of y on x.

The model of the diagnostic parameter variation ξ in time based on the regression equation takes the following form:

$$\xi = \xi_0 + t/a , \qquad (1.12)$$

where ξ_0 – initial value of the parameter; a – regression coefficient, which determines the slope of a line.

Obviously, the OD performance time to failure t_{dif} will be defined by the acceptable value of the diagnostic parameter:

$$t_{dif} = (\xi_{al} - \xi_0)a . \qquad (1.13)$$

The electrical equipment, however, comprise objects (electric machines windings) for which this value is impossible to be set. What can be done in this case?

Let's consider the equivalent circuit of an electric machine winding (Fig.1.14). Here Rg – resistance of the known value. For the case under consideration the forecast is primarily aimed at determining the residual operation time. The diagnostic parameters are $\Xi = (L, R_1, C_1)$, where L – equivalent inductance of winding; R_1 – equivalent resistance of winding; C_1 – equivalent capacitance of winding.
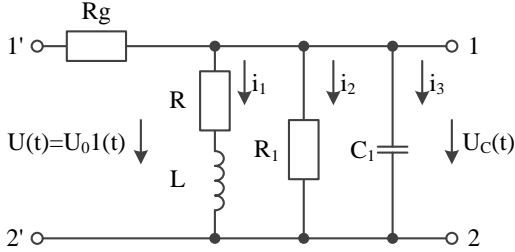
Figure 1.14 – Equivalent circuit of an electric machine winding

Due to the fact that the inductance changes in a step-like manner with the occurrence of shorted turns, this parameter is not suitable for the forecasting problem. The diagnostic parameters R_1 and C_1 characterize the state of insulation, which is subject to ageing and changes monotonically. This problem is quite difficult to solve, since acceptable values of parameters R_1 and C_1 of the electric machine winding are unknown.

The source data for forecasting will be values of diagnostic parameters R_1 and C_1, in general case ξ_{ij} for N machines in the points of time t_j, where $i = \overline{1, N}$; $j = \overline{1, n_i}$. The value for each object is computed using the method of regression analysis according to the measured parameters [11]:

$$a_i = \frac{n_i \sum_{j=1}^{n_i} t_j^2 - \left(\sum_{j=1}^{n_i} t_j \right)^2}{n_i \sum_{j=1}^{n_i} \xi_{ij} t_j - \sum_{j=1}^{n_i} \xi_{ij} \sum_{j=1}^{n_i} t_j} ; \qquad (1.14)$$

$$\xi_{oi} = \frac{1}{n_i} \sum_{j=1}^{n_i} \xi_{ij} - \frac{1}{n_i} \sum_{j=1}^{n_i} \frac{t_i}{a_i} . \qquad (1.15)$$

To forecast residual operation time of the electric machine windings, we need to determine the acceptable value of diagnostic parameters R_{1al} and C_{1al}, that is ξ_{al}. To do this, mean values for linear regression are calculated:

$$a = \frac{1}{N} \sum_{i=1}^{N} a_i ; \qquad \xi_0 = \frac{1}{N} \sum_{i=1}^{N} \xi_{oi} .$$

Applying (1.12), we can perform forecasting.

In some cases, for example, winding insulation resistance of electric machines, it is impossible to set an acceptable parameter value. In this case it can be defined in the following way.

Basing on the collected statistic data we define the mathematical expectation of the failure time:

$$M(t_{dif}) = (\xi_{al} - \xi_0)a, \qquad (1.16)$$

whence we get

$$\xi_{al} = \xi_0 + M(t_{dif})/a. \qquad (1.17)$$

This value is taken as the acceptable boundary value of the diagnostic parameter.

Then for the *i*-th electric machine the failure time can be predicted, having applied the formula:

$$t_{difi} = (\xi_{al} - \xi_{oi})a_i = [\xi_0 + M(t_{dif})/a - \xi_{oi}]a_i. \qquad (1.18)$$

Let's find the time of failure-free operation from the moment of the end of observations. The difference $\delta_0 = \xi_{al} - \xi_0$ – good operation time, a $\delta_0 = \xi_{al} - \xi_1$ – residual operation time. Using the formula of linear model of diagnostic parameters variation, we find the residual operation time $\tau_{r.o.i}$ for the *i*-th electric machine:

$$\tau_{r.o.i} = (\xi_{al} - \xi_1)a_i = [\xi_0 + M(t_{dif})/a - \xi_{oi}]a_i. \qquad (1.19)$$

To solve this task we can take previously collected information on the variation of diagnostic parameters of the electric machine in operation. Such dependences R_1 and C_1 for two electric machines are shown in the Fig. 1.15.

Thus, the method involves [18]:

1) selection of the monotypic OD being operated in equal conditions;

2) measuring of diagnostic parameters values ξ_{ij} for the entire set of ODs in certain time intervals t_j;

3) computation of the mean values $\bar{\xi}(t_j)$ of all ODs for the fixed point of time t_j;

4) defining the regression coefficient *a* by the parameters values in points of time t_j;

5) defining mean time of failure-free operation T_{mean};

6) computation of allowable value ξ_{al};

7) defining the residual operation time.
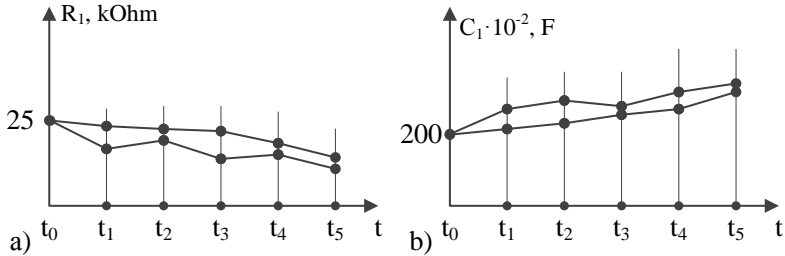
Figure1.15 – Variation of parameters R_1 and C_1

The considered method can be used to evaluate the state of various electrical equipment: electric machines, cables, transformers, converters, secondary cells, etc.

The obvious drawback of trend calculations with the help of linear regression is the assumed hypothesis of its linearity, since in actual practice the diagnostic parameters can vary exponentially due to wearing or be saturated.

Probabilistic forecasting

The tasks of probabilistic forecasting resolve themselves into defining the probability of the predictable process overrunning (not overrunning) the set limits.

Thus, mathematical problems of the probabilistic forecasting are formulated in the following way. The values of the time function (diagnostic parameter) $\xi(t)$ are known in points of time t_i, $i = \overline{1,n}$; $t_i \in T_1$. We need to determine the probability that the value of function $\xi(t)$ does not fall outside the acceptable limits ξ_{al} in the points of time t_{n+j}; $j = \overline{1,m}$, $t_{n+j} \in T_2$, that is $P\{\xi_{n+j} > \xi_{al}\}$ [10].

It's quite easy to determine the probability, if we know the probability distribution law for the diagnostic parameter:

$$P\{\xi_{n+j} > \xi_{al}\} = \int_{\xi_{al}}^{\infty} f_{n+j}(\xi)d\xi, \qquad (1.20)$$

where $f_{n+j}(\xi)$ – probability density function of the value ξ in the time intersection t_{n+j} with expected mean $m_{n+j}(\xi)$ and *dispersion* $\sigma^2_{n+j}(\xi)$.

The distribution function F(ξ) of the random value ξ in the time intersection t_i is related to the probability density function $f(ξ)$ by the following relation:

$$f(\xi) = dF(\xi)/d\xi; \quad F(\xi) = \int_{-\infty}^{\infty} f(\xi)d\xi.$$

In practice, the values of diagnostic parameters are usually distributed in accordance with the normal law:

$$f(\xi) = \frac{1}{\sigma_\xi \sqrt{2\pi}} \exp\left(-\frac{(\xi - m_\xi)^2}{2\sigma_\xi^2}\right), \tag{1.21}$$

where m_ξ – expected mean; σ_ξ – root-mean-square deviation (characterises values scattering with respect to the expected mean); $\sigma_\xi^2 = D$ – dispersion.

$$m_{\xi 1} > m_{\xi 2}, \quad \sigma_{\xi 3} > \sigma_{\xi 2} > \sigma_{\xi 1}$$
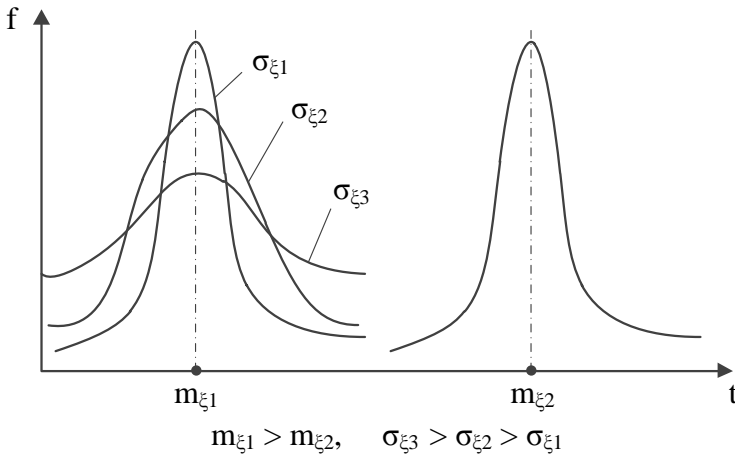
Figure 1.16 – Normal law of distribution

Those values are considered in the following way:

$$m_\xi = \frac{1}{n}\sum_{i=1}^{n}\xi_i \ ; \ \sigma_\xi = \sqrt{\frac{1}{n-1}\sum_{i=1}^{n}(\xi_i - m_\xi)^2} \ .$$

If the probability distribution law is normal, the probabilistic forecasting can be narrowed down to the forecasting of the variation of an expected mean.

The illustration of formulation and solution of the probabilistic forecasting problem using statistic extrapolation is shown in Fig. 1.17.

Whereas one must [18]:

• define on the interval T_1 m_ξ and σ_ξ for each time intersection;

• carry out interpolation of the values m_ξ and obtain the polynomial $F(t)$;

• carry out extrapolation m_ξ and σ_ξ in the required time t_{n+j};

• calculate the probability of the diagnostic parameter falling/not falling outside the acceptable limits.

In order to ensure the required prediction accuracy while performing the probabilistic forecasting for each time intersection, we need to determine the probability distribution law of the parameter values; therefore, we need a sample consisting of about 30-50 monotypical ODs. The amount of the time intersections considered to interpolate the nature of parameter variation is selected in the same way as for deterministic forecasting.
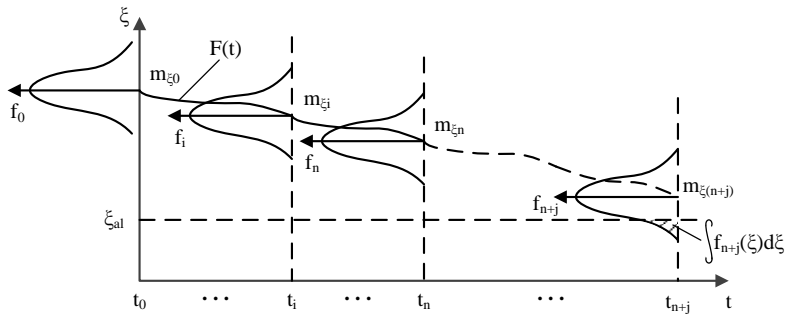
Figure 1.17 – Probabilistic forecasting

Forecasting applying the statistical classification method

The statistical classification is based on the theory of pattern recognition. Pattern recognition implies the attribution of the phenomenon or the object under consideration by their image to one of the known classes of objects or phenomena. The assumption is that each class is characterized in a certain way, inherent in each image from the multitude of images composing this class.

It requires the solution of two problems. *Classes formation*, often being interpreted as *learning*, in which the *similarity measure* is determined on the basis of the study of each class images, or a *class description* is provided, and the actual *recognition*, in which the *similarity measure* of the image's class is determined as well.

On the basis of the results obtained, we decide to attribute images to the class, to which the OD similarity measure is maximal.

31

A certain class membership of an image is characterised by the *similarity function*, with the help of which the probability of this class membership is determined. It should be noted that the attribution of an image to a certain class can be based, in fact, not on similarity (proximity), but on the differences between classes.

Solving the OD forecasting problem, we consider the *classes* are considered R^γ, $\gamma = \overline{1,m}$, which are divided into (Fig.1.18):

parametric ones $R_\xi^\gamma : R_\xi^1 = \xi_0..\xi_1,\ R_\xi^{21} = \xi_1..\xi_2,...R_\xi^m = \xi_{m-1}..\xi_m$,

where $\xi_i...\xi_j$ – the interval in the tolerance zone;

time ones $R_T^\gamma : R_T^1 = T_0..T_1,\ R_T^2 = T_1..T_2,...,R_T^m = T_{m-1}..T_m$,

where $T_i...T_j$ – is the time interval.

A class multitude and magnitude are determined by the OD specific features. They unite objects that have identical parameters of their state, a set of properties, etc. Each time class characterizes the operating life, and parametric one - the performance margin.

Classes R^γ present certain standards (prototypes, portraits). They are set on the basis of tests. In doing so, we determine the extrapolation links F^γ, that connect the diagnostic parameters values with classes.

The classes are to be separated from each other. If the classes vary significantly, it is easy to find the boundary; if they overlap, it becomes complicated. The state is recognizable at the boundary. The classes boundaries (Fig. 1.19) can be set by the method of zones, applying the following rule for its solution:

$$d_s = \begin{cases} -1, & \text{if} \quad \xi \leq \xi_1^L; \\ 0, & \text{if} \ \xi_1^{\text{н}} < \xi < \xi_1^U; \\ +1, & \text{if} \quad \xi \geq \xi_1^U. \end{cases} \qquad (1.22)$$

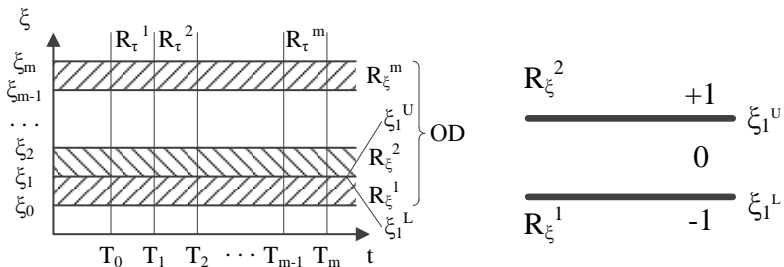The larger the zone '0' is, the more reliable the recognition is.

Figure 1.18 – Parametric and time classes   : 1.19 – Class boundary

If the object's state is evaluated by n parameters, the proximity measure is calculated as a sum:

$$d_\Sigma = \sum_{i=1}^{n} d_i \; . \tag{1.23}$$

For example (see. Fig.1.19), if $d<0$, that the OD is attributed to the class R^1, if $d>0$, in it attributed to the class R^2. If $d = 0$, the OD cannot be classified with the help of this method [18].

The forecasting problem while using the statistical classification method (objects recognition) is formulated in the following way.

The object state is characterized by the set $\Xi = \{\xi_i\}$ having m diagnostic parameters: ξ_j , $j = \overline{1,m}$ (in the simplest case – one). We know the values ξ_i in the point of time t_o or in the limited time interval $[t_o, t_l]$. We need to to make a decision concerning the object membership, according to its state, in one of the known classes R^γ .

Such a statement of a forecasting problem assumes that each set $\Xi = (\xi_{j1}, \xi_{j2}, ..., \xi_{jn})$ of diagnostic parameters values ξ_{ji} , $i = \overline{1,n}$, that characterizes a certain class of states has a corresponding durability or a degree of performance ability of an object.

The forecasting procedure involving the methods of statistical classification implies:

1) determining the initial sample of N objects with guaranteed operational period T_z. Each object of the sample N has a certain corresponding operational period t_i, $i = \overline{1, N}$;

2) based on the relation of values T_z and t_i objects are divided into classes;

3) the description of each object of diagnostics with m-dimensional state vector;

4) selection or construction of the recognition function F^γ or the decision rule d;

5) the actual recognition, i.e. the object's attribution to a certain class according to its state.

As it was stated above, the first two actions belong to learning problems' solving, that is why they are often called the *learning* stage, and the latter three ones correspond to the *recognition* stage, and they are called *basic*.

Thus, if the object's state is characterized by a state vector:

$$\Xi = (\xi_1, \xi_2, \dots \xi_m),$$

Then during the learning we receive vectors Ξ^γ forming the classes R^γ.

It means that performing probabilistic or statistical processing of vectors $\Xi \in R^1, \Xi \in R^2$, within each class R^γ we can describe a state with the help of a distribution density function $f^1(\Xi)$, $f^2(\Xi)$.

Depending on the manner the class is described or what the the setting up of the problem requires, the classification of vectors is performed by deterministic or probabilistic methods.

While applying deterministic methods, we use distances as the proximity measure:

$$d^1 = \Xi_\ni^1 - \Xi_i, \quad d^2 = \Xi_\ni^2 - \Xi_i, \dots,$$

where $\Xi_\ni$ – the reference value of the parameter of γ-th class.

Minimum distance $d_{\min}^\gamma$ indicates the object's membership in the class R^γ.

Probabilistic methods assume computation of the probabilities values $P^1(\Xi_i \in R^1)$, $P^2(\Xi_i \in R^2)$,.... Maximum probability value $P_{\max}^\gamma$ indicates the object's membership in the class R^γ.

Thereby the following is required [18]:

– learning, that is obtaining a range of statistical data by values $\xi(t)$;

– development of the discriminant function, i.e. an equation of surface, which divides classes R^γ in space.

For classes formation during the learning we need to have several hundred measured values of diagnostic parameters. The forecasting by statistical classification methods is mainly applied in series production, where a considerable "learning" sample is available.

LIST OF REFERENCES FOR CHAPTER 1

1. Kalyabin VP, Rybakov L. M. Reliability and diagnostics of electric power units: Study guide. /Mari State University – Yoshkar-Ola: 2000. – 357pp.:ill.
2. Gouk Yu.B. Reliability analysis of electric power units. – Leningrad: Energoatomizdat Publ., 1989. – 244 pp. ill. – (Reliability and Quality).
3. Gulyaev V. A., Konstandy G. G. Technical diagnostics. Methods for determination of the frequency of electric power systems diagnosing. – Kiev: Engineering, 1987. – 200 c.

4. Kalyabin V. P., Mozgalevsky A. V., Galka V. L. Reliability and technical diagnostics of shipboard electrical equipment and automatic equipment: Manual. – St. Petersburg: Elmore, 1996. – 296 с.
5. Rozanov M. N. Reliability of electric power systems. 2-nd Rev. and Ext.Ed. – Moscow: Energoatomizdat Publ., 1984. – 200 с.
6. Rybakov L. M., Khalilov F. K. Improving operational reliability of transformers and high voltage electric motors. – Irkutsk: Irkutsk University Publishers, 1991. – 155 с.
7. Svi P. M. Methods and means of the high voltage equipment diagnostics. – Moscow: Energoatomizdat Publ., 1992. – 239 с.
8. Ushakov V. Ya. Insulation deterioration and methods of its condition monitoring. Study guide. – Tomsk: Tomsk Polytechnic University Publishers, 1993. – 368 с.
9. Fokin Yu. A. Reliability and efficiency of electric power grids. Moscow: Higher School Publishers, 1989. – 151 с.
10. Sinchuk O. M., Sinchuk I. O., Boyko S. M., Karamanets F. I., Yalova O. M., Parkhomenko R. O. Renewable electric energy sources in the structure of power supply systems of iron ore mining enterprises. (Analysis, prospects, projects): monograph. Kryvyi Rih: PE Shcherbatykh O.V. Publishing House, 2017. 152 pp.
11. World Energy Outlook –2015, OECD/IEA, Paris.
12. Ukraine's Power Industry Strategy for the period till 2035. // The Ministry of Energy and Coal Industry of Ukraine website: [electronic source]: http://mpe.kmu.gov.ua.
13. Skalkyn F. V. Energy and Environment / F. V. Skalkyn, A. A. Kanayev, I. Z. Kopp. – Leningrad: Energoizdat Publ., 1981. – 280 pp.
14. World Energy Resources; in P. S. Neporozhnyi, V. I. Popkov (Eds.) – Moscow: Energoatomizdat Publ., 1995. – 232 pp.
15. Basic parameters of the national economy energy supply of for the period until 2020. Stogniy B. S., Kyrylenko O. V., Prakhovnik A. V., Denisyuk S. P., Nehoduiko V. O., Pertko P. P., Blinov I. V. – Kyiv: Publ. Institute of Electrodynamics of the National Academy of Sciences of Ukraine, 2011. – 275 pp.
16. Smart Power Grids – Talking about a Revolution // IEEE Emerging Technology portal, 2009.
17. Sinchuk I. O. Renewable and Alternative Energy Sources: study guide / I. O. Sinchuk I. O. Boyko, O. Ye. Melnyk // study guide – Kremenchug: PE Shcherbatykh O. V. Publishing House, 2015. – 270 с.
18. Power industry of Ukraine: Current State and Development Trends// National Security and Defence. – 2012. – № 6(135). - pp. 2-41

CHAPTER 2
DIAGNOSTICS OF ELECTRIC MOTORS PARAMETERS
(Sinchuk I. O., Smenova L. V., Boiko S. M.)

The electrical machines ruggedness, being one of the most important technical and economic factors, is of primary significance for the national economy, since it is one of the additional sources of increasing the operational fleet of electrical machines.

Electric drives with d.c. motors. Considerably reliable statistical material regarding the operational reliability of electric drive systems has been accumulated. Studies in this direction usually repeat the known results, so there is no need to perform them [1, 2].

The greatest number of failures in d.c. machines happen in the commutator-and-brush unit and in bearings [3, 4]. In electrified transport systems the mentioned failures account for 44-66%; in the excavator drive - over 60%. Typical damages of the commutator include its deformation due to uneven wear, burning and fusion of the commutator bars during unfavourable commutation.

Damages to the frame insulation, though less vast, typically have more severe consequences. Generally, this is an insulation breakdown of between the section conductors by steel stacking; commutator necks sealing off the commutator bars; the destruction of the binding bands of the armature winding. The consequences severity of such damages is accounted for inopportune disconnection due to imperfections of protection, on the one hand, and the impossibility of instantaneous motor stopping in the vast majority of mechanisms due to the response delay of the rotating parts, on the other hand.

Damage to the field winding, intermediate poles and the compensation winding is mainly related to the breakdown of the frame insulation. It should be emphasized that compensatory windings fail more often in thyristor electric drive systems. As far as the mechanical damages are concerned, the bearings failure is the most typical one: wearing-out of liners, destruction of balls, separators, etc.

Electric drives with induction motors. In the majority of cases [5] the motors with capacity over 5 kW break down: due to turn-to-turn short circuits - 93%, turn insulation breakdowns - 5%, slot insulation breakdowns - 2%. Mechanical damages account for about 8%. Damages to asynchronous motors are mainly of operational nature (up to 50%), technological causes associated with manufacturers account for about 30%. Failures with short circuits in the stator winding have different nature: two-phase mode operation; local overheating of various nature, severe starting conditions, etc. The repair of electrical machines involves a certain

processing of the stator and rotor, i.e. with operations that modify the properties of construction materials, which are not subject to repair.

Electric drives with synchronous motors. From a constructive point of view, synchronous motors are more complex than induction ones. The indicators of reliability of machines with regard to the stator and rotor windings are clearly defined [6]. Turn-to-turn short circuits as well as sections short circuits to frame are the main causes of stator windings failures. The causes of the synchronous machines stators failure are, in their turn, diverse, and their classification depends on the technology of machines manufacturing, operating conditions (frequency of synchronous machines starting, etc.). Furthermore, the most vulnerable elements of the stator winding design are stator end windings, in particular, due to insulation failure caused by mechanical stresses occurring during the starting. The value and nature of the stresses depend on the level of the supply voltage and the voltage at the terminals during the starting, the impact itself on the winding depends on the starting duration. The environment and the service culture have a significant impact.

The rotors breakdown is caused by faults in the starting and damper windings, the field winding fault. Damage of the starting winding is typically caused by severe starting conditions, in particular, when starting under load, and it depends on the level of the supply voltage, etc. Experience has shown that in large power grids, the stator winding breaks down more often, i.e. kinetic force is significant, while the starting time is minimal. In case of considerable undervoltage under the influence of starting currents, the starting winding is damaged more often due to the increase in the starting time.

2.1 Parameters determination in induction motors systems

The detailed analysis of the current state of the systems of maintenance and repair of complex technical facilities [14, 15] proves the necessity of transition from the system of planned preventive maintenance to the strategies of control the operating reliability of these facilities according to their technical condition. The advantages of such a transition from the point of view of labour saving, material and financial resources saving are apparent, and in the market economy they are indispensable. However, this transition is possible only if technical diagnostic systems and/or monitoring systems for the facilities' technical condition are created. The theory of such systems is currently not sufficiently represented in the scientific works of foreign and Ukrainian scientists, and the practical implementation of this class systems is at the initial stage of its development and far from complete. Creating of modern diagnostics and monitoring systems for complex technical objects requires:

− primary measuring instrumentation for technical parameters;

− secondary information and computing hardware for processing and visualization of collected data;

− various information technologies or, in other words, the rules for measuring and collecting technical signals, algorithms for converting these signals into digital diagnostic data, and the complexes of programs for conversion, storage, visualization and logging of collected data using mathematical state transition models (in diagnostic technologies) and degradation processes models (in monitoring technologies) of the monitored objects' state.

Information technology of diagnostics. It allows: to obtain an object's state evaluation on the basis of protocols of technical parameters measuring and their exclusion protocols, to determine types of faults by parametric and/or spectral analysis and/or using information technologies for fault recognition systems. If at the same time there is a possibility to obtain a single document − a technical state certificate, in which the exclusion protocols and the object's faults protocols are simultaneously listed, the diagnostic information technology becomes the information technology of the object certification. Classification of diagnostics types distinguishes functional and test diagnostics of technical objects. Functional diagnostics, which is carried out on a operation (functioning) object and is typically performed with the accuracy of determining one of its two states: (nonfault-faulty, operable-nonoperable, adequately functioning - inadequately functioning), in most cases does not satisfy the owners of objects, and then the functional diagnostics is applied with the three-level state evaluation (nonfault-faulty, but operable-nonoperable). In both cases, we refer to a general functional diagnosis or a general state evaluation of the object and the diagnostics resolves itself to determining one of the above states of the object using state transition models. The main disadvantage of general functional diagnostics is that it does not give answers to such questions important for users as [6-10]:

− What parts, blocks and components of the object have faults?

− What types of faults are in parts, blocks, components and the entire object?

− When will the failure of a part, block, component or the entire object happen?

You can answer the first question if you use functional diagnostics with the object state evaluation based on all its technical and technological parameters. In this case, this refers to a parametric functional diagnostics, and it is quite obvious that to ensure such monitoring we need a strictly defined set of diagnostic parameters characterizing the state of a part, a

block, a component and an entire object; if it is a three-level state of the object, we need to know exactly their acceptable, extreme limit and over-extreme limit values. In this case, the diagnostics resolves itself to measuring the diagnostic parameters and comparing them with the acceptable, extreme limit and over-extreme limit values. In such case, the set of measured parameter values presents the object state protocol, and the set of parameters which values are out of range presents an exclusion protocol for parameters. However, in this case, having performed the parametric functional diagnostics, we can only note a certain state, while it is impossible to indicate the types of faults and the time of the failure occurrence in the part, block, or the entire object. Presently, functional diagnostics in its pure form is generally not used. At least, it is supplemented by the function of predicting the values of the observed parameters by its trend in time and by the function of determining the dates of the nearest technical inspection of the monitored object.

Information technology of fault detection. It allows you to answer the question what kind of faults are in the object. In doing this, we need to know the criteria of faults in parts, blocks, components and monitored objects in general. To answer the question of what types of faults are in the object, we need to implement the fault detection function. In doing this, we need to know the criteria of faults in parts, blocks, components and monitored objects in general. Correctly selected criteria allow us to detect partial and complete, stable and unstable, obvious and latent defects and faults. The criterion of fault, as well as the criterion of a defect, is called the over-extreme limit and extreme limit value of one or several diagnostic parameters, respectively. The failure criteria are the basis of any method of fault identification. Currently, the most widespread among of all the known methods are three types: the manual analysis method, the method of creating deterministic expert systems and the method of creating probabilistic expert systems. The final product of the application of any of the methods considered is the protocol for detection of hidden defects, faults and destruction [11].

Information technology of certification. In recent years, in the field of monitoring the objects technical condition the certification (inspection) of the monitored object state has been used instead of the functional diagnostics. The certification is essentially a combination of general functional diagnostics, parametric functional diagnostics with logging of exclusions of the monitored parameters admissible values, and identification of faults types with logging of detected defects and faults.

Information technology of monitoring. This technology, being a continuous or intermittent observation of the technical state of objects, has broader functionality and generally includes: diagnostics (evaluation of the

current state), genesis (evaluation of the past state) and forecast (evaluation of the future state) of the monitored objects. Monitoring based on spectral, correlation and harmonic analysis of diagnostic data ensures scientific validity of the following: to forecast failures and to plan, in this regard, terms and scope of equipment repairs, manpower costs, material and financial costs in the maintenance and repair system, determine sufficient criteria for the objects state evaluation, determine the values of criteria for the objects state evaluation, identify the characteristic features of faults. To determine when the failure occurred or will occur, we need a function of genesis and prediction the values of the diagnostic parameters. These functions are implemented by methods of the technical state monitoring. At present, several monitoring methods are known. The key distinguishing features of these methods are the rules used to determine a fault-free shutdown of the operation of the monitored object. Here are some of these rules [12]:

− pre-start check rules,

− rules of the optimal shutdown according to the criterion of service life efficiency,

− rules of minimizing the time to failure,

− rules of guaranteed success or a game approach.

Any of these rules implies the use of a mathematical model of the equipment degradation processes to determine the exact date of a faulty object shutdown. In this case, mathematical models are of situational nature, i.e. after each measurement of the diagnostic parameters, the trajectory of the parametric vector in the space of its values is defined more accurately. Presently, the most widespread are two methods of monitoring the technical state of an object by fault-free shutdown of an object operation by the rule of pre-start check. The basic concept of the first method is to determine the date of the object shutdown by the date of intersection of the polynomial of the third degree used for extrapolation; this polynomial approximates the process (trend) of the monitored parameters with the level of the over-extreme values of these parameters. The basic concept of the second method is to determine the date for the object shutdown by the date of intersection of the polynomial of the third degree used for extrapolation; this polynomial approximates the process of increment to the arithmetic mean values of the monitored parameters, with the level of the over-extreme values of these parameters. The second method gives a later date of the shutdown and can be used to determine the date of maintenance or repair, while the first method can be used to determine the due date of the next inspection of the object [13].

Currently, methods of machines and mechanisms maintenance are generally divided into three types [10-20]:

1. The first type is the equipment maintenance after its failure.

In this case, machines and equipment operate before their breakdown [5]. Basically, this applies to cheap auxiliary stand-by equipment, when the replacement of equipment is cheaper than the costs for its repair and maintenance.

If the stand-by equipment is absent/not available for the period of repair, the operation has to be stopped. Often, during the equipment operation before its breakdown, periodic measurements of the machine vibration state are also performed, which allow us to reduce the repair time due to the possibility to determine, in the first approximation, the time when the machine may break down, and thus provide the maintenance personnel with spare parts in due time.

2. The second type of maintenance is the equipment maintenance as per the procedures.

In this case, the maintenance is carried out in accordance with the manufacturer's recommendations at regular intervals, for example, weekly or monthly, regardless of the technical condition of the equipment. This kind of maintenance is usually called a planned preventive (routine) one. If the maintenance frequency is defined by the methods of statistical analysis, then in accordance with the regulatory documents, the period between maintenance usually comprises the time during which not less than 98% of the equipment operates without failures.

The servicing in compliance with the maintenance schedule, at least, remains the possibility to use the manufacturer's warranty. But it develops that at least 50% of all technical services as per the maintenance schedule are carried out without their actual need. What is more, for many machines, maintenance and repair as per the maintenance schedule do not reduce the frequency of their failure [5].

Moreover, the operational reliability of machinery and equipment after maintenance (if maintenance involves disassembling of the mechanism or parts replacement) often decreases, sometimes temporarily, until they are run-in, and sometimes this reliability reduction is caused by installation defects that were absent before maintenance.

3. The third type of maintenance is a condition-based one. [5].

As far as this type of maintenance is concerned, the condition of machines and mechanisms is monitored either periodically (in the absence of defects), or depending on the diagnosis results and the technical condition forecast.

In this case the maintenance is carried out only when it is necessary due to the oncoming high probability of the equipment failure. Thus, the

operating of properly functioning mechanism is not interrupted by human intervention.

2.1.1 Analysis of the evaluation methods of induction motors' state and quality

Generally accepted indexes, regulated by standards, and able to determine the quality of any motors, including traction induction ones, are: efficiency, power factor, maximum torque M_M, initial starting torque M_S, initial starting current I_S [21].

These indexes characterize the induction motor (IM) operational mode, when electromagnetic transient phenomena are either absent or can be neglected.

Using IM (induction motors) in electric drives in traction electrotechnical systems of mine electric locomotives, operated in conditions of dynamically quick changing loading, the use of these indexes, which characterize static processes, is hampered, since along with the indexes that evaluate the static properties of IM, we need to introduce the additional indexes that evaluate dynamic properties and results of operation of the traction induction motors. Such indexes may be, for example, the magnitude of shock electromagnetic torque during starting or emergency braking, the value of electrical losses during ripple loading, etc.

These estimates of the state and quality of TIM (traction induction motors) in dynamic modes can also be obtained if the motor parameters are known in all possible ranges of rotor speed variation.

Let's assume, as in [7], that the parameters of asynchronous electric machines are coefficients in front of independent variables in the equations describing the transformation of electromechanical energy. Typically, independent variables are currents. The equations can be either differential or complex or algebraic ones.

Parameters of traction electrical machines, including asynchronous ones, are resistance, and inductive reactance and moment of inertia.

As a result, two main ways of obtaining these parameters is logically determined: the computational, and combined experimental and computational [22].

Computational methods may imply the definition of only a part of the TIM parameters, considering the latter unknown. For example, [8, 9] we determine the leakage inductances of a rotor chain and the inductance of the magnetizing circuit of an induction motor. Here input data is the current and phases voltage of a stator. Leakage inductance and the stator resistance are determined in the no-load test; while the rotor resistance is determined on the basis of data obtained in the short circuit test. We consider the steady state operation of the motor. The method of computation, as we already

have noted, provides for the determination of inductances only. Therefore, the results obtained can be considered valid only for one operational point or the area of the TIM (rated) characteristic, since the variation of the rotor resistance during profound change of the rotor speed of rotation is not taken into account.

It should be noted that in [8, 9] the mathematical model of TIM is used [57]. There is a common approach to constructing an algorithm for determining parameters; it is a determined procedure.

Besides the determined procedures for definition of TIM parameters, search procedures are considered, for example, in [10, 11]. The concept of the latter is to determine the iterative search procedures in order to minimize the differences between the experimental data and the computation ones. At the same time, initially, the TIM required parameters can be set approximately, and then defined more precisely to values that provide the maximum approximation of the computation and experimental data. In [12], based on the use of the mathematical model of TIM for [13], the TIM electromagnetic parameters are determined on the basis of no-load test and short circuit test. Therefore, it is assumed that the parameters of the rotor circuit are linearly dependent on the angular rotation rate of the rotor. Furthermore, in [12], the static mechanical characteristic of the motor is additionally found by experiment. In view of this, the procedure of the parameters determining is divided into three stages. At the first stage - we determine the approximate initial values of the required parameters and the nature of their variation, depending on the speed of rotation of the rotor. At the second stage - the static mechanical characteristic of an induction motor is recorded. At the third stage - an iterative procedure is implemented in order to minimize the deviation of the experimental curve from the computational one.

One of the known ways of the IM parameters determining is based on assuring certain conditions for power supply of an induction motor and recording the phenomena that occur. For example, [14] describes the method of determining the IM parameters based on measurements with a direct current passing through the stator winding.

Having analyzed the methods of determining the IM parameters, we can state that a significant part of these methods is focused on the determination of parameters in a limited area of motors characteristics. For example, in [15] IM parameters are defined on an experimental basis, but saturation of a machine is not taken in consideration. [14, 16, 17] define parameters for a limited range of variation of rotor speed [7, 9] here the rotor resistance or the rotor leakage inductance and the inductance of the magnetization circuit are considered constant. The technique is known when measurements are made if the rotor is locked [18, 19].

Consequently, a significant part of the methods for determining the IM parameters has a limited range of application.

However, the possibility of using computers, i.e. numerical methods, for this purpose is the solution of the above part of the problems.

The use of mathematical models for this purpose should be planned when creating a system of identification and diagnostics, and the models themselves should allow their direct application in the control process. This basic condition requires a direct relation between the models development and selection of the structure of operations conducting, as well as appropriate information support, new methods of operations conducting, and even new forms of documentation. This requirement is due to the fact that mathematical models must be seamlessly incorporated into the flow of control system operations.

The use of mathematical models in the operation of the control system requires the availability of the appropriate technical standards base, classifiers, on-line corrected data, appropriate technical support, etc. The lack of all these factors is one of the reasons for the insufficient application of mathematics in identification and diagnostics systems.

The second reason is purely 'mathematical' one. To apply a mathematical model, we need to have it. The complexity of real problems, the need to record multiple, often quite heterogeneous, parameters and constraints, nonlinearities, and occasional events complicate the development of actual mathematical models, which can be directly used in control processes to obtain better management solutions. Practice proved that administrative control requires its 'own' mathematics, because the classical analytical methods that are successfully applied in the management of technical facilities often 'do not work' in managerial control systems (though in some cases, their application allows us to obtain the required results). Analytical methods are suitable when the model represents a system of relatively small number of linear or difference equations of the first or second order. Analytical methods are not suitable in the case of high orders, the need for accounting nonlinearities, random disturbances. In practice, there are not so many problems that can be solved by classical optimization methods or mathematical programming methods.

The application of analytical methods in identification and diagnostic systems is associated with the solution of optimization problems, i.e. with finding the extreme values of some functions that describe the connection of the chosen optimality criterion with the parameters that determine their value under the existing constraints. It is the complexity of obtaining such a functional dependence, which can be resolved by analytical methods and directly used during control, that has led to the limited use of analytical methods in identification and diagnostic systems.

In the field of mathematical methods application for identification and diagnostics, significant research works are in progress; they can be provisionally divided in two directions. The first direction is associated with the use of a traditional analytical approach, the second one - with the development and implementation of mathematical methods that take into account the specific features of control, and which are directly designed for application in the control process. The first direction (the above mentioned one) develops approximate models which, although they oversimplify the mathematical description of the real processes, but allow us to obtain the necessary data.

Let's note that the complexity of the problems of control, identification and diagnostics, the large dimension of mathematical equations, which are models of these problems, typically make it unrealistic and inappropriate to develop single 'global' models that describe the operation of the entire control system, its individual functions.

As it has been already noted above, automation of the functions performance is carried out by transferring individual problems and their complexes to computers. In the process of decomposition of functions, the mathematical model of an entire function is a set of mathematical models of individual problems (obviously, it means the complex of interconnected models, and not about their simple set). Models should be constructed in such a manner, so that they are not only equivalent to real problems, but also could be solved using existing computing means. It should be noted that it's by no means always that such a complex can be developed.

The second direction, associated with the development of so-called algorithmic methods, which are directly intended for operation in control systems, is now rapidly developing. These are methods of numerical analysis, or machine simulation.

Thus, the problem of the parameters identification and diagnostics of the state of traction induction electric drives has not been completely solved up to the present moment. With regard to TIM in traction electrotechnical system on board of mine electric locomotives, these issues regarding the determining characteristics of the modes and conditions of the mine electric locomotives operation have not yet been considered at the right scientific level. Taking into account all these facts, we can formulate the following generalized requirements for research and implementation of their results:

− in order to obtain real information about the state of the parameters of the traction induction motor, we should ensure a variation in the rotor's rotation speed in the range from zero to the rated value;

−information about the TIM state should be obtained by the minimum number of sensors which should not be mounted on the motor according to the design;

−the initial result in the monitoring process should be the value of the electromagnetic and mechanical parameters of the TIM (traction induction motor) in the full range of the rotation speed variation.

2.1.2 Generalized algorithm of induction motors diagnostics and identification

The previously proposed and grounded sequence of operations during the identification of electrical parameters and the diagnostics of traction induction motors in the traction electrotechnical system of mine electric locomotives is as follows (Fig. 2.1).

We form the model of the object for monitoring, which includes:

−the type of traction induction motor;

−the type and features of the frequency converter operation: balanced and unbalanced operating modes with separate voltage and frequency regulation; the possibility of forming a constant voltage in the given load circuits (phases of an induction motor);

−the possibility to set the necessary operating modes: start, braking, continuous rotation, DC excitation;

−conditions of a traction electrotechnical system operation: the nature and possible volume of the traction load, applied to the shaft of the motor moment of inertia of the mechanism, which depends on the load of the mine electric locomotive.

The choice of structure - the sequence of identification operations is determined by the mode of operation, which is preformed in a certain way during the execution of the commands of the electric locomotive driver.

In the course of automatic control of the electric locomotive, the structure of the object's model is determined by the commands of the operator.

In this case, the following modes of the traction electrotechnical system operation, which is required for identification, are tested: successive two-phase connection of the motor's stator to a constant voltage [17-23], the motor starting with a given amplitude and the frequency of the supply voltage. In this case, the measured parameters of TIM are - the values of phase voltages, currents and rotation speed. Formatted by the microprocessor control system of traction electrotechnical unit, the data is transmitted by the corresponding channels to the on-board computer, which contains the necessary software for identifying these parameters and diagnosing the motor condition.

The arrays of data on transient processes, required to diagnose and identify the parameters, are loaded in the RAM (random access memory) of the on-board computer:

$-$ three data arrays $I_{a1...aN}$, $I_{b1...bN}$, $I_{c1...cN}$ on phase currents and three data arrays $U_{a1...aN}$, $U_{b1...bN}$, $U_{c1...cN}$ on pairwise phase connection to constant voltage U_n (that is, the phases ab are connected the first, then phases bc and finally - ca);

$-$ three data arrays $I_{a1...aN}$, $I_{b1...bN}$, $I_{c1...cN}$ on currents in three phases and three data arrays $U_{a1...aN}$, $U_{b1...bN}$, $U_{c1...cN}$ on three-phase voltages during starting or operating mode;

$-$ if the sensor of the rotation speed is installed, a corresponding data array is generated $- \omega_{1....N}$.

The processing of experimental data consists in scaling, regularizing the adjustment of data arrays with the expected results of computation based on the mathematical models of the object being identified. Scaling for measured values, which represent the transient process, with the accuracy required for solving identification problems, is determined by the admissible error of further calculations and presents a separate problem [24].
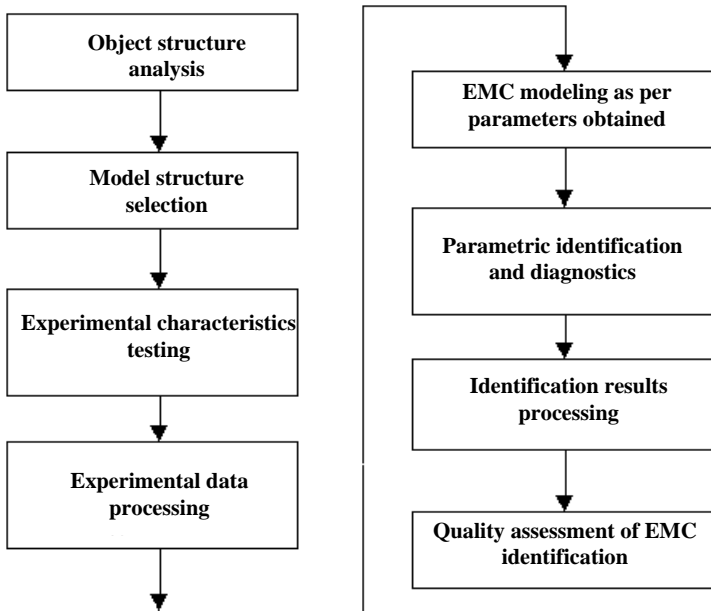
Figure 2.1 – The sequence of operations during the identification and
diagnostics of traction induction motors' parameters

Based on the analysis of transient processes in the electromagnetic
circuit of the stator circuit, we developed an algorithm for identifying the
resistances, inductances and interdependencies of the TIM stator and rotor,
which involves turning on of the traction electrotechnical system, measuring
and storing the values of the required coordinates (currents, voltages,
rotation speeds) and calculations of transient and real time steady processes.
The processing of identification results is an integral part of the
diagnostics. The diagnostic algorithm of the state of TIM parameters is
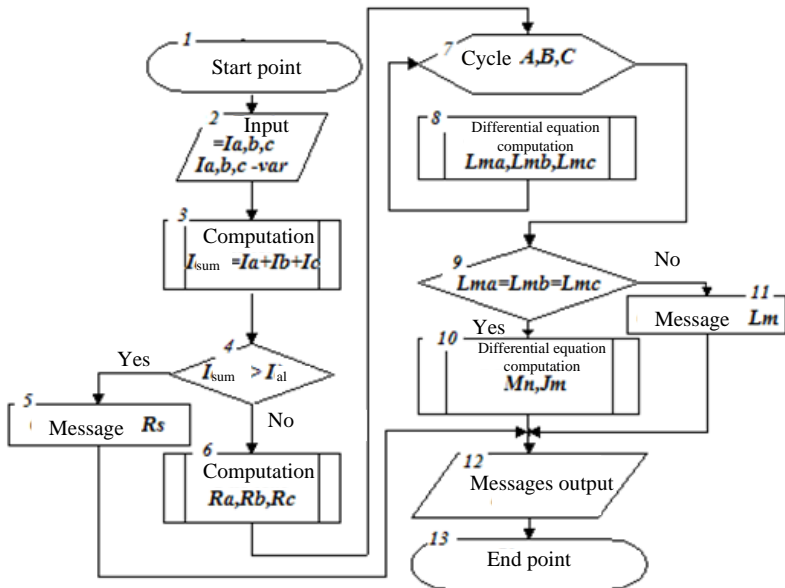presented in Fig. 2.2

Figure 2.2 – Diagnostic algorithm of the state of electrical parameters of a
traction induction motor

Comparing the values of currents in each phase for a certain time,
for example, the starting time or connection to a constant voltage, the time
intervals of the transient process and the steady one are determined.
Diagnostic procedures are carried out after the data arrays on phase
currents and stator voltage (Block 1) have been received and scaled and

basing on the results of the deviation of data on coordinates, which were measured and calculated during the simulation.

The computation of the phases' resistances according to the stator currents' data when the stator is connected to the constant stator voltage (Block 6 Figure 2.2), and their comparison with the catalogued (nameplate) data, allows us to conclude that there are turn faults or interruption of parallel branches in stator windings.

The diagnostic algorithm of the interruption of squirrel-cage rotor bars is performed if the resistances of the stator winding have acceptable values and is as follows.

At the section of the steady process, the instantaneous values of the stator's phase currents are summed up (Block 3) and their sum is compared with the admissible value of the deviation (Block 4), which is determined by the current requirements for TIM. Exceeding the admissible deviation indicates the presence of zero sequence and asymmetry in a three-phase system. It indicates a damage to the TIM rotor, and a corresponding message is produced (Block 5).

With an allowable value of a current of zero sequence, the calculation of stator and rotor resistances is carried out by the block 6.

Performed in three phases, the cyclic computation of the roots of the characteristic equation for an electromagnetic contour of each pair of phases (Blocks 7, 8), connected to the constant voltage, and the comparison of the obtained values between themselves (Block 9) allows us to estimate the state of the magnetic system of the induction motor by symmetry and permeability (blocks 11, 12).

Determination of the main magnetic flux density or the inductive resistance of the magnetization loop according to the values of the time constants of the electromagnetic loop enables us to predict the main TIM operating parameters and determine the permissible load of the motor (block 12).

To determine the permissible load of TIM, let's make the following assumptions.

Nowadays to solve various problems related to the frequency and parametric control, creation of automatic regulation and optimal control systems, increase of power performance of electric drive systems equipped with TIM, the most common solution is the vector representation of a.c. machines coordinates. Taking into account that the electromagnetic torque of an a.c. machine [11] in the vector representation

$$M_{ET} = \frac{m}{2} p L_\mu Im\left(\dot{I}_S \dot{I}_r^*\right) = \frac{m}{2} p L_\mu (I_{S1} I_{r2} - I_{S2} I_{r1}), \qquad (2.1)$$

and the stator and rotor currents are interconnected with known dependences, we will assume that the TIM electromagnetic torque is proportional to the square of the stator current

$$M_{ET} = \sim K_{AD} L_\mu I_S^2 \qquad (2.2)$$

Accordingly, the losses of $\varDelta P$ in TIM and its heating are also directly proportional to the square of the stator current I_S^2.

Thus, the allowable load torque on the TIM shaft

$$M_{al} = \sim K_{AD} L_\mu I_{S\,rat}^2, \qquad (2.3)$$

which clearly determines the allowable load of the electric locomotive train.

A motor operation with the permissible design load increases its service life.

Moreover, if the motor operates with the permissible design load, it increases its interrepair time.

2.1.3 Determination of rotor and stator mutual inductance in an induction motor

The mathematical apparatus for solving this problem is as follows.

The system of linear inhomogeneous differential equations with respect to current $Ia(t)$ and stator flux linkage ψ_a with two-phase connection to a constant voltage U_p, which describes transient processes in the electromagnetic loop of the stator circuit, has the form:

$$\frac{dI_a}{dt} = AL_r U_p - I_a AL_r \left(R_S + R_r \frac{L_\mu^2}{L_r^2} \right) + \psi_a AL_r \frac{R_r}{L_r}$$

$$\frac{d\psi_a}{dt} = 1.5 \frac{L_\mu}{L_r} I_a - \frac{R_r}{L_r} \psi_a \qquad (2.4)$$

Solving the system with respect to the stator current:

$$I_a(t) = \frac{U_p}{R_{Sr}} \left(1 - A_1 e^{tp_{i1}} - A_2 e^{tp_{i2}} \right), \qquad (2.5)$$

where $Ia(t)$ – stator current; U_p – constant voltage applied to stator windings; R_S, R_r – stator and rotor resistances respectively; L_S, L_r – stator and rotor inductance respectively; L_μ – stator and rotor mutual inductance; ψ_α – stator flux linkage; R_{sr} – design stator resistance; p_{i1} and p_{i2} – are the roots of the characteristic equation of system (2.1), which are negative and inversely proportional to the electromagnetic time constants T_{l1} and T_{l2} of stator circuits; A1 and A2 – are constant coefficients determined by the initial conditions of the system (2.1), $A=(LsLr-L\mu^2)^{-1}$ – is a design coefficient of TIM [10].

With allowable deviations, using data arrays on transient processes, we perform the search for characteristic points needed to determine the stator and rotor mutual inductance L_μ. The algorithm for determining the characteristic points is as follows. The data sheet of the transient process at constant current of the motor is approximated by two linear graphs L_{n1} and L_{n2}, which characterize the initial and final time periods of the transient process. The point of the graphs' intersection defines a characteristic point with a temporary coordinate T_{per}, relative to which the values of currents are chosen to determine the stator and the rotor mutual inductance L_μ.

The intersection point T_{per} is determined by the following algorithm.

According to the values of current, we determine the coefficients of the equations of linear relations of current variation on line sections, which occurs at the beginning and at the end of the transient process.

In general case, the equation of a straight line L_{n1} has the form:

$$I(t) = a + b\ t$$

Current I_0 and I_1 in the points of time t_0 and t_1 respectively will be equal to:

$$I_0 = a_1 + b_1 t_0 \tag{2.6}$$
$$I_1 = a_1 + b_1 t_1.$$

Solving the obtained system of equations with respect to constant coefficients a_1 and b_1, we obtain

$$a_1 = \frac{I_0 t_1 - I_1 t_0}{t_0 - t_1}$$
$$b_1 = \frac{I_1 - I_0}{t_1 - t_0}, \tag{2.7}$$

then the equations of lines L_{n1} and L_{n2}:

$$L_{n1}(t) = \frac{I_0 t_1 - I_1 t_0}{t_0 - t_1} + \frac{I_1 - I_0}{t_1 - t_0}\ t$$
$$L_{n2}(t) = \frac{I_2 t_3 - I_1 t_2}{t_2 - t_3} + \frac{I_3 - I_2}{t_3 - t_2}\ t. \tag{2.8}$$

The point of intersection T_{per} is determined on the basis of the condition $L_{n1} = L_{n2}$:

$$T_{per} = \frac{\dfrac{I_2 t_3 - I_1 t_2}{t_2 - t_3} - \dfrac{I_0 t_1 - I_1 t_0}{t_0 - t_1}}{\dfrac{I_1 - I_0}{t_1 - t_0} - \dfrac{I_3 - I_2}{t_3 - t_2}}. \tag{2.9}$$

Based on the condition of the discrete pitch size, we determine the ordinal numbers of the current coordinates Kt_1 and Kt_2, which will be used as a basis for calculations of parameters:

$$Kt_1 = \frac{T_{per}}{\Delta t} - N,$$

$$Kt_2 = \frac{T_{per}}{\Delta t} + N, \qquad (2.10)$$

where N – is an integral number, selected during the software debugging.

The characteristic equation roots P_{i1} and P_{i2} of the stator circuit are described by the equations:

$$P_{i1} = -\frac{A(R_S L_r + R_r L_S)}{2} - \frac{A}{2}\sqrt{(R_S L_r + R_r L_S)^2 + 4 R_S R_r L_\mu^2}; \qquad (2.11)$$

$$P_{i2} = -\frac{A(R_S L_r + R_r L_S)}{2} + \frac{A}{2}\sqrt{(R_S L_r + R_r L_S)^2 + 4 R_S R_r L_\mu^2}$$

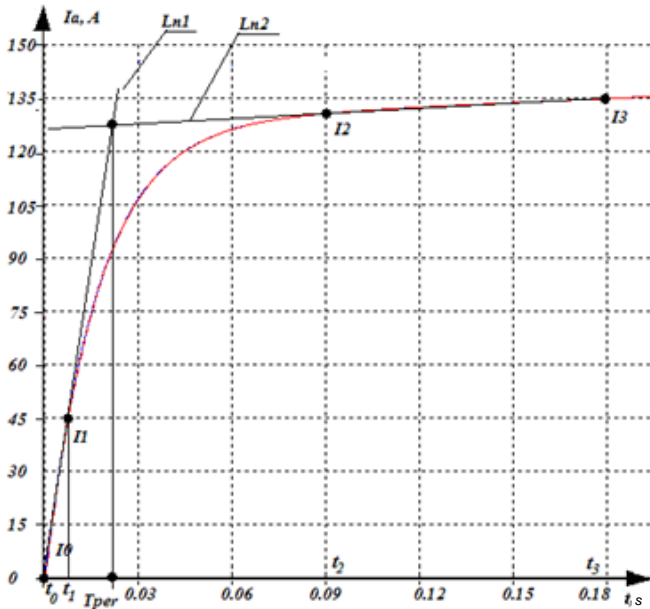and determined with respect to the coordinate point $Kt_{per} = T_{per}/\Delta t$.

Figure 2.3 – Approximation graph of the current transient process in a traction induction motor

By values of currents with respect to the coordinate K_{t2} we choose N_k values of currents I_{p2} and I_{p2-1}, that are applied to determine the values of the characteristic equation roots P_{i2} and P_{i1} using the following formulae:

$$dI_{21} = \frac{I_{Ip2} - I_{Ip2-1}}{\Delta t}, \tag{2.12}$$

$$dI_{22} = \frac{I_{Ip2+10} - I_{Ip2-1+10}}{\Delta t}, \tag{2.13}$$

$$P_{i2} = \frac{dI_{21} - dI_{22}}{I_{Ip2+10} - I_{Ip2-1+10}}, \tag{2.14}$$

$$P_{i1} = \frac{1}{I_{p1}} Log \frac{I_{ust}(1 - e^{P_{i2}K_{t2}\Delta t}) + I_{Ip2}e^{P_{i2}K_{t2}\Delta t}}{I_{Ip2} - I_{Ip2}P_{i2}}, \tag{2.15}$$

$$D_a = \frac{I_{ust}(1 - e^{P_{i2}K_{t2}\Delta t}) + I_{Ip2}e^{P_{i2}K_{t2}\Delta t}}{I_{ust}e^{P_{i2}K_{t2}\Delta t} - I_{Ip2}e^{P_{i2}K_{t2}\Delta t}}, \tag{2.16}$$

Figure.2.4 shows a graphic annex to the algorithm of determining the characteristic equation roots P_{i1} and P_{i2} of the induction motor' stator circuit.
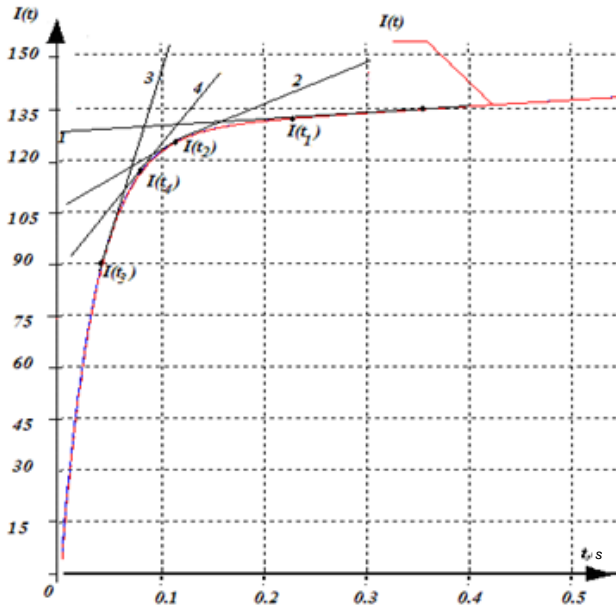
Figure 2.4 – Graph of the current transient process in a traction induction
motor

Applying the formulae of the first terms of the power series expansion for the equations:

$$P_{i2} = \frac{dI_{21} - dI_{22}}{I_{Ip2+10} - I_{Ip2-1+10}},$$ (2.17)

$$P_{i1} = \frac{1}{I_{p1}} Log \frac{I_{ust}(1 - e^{P_{i2}K_{t2}\Delta t}) + I_{Ip2}e^{P_{i2}K_{t2}\Delta t}}{I_{Ip2} - I_{Ip2}P_{i2}},$$ (2.18)

$$D_a = \frac{I_{ust}(1 - e^{P_{i2}K_{t2}\Delta t}) + I_{Ip2}e^{P_{i2}K_{t2}\Delta t}}{I_{ust} e^{P_{i2}K_{t2}\Delta t} - I_{Ip2} e^{P_{i2}K_{t2}\Delta t}},$$ (2.19)

we obtain approximate formulae for determining the values of the characteristic equation roots P_{i1} and P_{i2} of the electromagnetic loop in the induction motor' stator circuit:

$$P_{i2}^1 = \frac{dI_{21} - dI_{22}}{I_{Ip2+10} - I_{Ip2-1+10}},$$ (2.20)

$$P_{i1}^1 = \frac{1}{I_{p1}} Log \left[\frac{(I_{ust} + I_{Ip2})P'_{i2}K_{t2}\Delta t}{I_{Ip2} - I_{Ip2}P'_{i2}} \right],$$ (2.21)

$$D_a^1 = \frac{I_{ust}P'_{i2}K_{t2}\Delta t + I_{Ip2}(1 - P'_{i2}K_{t2}\Delta t)}{(I_{ust} - I_{Ip2})(1 - P'_{i2}K_{t2}\Delta t)}.$$ (2.22)

Let's use the power series expansion of a logarithmic function and restrict ourselves to the first two terms, since the argument of the logarithmic function is of order 10^{-3}-10^{-4}. Thus, we can define the value P_{i1} by applying the following formula:

$$P_{i1}^1 = \frac{1}{I_{p1}} \left\{ \left[\frac{(I_{ust} + I_{Ip2})P'_{i2}K_{t2}\Delta t}{I_{Ip2} - I_{Ip2}P'_{i2}} - 1 \right] - \frac{1}{2} \left[\frac{(I_{ust} + I_{Ip2})P'_{i2}K_{t2}\Delta t}{I_{Ip2} - I_{Ip2}P'_{i2}} - 1 \right]^2 \right\}.$$ (2.23)

It is sufficient to perform the averaging of the values of the time constants P_{i1} and P_{i2} with the five adjacent values of current near the points with coordinates I_{P1} and I_{P2}.

The analytic expression of the difference ΔP of the characteristic equation roots P_{i1} and P_{i2} of the TIM stator's electromagnetic loop:

$$\Delta P = P_{i2} - P_{i1} = A\sqrt{(R_S L_r + R_r L_s)^2 + 4R_S R_r L_\mu^2}.$$ (2.24)

Taking into consideration that $A = \frac{1}{L_S L_r - L_\mu^2}$, we obtain equality:

$$\Delta P(L_S L_r - L_\mu^2) = \sqrt{(R_S L_r + R_r L_s)^2 + 4R_S R_r L_\mu^2}.$$ (2.25)

Taking into account $Ls = Kls \cdot L\mu$ and $Lr = Klr \cdot L\mu$ the square equation with respect to $L\mu$ will be written as:

$$L_\mu^2 + L_\mu \frac{\Delta P}{K_{LS}P_{i1}P_{i2}} + \frac{K_{Lr}R_S^2}{K_{LS}P_{i1}P_{i2}(K_{LS}K_{Lr}-1)} = 0. \quad (2.26)$$

Solution of the obtained equation determines the mutual inductance of TIM stator and rotor:

$$L_{\mu 1,2} = -\frac{\Delta P}{2K_{LS}P_{i1}P_{i2}} \pm \sqrt{\left(\frac{\Delta P}{2K_{LS}P_{i1}P_{i2}}\right)^2 - \frac{K_{Lr}R_S^2}{K_{LS}P_{i1}P_{i2}(K_{LS}K_{Lr}-1)}} \quad (2.27)$$

We choose the value of the stator and rotor mutual inductance $L\mu$ with plus sign $(+)$ before a radical.

The second method for determining the mutual inductance $L\mu$ of stator and rotor is as follows.

The values of the characteristic equation roots P_{i1} and P_{i2} of the electromagnetic loop in the stator circuit are determined by semigraphical method according to the formulae. We determine the sum of the characteristic equation roots P_{i1} and P_{i2}

$$P_{i1} + P_{i2} = -(R_s L_r + R_r L_s), \quad (2.28)$$

Taking into account $K_{lr}=L_r/L\mu$; $K_{ls}=Ls/L\mu$; $K_{sr}=R_r/R_s$; $K_{sr}=P_{i1}P_{i2}L\mu^2$ $(K_{ls}K_{lr}-1)/Rs^2$ we obtain the formula for calculating the stator and rotor mutual inductance

$$L\mu = \frac{R_{SR}((D_a-1)P_{i1}+P_{i2}))}{K_{ls}P_{i1}P_{i2}(1+D_a)}. \quad (2.29)$$

If we know the stator and rotor leakage inductances, which determine the complete inductances taking account of the stator and rotor mutual inductance

$$L_S = L_\mu + L_{SK}, \quad (2.30)$$

$$L_r = L_\mu + L_{RK}, \quad (2.31)$$

we get the second version of the main inductance computation.

Let's introduce notations: $B = R_s + R_s K_{RS},$ $C = R_S(L_{RK} + K_{RS}L_{SK}).$

Having converted the equation into the equation

$$\Delta P(L_S L_r - L_m^2) = \sqrt{(R_s L_r + R_r L_s)^2 + 4R_s R_r L_m^2}, \quad (2.32)$$

we obtain the solution in the form:

$$L_{\mu 1,2} = -\frac{2BC - \Delta P(L_{SK} - L_{RK})}{2(B^2 + C^2 + 4R_S^2 L_{SK}K_{RS})} \pm$$

$$\pm \sqrt{\frac{(2BC - \Delta P(L_{SK}-L_{RK}))^2}{4(B^2+C^2+4R_S^2 L_{SK}K_{RS})^2} + \frac{4\Delta P L_{SK}L_{RK}}{(B^2+C^2+4R_S^2 L_{SK}K_{RS})^2}}. \quad (2.33)$$

The procedure for calculating the definition (improved precision) of the coefficient Kls, represented by the structural scheme in Fig. 2.6, is the following

Operator 2 provides the input of the data array on current $Ia_1...Ia_{ktu}$, which in obtained in an experimental way, and pre-calculated values of Rs, Rr, Kls, Klr, P_{i1}, P_{i2}. Operator 3 calculates the value of ΔI_0 by means of numerical integration of the experimental current data array [25].
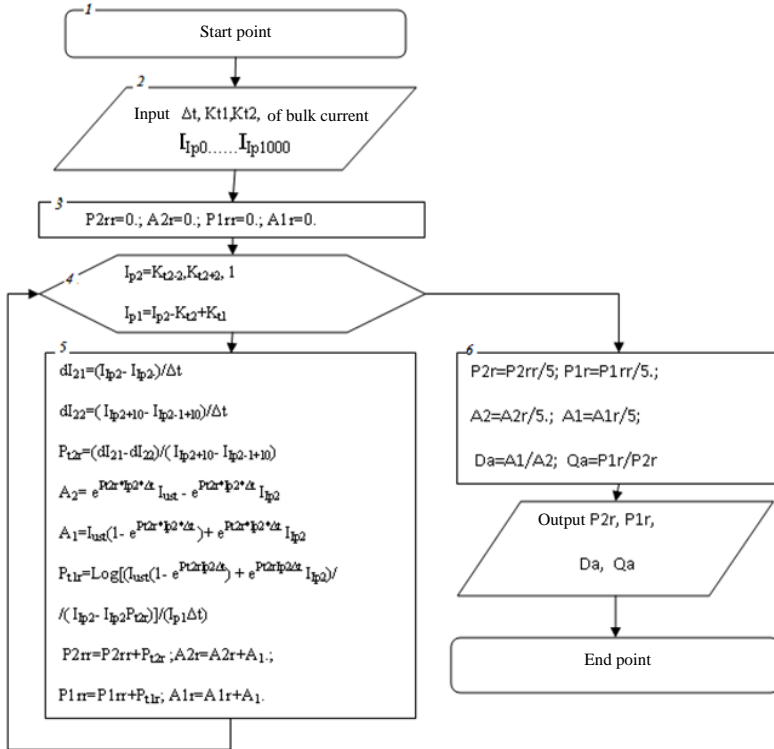

Figure 2.5 – Algorithm of determining the values of the characteristic equation roots P_{i1} and P_{i2} of the electromagnetic loop of the stator circuit in the TIM stator using transcendental functions

Operator 4 changes the design coefficient Kls by the value. Operator 5 performs computation of the stator and rotor windings' inductances, which are used during solving the system of differential equations. Operator 6 integrate numerically the system solution - the data array of computated current and its value ΔI_1 is compared with ΔI_0. Logical operator 7 verifies the condition $\Delta I_0 < \Delta I_1$.
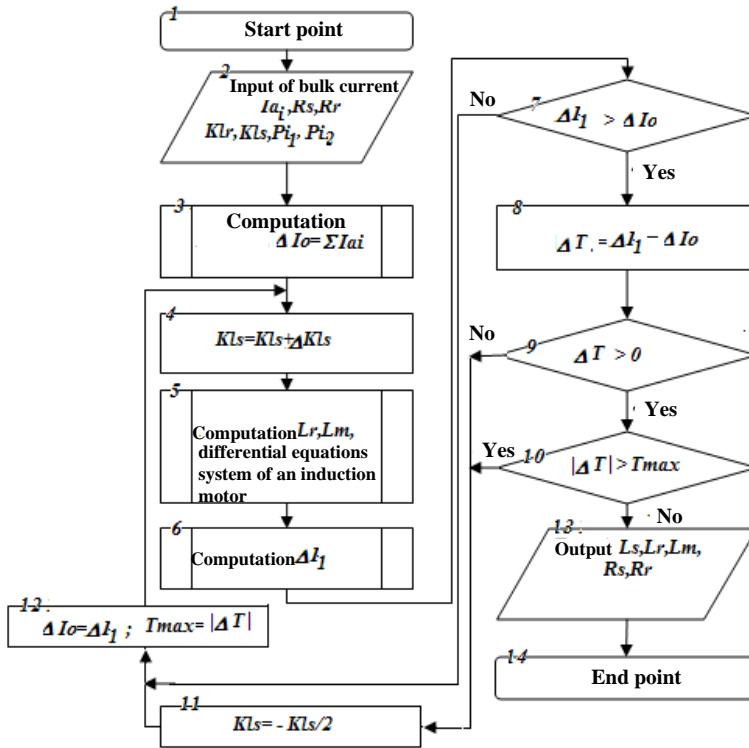
Figure 2.6 – Structural diagram of algorithm for computation of inductive
resistances of a traction induction motor

If the condition is satisfied, the difference ΔT and the sign between the output and the computed integral values are determined (operators 8,9,10). In the case of the sign ΔT changing, the sign of the coefficient ΔKls changes to the opposite, and ΔKls is divided by 2. The process continues until the condition $\Delta T > \Delta T_{max}$ is met, where ΔT_{max}– specified minimum error value [26].

Initial parameters of an induction motor having 55kW capacity, calculated as per catalogued data:

Rs= 6.7000002E-02 Ohm; Rr= 3.2000002E-02 Ohm; Ls= 2.9400000E-02 H; Lr= 2.9700000E-02 H; $L\mu$= 2.8700000E-02 H; Jm=

12.20000 kgm^2; M_T=44.00000 Nm; Lsk= 0.0700000E-2; Lrk= 0.100000E-2; Klr= 1.034843; Kls= 1.024390; Ksr= 0.4776120.

The data sheets of the transient process according to the stator current in the induction motor during its connection to the constant voltage in case of *Kls* variation by the value equal to –*ΔKls*, and the process computed according to the catalogued data are shown in Fig. 2.7. The initial approximation step *ΔKls*=0,016, initial approximation *Kls*=1,17. Start time of the transient process t_0=0.0, end time – t_k = 8.000000 s.

The value of parameter *Kls* in *N* - th approximation:

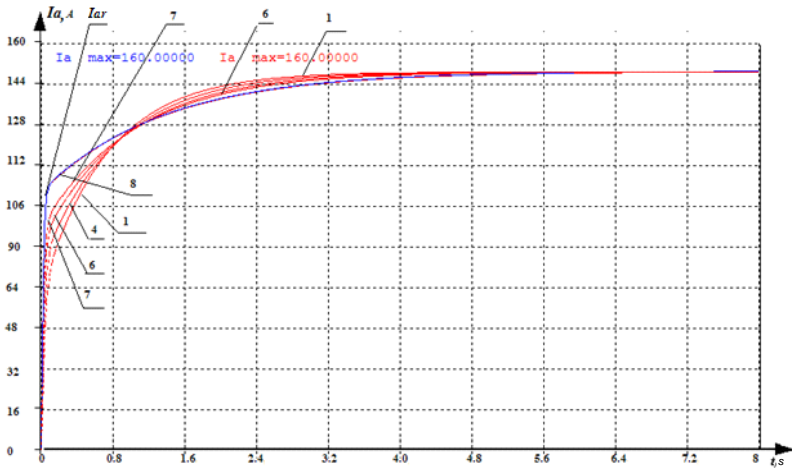|	
Kls= 1.170000	N approx = 0;
Kls= 1.154000	N approx = 1;
Kls= 1.138000	N approx = 2;
Kls= 1.122000	N approx= 3;
Kls= 1.106000	N approx = 4;
Kls= 1.090000	N approx = 5;
Kls= 1.074000	N approx = 6;
Kls= 1.058000	N approx = 7;

Figure 2.7 – Data sheets showing variations of the current of a stator with
two-phase connection to the constant voltage in the process of
determination of optimal *Kls*

The identifiable TIM parameters are computed according to measured currents in the transient processes during the starting and steady operating modes: *Rs*=0.067088157 Ohm; *Rr*=0.030110942 Ohm;

Ls=0.029435014H; *Lr*=0.027862389H; *Lm*= 0.027821375H; *Jm*= 11.59000 kgm^2; *Mng*= 48.40000 Nm; *Klr*=1.001474; *Kls*=1.058000; *Ksr*=0.4488265.

The errors between the initial and design values computed and determined by the electric parameters, which are obtained with the help of the proposed algorithm are:

Δ Rs=0.0 67088157- 0.06700000=0.000088157 Ohm; *Δ Rs*=0.13%

Δ Rs= 0.030110942-0.030000000=0.000110942 Ohm; *Δ Rs*=0.36%

Δ Rs= 0.029435010-0.029400000=0.000350100 Ohm; *Δ Rs*=1,20%

Δ Rs= 0.028862389-0.029700000=0.001837611 Ohm; *Δ Rs*=2.60%

Δ Lμ=0.027821375-0. 02870000=0.000878625 Ohm; *Δ Lμ*=3.06%

ΔKlr=1.034843-1.0014740=0.033369 s; *ΔKlr*= 3.20%

ΔKlr=1.024390-1.0580000=0.033610 s; *ΔKlr*= 3.176%

ΔKsr=0.477612-0.4488265=0.028786 s; *ΔKsr*=6.416%

2.1.4 Determination of mechanical parameters of a traction induction motor and mechanism

The computation of transient processes for determining the torque *Mg* on the motor shaft is performed with the help of a data array on current at a constant rotation speed. Approximation step *Δ Mg*= 9.36 Nm, initial approximation *Mg* =9.68 Nm. The algorithm for determining the load torque and the program for its implementation is the same as in the previous case (Fig. 2.8).

It allows us to unify the algorithmic, software and technical support of the complex of identification and diagnostics of an induction motor parameters. The difference between algorithms, in which the way of determination of the load torque and the moment of inertia differ from the one given in Figure 2.6, is that in block 4 the approximation by either the load torque or by the moment of inertia is formed. The load torque is defined the first, and its value is transmitted with the data to identify the moment of inertia. This is due to the fact that the process of starting will be affected by the load torque and the moment of inertia with the same voltage supply. The load torque is defined by the data of a steady mode, that is, at a constant rotor speed, when the moment of inertia does not affect the current transient process [27].
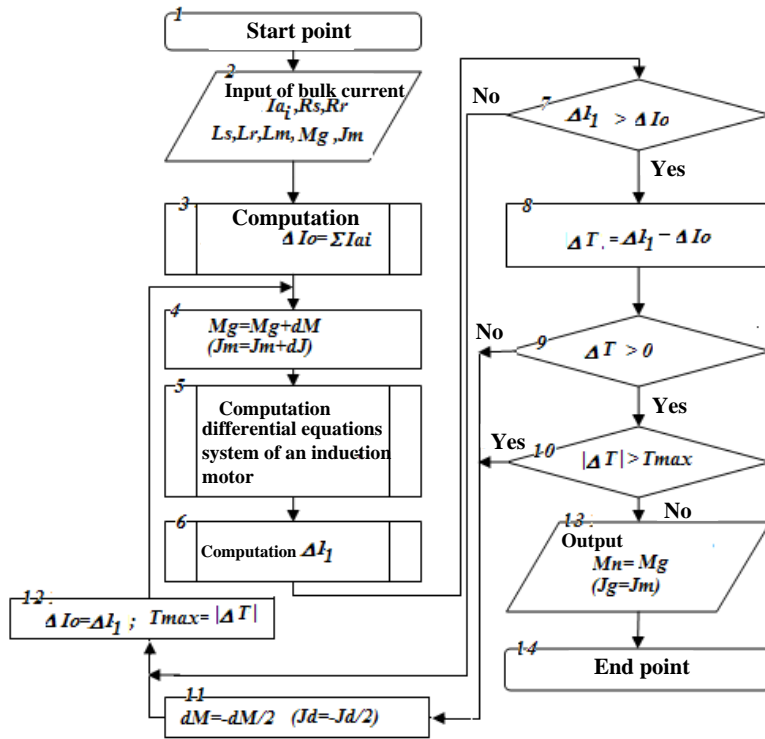
Figure 2.8 – Algorithm for determining the load torque of a traction
induction motor

The data sheets of the calculated and reference transient process
(by current) during determination of the load torque on the motor shaft are
shown in Fig. 2.9.

The value of the load torque in *N*-th approximation:

Mg=   9.68000 Nm; *N approx* = 0;

Mg= 19.36000 Nm; *N approx* =1;

Mg= 29.04000 Nm; *N approx* = 2;

Mg=38.72000 Nm; *N approx* = 3;

Mg=48.40000 Nm; *N approx* = 4.
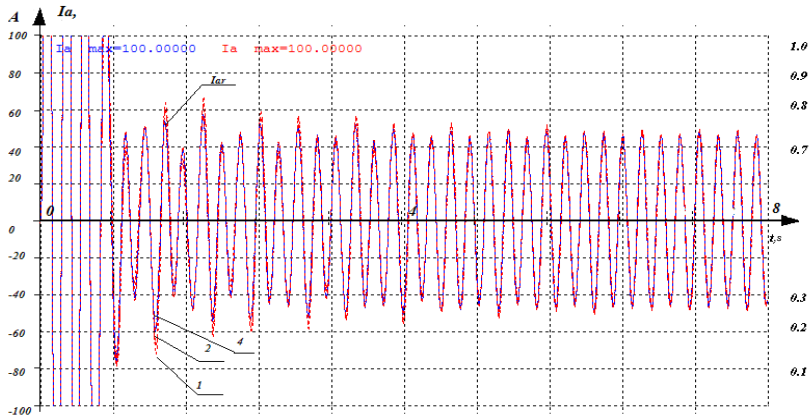
Figure 2.9 – Data sheets of a stator current variation during starting and steady motion, for determination of the torque on the motor shaft

The algorithm for determining the total inertia moment applied to the rotor shaft of TIM and the mechanism is shown in Figure 2.10. Determination of the total inertia moment is carried out by comparing the data of the transient process by the stator current in the starting mode, if the amplitude and the frequency of the supply voltage are known. The instantaneous values of supply voltage can be set by computation or by measured voltage data. In the Fig. 2.11 shows the data sheets of the rotation speed transient process when approaching by the moment of inertia [28].

Therein, the error in the difference between measured and computed transient processes is calculated by the values of the phase current of the stator.

The identification of the moment of inertia was performed under the following conditions: Approximation step $\Delta \ Jm=$ 1.22 kgm^2; initial approximation $Jm=$27.45kgm^2.
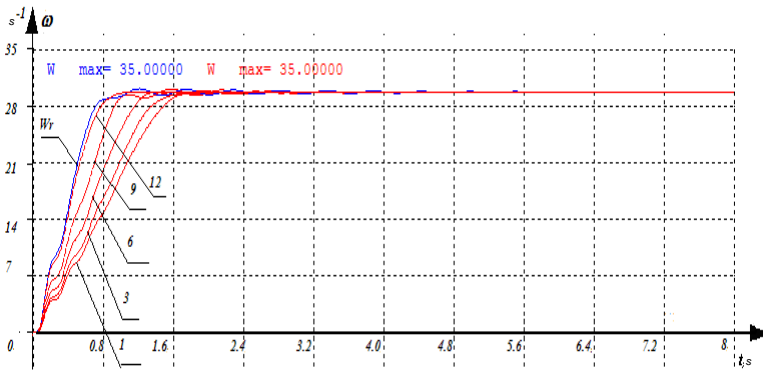
Figure 2.11 – Data sheets of the rotation speed while determining the total
inertia moment on the TIM shaft of an electric locomotive

The value of the moment of inertia in *N*-th approximation:
Jm= 27.45000 kgm^2, *Nprb*=0;
Jm= 26.23000 kgm^2, *Nprb*=1;
Jm= 25.01000 kgm^2, *Nprb*=2;
Jm= 23.79000 kgm^2, *Nprb*=3;
Jm= 22.57000 kgm^2, *Nprb*=4;
Jm= 21.35000 kgm^2, *Nprb*=5;
Jm= 20.13000 kgm^2, *Nprb*=6;
Jm= 18.91000 kgm^2, *Nprb*=7;
Jm= 17.69000 kgm^2, *Nprb*=8;
Jm= 16.47000 kgm^2, *Nprb*=9;
Jm= 15.25000 kgm^2, *Nprb*=10;
Jm= 14.03000 kgm^2, *Nprb*=11;
Jm= 12.81000 kgm^2, *Nprb*=12;
Jm= 11.59000 kgm^2, *Nprb*=13.
The specific feature of determining the mechanical parameters is
their variation in the course of operation, since the load torque on the motor
shaft and the moment of inertia are proportional to the loading of the
electric locomotive.
The parameters of the TIM under study are calculated on the basis
of currents measured in transient processes during starting as well as in
steady operating modes: Jm=11.59000 kgm^2; *Mng*= 48.40000 Nm;
Design values of electromechanical time constants of the TIM
under study are: *Tω1*=0.01794854 s;*Tω2*= 0.2464656 s.

The error between the actual values of the inertia moment, the load torque, and the computed approximate values of the load torque and the computed inertia moment is defined by approximation and comprises:

$$O_{шм} = 100\frac{|\Delta J_m|}{J_m} = 100\frac{|48,4 - 44,0|}{44,0} = 10\%$$

$$O_{шн} = 100\frac{|\Delta M_{gm}|}{M g_m} = 10\%$$

For TIM with a proposed design capacity of 55 kW with a reduced iron permeability, the actual parameters have the following values: Rs=6.7000002E-02 Ohm; Rr=3.2000002E-02 Ohm; Ls=2.5700001E-02 H; Lr=2.6000001E-02 H; $L\mu$=2.5000000E-02 H; Jm=12.2 kgm^2; Mxx= 44.0 Nm; Klr=1.034843; Kls=1.024390; Ksr=0.4776120. Computation time – 4 s.

Data sheet of transient processes according to the stator current, the induction motor torque, and the rotation speed during across-the-line starting of the motor on the reduced voltage, calculated with the help of the proposed mathematical model, are shown in Fig. 2.12 - 4.14.

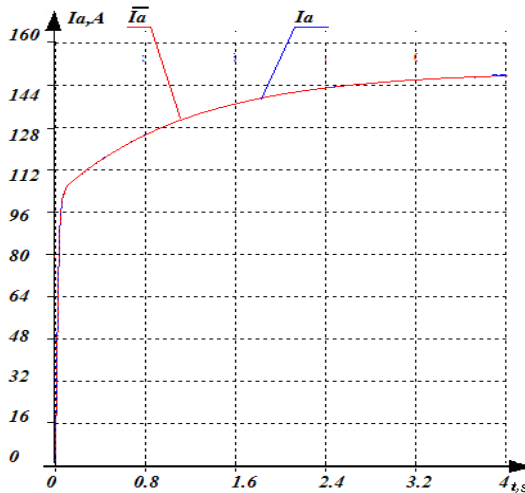Figure 2.12 – Data sheet of the transient process according to the current of TIM stator

(L_μ=0.025 H) during connection to the constant voltage
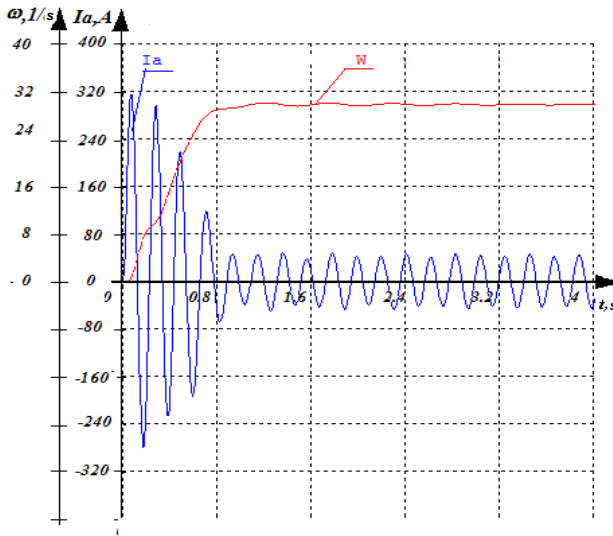
Figure 2.13 – Data sheets of the transient process according to the current
and TIM rotation speed (L_μ=0.025 H) during the starting
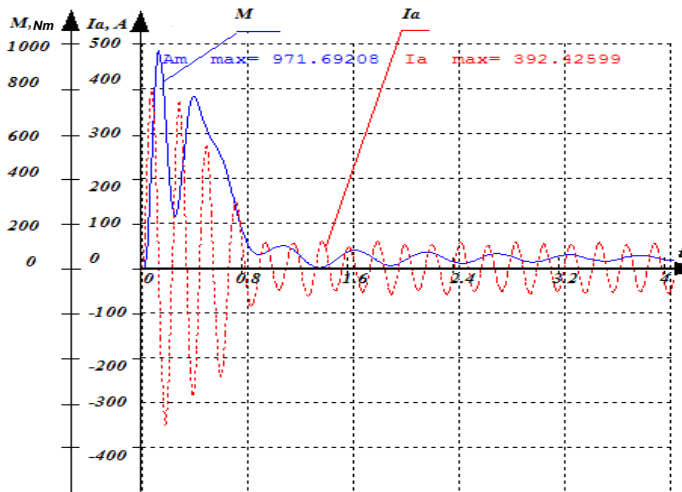
Figure 2.14 – Data sheets of the transient process according to the TIM
torque and its stator current ($L\mu$=0.025 H) during the starting

During the process of identifying the main magnetic flux density $L\mu$, the intermediate results of the values of the computed and actual processes (Fig. 2.15) are provided for the following N approximations:

$L\mu=$ 2.6724499E-02 H; $N\ approx=0$;
$L\mu=$ 2.6224500E-02 H; $N\ approx=1$;
$L\mu=$ 2.5724500E-02 H; $N\ approx=2$;
$L\mu=$ 2.5224501E-02 H; $N\ approx=4$;
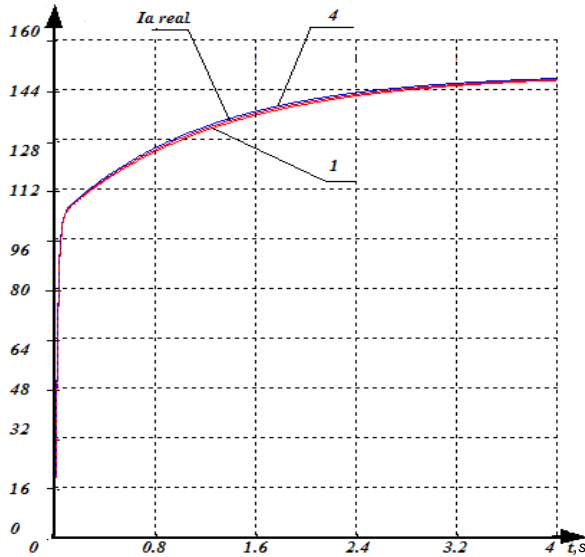
Figure 2.15 – Computed and reference data sheets of the TIM stator current (L_μ=0,025 H) during connection to the constant voltage

Analysis of the results presented in Fig. 2.16 shows that determination of the values of electromagnetic time constants with the help of the proposed algorithm is performed with minor deviations from real values and assures more precise evaluation of the main magnetic inductance (magnetic flux density) value L_μ with high precision – in four approximations. Computation error is ΔL_μ=0.8% [28].

Determination of the load on the traction motor was performed by the method of successive approximation. Reference load – Mn=44 Nm. The approximation step is assumed to be equal to 5% of the rated torque of the traction induction motor.

Computation results for the following approximations:

Mg=0.000000Nm; $Napprox$=0;

Mg=8.000000Nm; $Napprox$=1;
Mg=16.00000Nm; $Napprox$=2;
Mg=24.00000Nm; $Napprox$=4;
Mg=32.00000Nm; $Napprox$=6;
Mg=40.00000Nm; $Napprox$=8;
Mg=48.00000Nm; $Napprox$=9;

are represented in the form of three data sheets of the reference stator current *Iareal*, the first and last 9th approximation, are shown in Fig. 2.16.

Load torque error comprises 10%.

Determination of the inertia moment of an electric locomotive Jm, applied to a TIM shaft, at five approximations with a known or calculated load torque Jn=12 kgm^2 is shown in Fig. 2.17.

Jm=22.40000 kgm^2; $Napprox$=0;
Jm=20.40000 kgm^2; $Napprox$=1;
Jm=18.40000 kgm^2; $Napprox$=2;
Jm=16.40000 kgm^2; $Napprox$=3;
Jm=14.40000 kgm^2; $Napprox$=4;
Jm=12.40000 kgm^2; $Napprox$= 5.
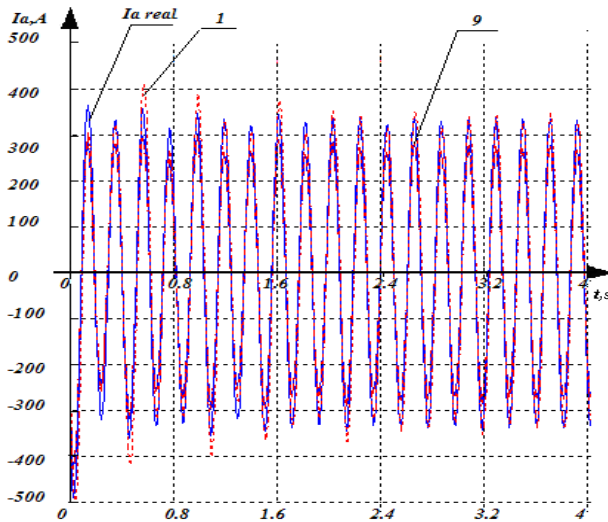
Figure 2.16 – Data sheets of calculations of the actual loading on the shaft of the traction induction motor, of the first and last approximation
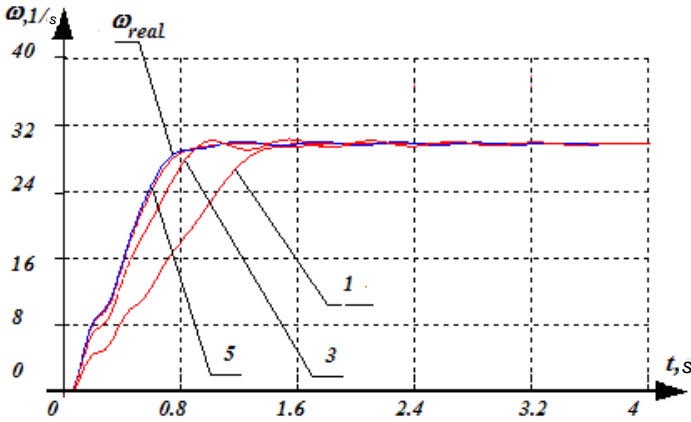
Figure 2.17 – Graphs of rotation speed transient processes at five approximations to $\omega real$ during determining the moment of inertia

As a result of the calculations, we obtained the following values of parameters of the induction motor under consideration: Rs=6.7084692E-02 Ohm;

Rr=3.2040451E-02 Ohm; Ls=2.5930787E-02 H; Lr=2.6233481E-02 H; $L\mu$=2.5224501E-02 H; Jm=12.40000 kgm^2; Mg=48.0 Nm; with known design coefficients of an electric motor: Klr=1.040000; Kls=1.028000; Ksr= 0.4776120.

Reference parameters of a traction induction motor (TIM): Rs=6.7000002E-02 Ohm; Rr=3.2000002E-02 Ohm; Ls=2.5700001E-02H; Lr=2.6000001E-02H; $L\mu$ =2.500000E-02; Jm=12.20000 kgm^2; Mxx=44.00000 Nm, Klr= 1.034843; Kls= 1.024390; Ksr=0.4776120 [29].

Variance between the calculated and reference parameters amount to: ΔRs=0.12%;ΔRr=0.12%; $\Delta L\mu$=0.08%; ΔLs=0.08%; ΔLr=0.08%.

Figs. 2.18 – 2.20 data sheets of TIM calculated and actual transient processes approaching the design parameters of a motor with 55 kW capacity and mutual inductance $L\mu$=0.02 H. Mutual inductance differs from the catalogued value by 24% and amounts to $L\mu$=0.0287 H. The parameters of the motor under consideration are: Rs=6.7000002E-02 Ohm; Rr=3.20E-02ОмOhm; Ls=2.0700000E-02H; Lr=2.1000000E-02H; Lm=2.0000000E-02 H; Jm= 12.20000 kgm^2; Mxx=44.00000 Nm. Design coefficients: Klr=1.034843; Kls=1.024390; Ksr=0.4776120, with time constants: $Ti1$=

1.7100694E-02s; *Ti2=*   1.349831 s; *Tw1*=1.8061439E-02 s; *Tw2*= 0.2596448 s.

Data sheets of the stator current of the motor connected to the constant voltage (Fig. 2.18), show that identification of the stator and rotor mutual inductance is achieved in 5 approximations [30-40].
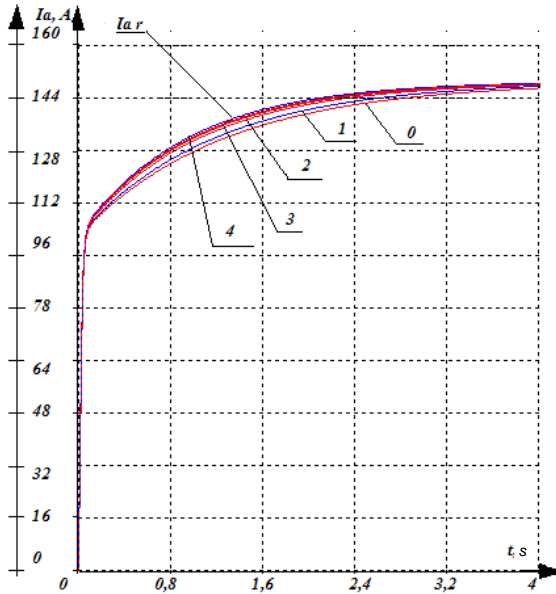
Figure 2.18 – Data sheets of the the stator current of the motor when approaching the value L_μ=0.02

Identification of the torque on the motor shaft is defined by the ninth approximation (Fig. 2.19).

Reference parameters: *Rs*=6.7000002E-02 Ohm; *Rr*=3.2000002E-02 Ohm; *Ls*=2.0700000E-02 H; *Lr*=2.1000000E-02 H; *Lμ*=2.0000000E-02 H; *Jm*=12.0; M*xx*=44.0.; *Klr*=1.034843; *Kls*= 1.024390; *Ksr*=0.4776120.
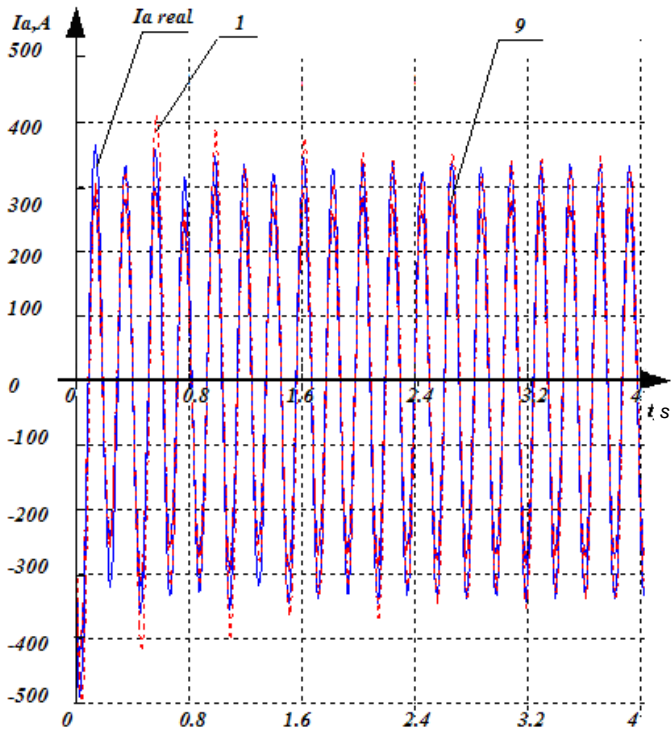
Figure 2.19 – Data sheets of the stator current of the traction induction motor with steady rotation speed

Determination of the moment of inertia *Jm* is performed by the sixth approximation (Fig.2.20).
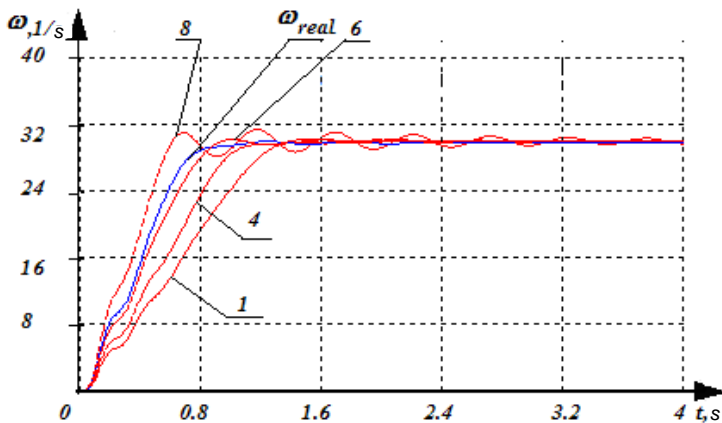
Figure 2.20 – Data sheets of the rotation speed transient processes
approaching in the inertia moment with the stator and rotor mutual
inductance is $L_\mu=0,02$H

Calculated values: $Rs=6.7083709$E-02 Ohm; $Rr=3.2039981$E-02
Ohm; $Ls=2.0712448$E-02 H; $Lr=2.1012625$E-02 H; $L\mu=2.0112025$E-02 H;
$Jm=12.4$; $Mng=48.0$; $Klr=1.050000$; $Kls=1.035000$; $Ksr=0.4776120$ [38].
Computation   error: $\Delta Rs=0.12\%$; $\Delta Rr=0.12\%$;
$\Delta L\mu=0.08\%$; $\Delta Ls=0.05\%$; $\Delta Lr=0.04\%$.

2.2 Determination of parameters of electric drive systems with synchronous motors

Synchronous motors for general industrial use are most complex in
describing the processes occurring in them in both static and dynamic
modes as compared to other types of electrical machines - asynchronous
ones and d.c. machines. To the same extent, the present methods of
determining the parameters of machines are complicated and laborious; the
operational properties of motors, including the starting characteristics,
depend on these parameters. The task of parameters determination has
specific features depending on the design of the stator and rotor systems, the
levels of the supply voltage and the excitation current. The determination of
parameters and characteristics is significantly complicated in the case of the
salient-pole machines, the presence of starting and damper windings on the
rotor [15]. In this regard, methods for determining the parameters of the
windings, generally accepted for induction motors, typically come out to be

unacceptable. It should be pointed out that the values of parameters of an electrical machine depend on the relative position of the stator and rotor windings. This property, however, receives little use in the parameters diagnostics as a positive property. Analysis of literature sources shows that when determining the parameters of electrical machines, we can state the lack of efficient use of open-phase modes (a motor powered via two phases, etc.), as well as polyharmonic power systems, circuits and power systems with resonant circuits in the stator and rotor. Bearing in mind these circumstances, we have a need to fill in the gaps and make operations of determining the synchronous machines parameters as trivial as the ones applied for asynchronous machines.

The parameters to be determined while testing synchronous motors after repair are as follows:

- the parameters of the resistances and reactances of the stator and rotor, moreover, in case of the stator these parameters must be determined for each phase separately. The stator resistances must be determined by the ammeter-voltmeter method with a constant operational current;

- iron losses of a synchronous motor. The process of their determination has the following specific features: at a synchronous speed, losses occur only in stator iron, which is magnetized with the mains frequency regardless of the value of excitation current.

One should determine the dependence of losses on power and excitation parameters in the following order. The synchronous motor without load (in compensator mode) is powered by the mains; its rotor rotates with a synchronous speed. In the experiment, for a number of values of the excitation current, the values of the voltage, stator current, and the components of the circuit power (active and reactive) are fixed [12] The obtained dependences of the stator current, the extent of stator copper losses, the stator iron losses, and the mechanical losses on the excitation current are shown in Fig. 2.20. The following values are noted here: ΔP_M - stator copper losses; ΔP_c - stator iron losses; ΔP_{meh} - mechanical losses of a synchronous motor; I_b - excitation current.
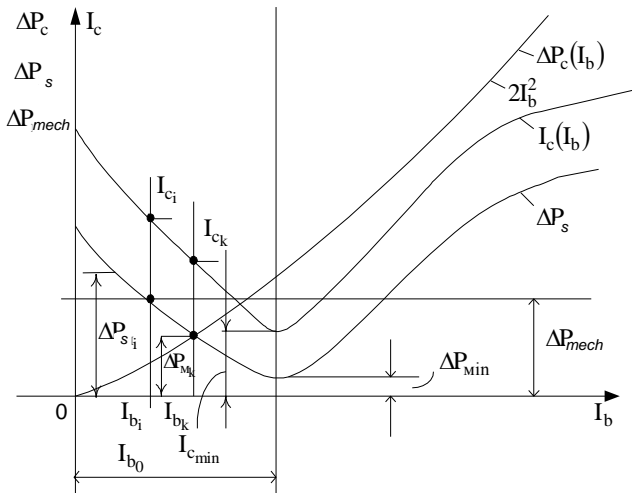
Figure 2.20 – Dependences of the stator current and the components of the motor total losses.

Determination of iron losses is not included in the test procedures stipulated by the standards. However, in the case of post-repair tests, this procedure should be considered mandatory due to the fact that iron is a structural material that significantly changes its characteristics during pre-repair procedures and the repair itself:

– starting, maximum and pull-in torque of the synchronous motor - as basic electromechanical properties;

– compensating ability of machines at different levels of supply voltage and excitation current. These parameters are also important after the completion of repair procedures.

Most of these parameters can be determined in the no-load test, as well as after obtaining the direct-axis and quadrature axis motor reactances.

Dependences for the components of power losses are defined as:

$$\Delta P_s = I_{c_a}^2 \cdot R_a + I_{c_b}^2 \cdot R_b + I_{c_c}^2 \cdot R_c; \ \Delta P_{mech} = M_{xx} \cdot \omega_0; \lim_{\delta x \to 0}$$

$$\Delta P_c = C \cdot \Phi^2 \approx \alpha \cdot I_b^2.$$

Mains power:

$$P_{c_i} = \Delta P_{s_i} + \Delta P_{mech_i} + \Delta P_{c_i}.$$

It corresponds to the following dependences for two values of excitation currents:

$$P_{c_i} = \sum_{a,b,c} \Delta P_{s_i} + \Delta P_{mech} + \alpha \cdot I_{b_i}^2;$$

$$P_{c_k} = \sum_{a,b,c} \Delta P_{s_k} + \Delta P_{mech} + \alpha \cdot I_{b_k}^2.$$

(2.34)

For two values of excitation currents I_{b_i} and I_{b_k} the corresponding values of the losses' components are shown. Their values forming the system, allow us to obtain the unknown α and P_{mech}:

$$\alpha = \frac{P_{c_i} - P_{c_k} - \sum\limits_{a,b,c} \Delta P_{s_i} + \sum\limits_{a,b,c} \Delta P_{s_k}}{I_{bi}^2 - I_{b_k}^2}$$

(2.35)

The case under consideration seems to be the simplest, since a quadratic dependence of the iron losses on the excitation current is proposed. The practical part of the question is somewhat more complicated: firstly, the dependence of iron losses can be different from quadratic one; secondly, the dependence can vary depending on the degree of iron saturation. Taking into consideration this fact, we may need to determine the normalized functional dependence of the losses on the excitation current with greater precision.

The problem can be solved in various ways. One of them is to separate mechanical losses from the sum of total losses. To do this, we must formulate a dependence:

$$P_{c_i} - \sum_{a,b,c} \Delta P_{s_i} = \Delta P_{mech} + \alpha I_b^\beta = f\left(\alpha, \beta\right)$$

(2.36)

For this purpose, the circuit power is measured P_c at several points, the losses in the stator windings are determined and the dependence is obtained $f(\alpha, \beta)$ as the difference between the total power and copper losses. An approximate dependence of the required function is shown in Fig. 2.21.

The obtained dependence can be approximated by one of the known methods in the form of a power polynomial.

$$f(\alpha, \beta) = a_1 \cdot I_b + a_2 I_b^2 + a_3 I_b^3 = \alpha \cdot I_b^\beta$$

(2.37)

From the dependence obtained, we can determine the coefficients α and β:

$$\alpha = I_1\left(a_1 + a_2 I_1 + a_3 I_1^2\right)\exp\left[\ln(I_1) - \frac{\ln\left[\dfrac{I_1\left(a_1 + a_2 I_1 + a_3 I_1^2\right)}{I_2\left(a_1 + a_2 I_1 + a_3 I_1^2\right)}\right]}{\ln\left(\dfrac{I_2}{I_1}\right)}\right];$$

$$\beta = -\frac{\ln\left[\dfrac{I_1\left(a_1 + a_2 I_1 + a_3 I_1^2\right)}{I_2\left(a_1 + a_2 I_1 + a_3 I_1^2\right)}\right]}{\ln\left(\dfrac{I_2}{I_1}\right)}.$$

The analysis performed shows relative simplicity of the operations for separating losses in a synchronous motor during its testing. It should be noted that the approach is based on the easily obtainable dependence of the stator current on the excitation current. It signifies greater possibilities for determination of losses and their correlations of different orders.
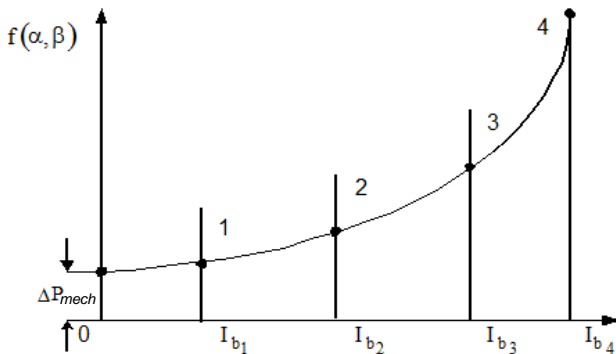
Figure 2.21 – Approximate dependence of the required function

The selection of particular circuits for testing synchronous motors without mechanical load should be made taking into account the obvious fact: circuit design solutions for synchronous motors should be the same (or sufficiently close) to the ones intended for asynchronous machines. A number of scientific works proved that the best preferable option for asynchronous motors is the stator circuit supply design with a symmetrical or asymmetric thyristor voltage controller [34]. A symmetrical thyristor voltage controller (TVC) means a three-phase regulator with symmetrical control. An asymmetric TVC implies various options of asymmetrical control, including stator windings' single-phase power supply in a star -

"zero" circuit,in a star - separate neutral circuit, and in delta circuit. The specifics of the application of such circuit design solutions are significant, they are caused by the synchronous machine complexity. This complexity is due to the asymmetry of the rotor windings, which are generally known to include a rotor field winding, a symmetrical or asymmetrical starting winding, a symmetrical or asymmetrical damper winding. The asymmetry parameters in the theory of electric machines are estimated by introducing two orthogonal axes – the longitudinal/direct d-axis and the transversal/quadrature q-axis, with the direct axis coinciding with the axis of the field winding, whereas the quadrature one is at an angle $\pi/2$. The field winding, depending on the circuit design, can be powered from d.c. power source, a.c. circuit, or can be open. The design circuit of a synchronous motor and the known windings is shown. In figure the following notations are introduced:

X_1 - stator leakage resistance; x_{ad} - direct-axis resistance to mutual inductance;

R_b - field winding resistance;

x_{fd} - field winding inductive reactance;

x_{kd} - direct-axis inductive reactance of shorted loops;

R_{kd} - short-circuited windings (staring and direct-axis damper one) resistance;

R_{kq} - quadrature-axis resistance of short-circuited windings;

x_{kq} - quadrature-axis inductive reactance.

Resistances $R_{\mu d}$ and $R_{\mu q}$ - are equivalent to direct-axis and quadrature-axis iron losses. In the steady state, the shorted loops have no impact on the processes passing in the motor. Due to this, the above equivalent circuits in such modes can be significantly simplified (loops $x_{fd}, R_b; x_{kq}, R_{kq}; x_{kd}, R_{kd}$ should be excluded of the circuit) [32].

Direct-axis and quadrature-axis equivalent circuits of a synchronous motor are shown [39, 42].

a)   b)
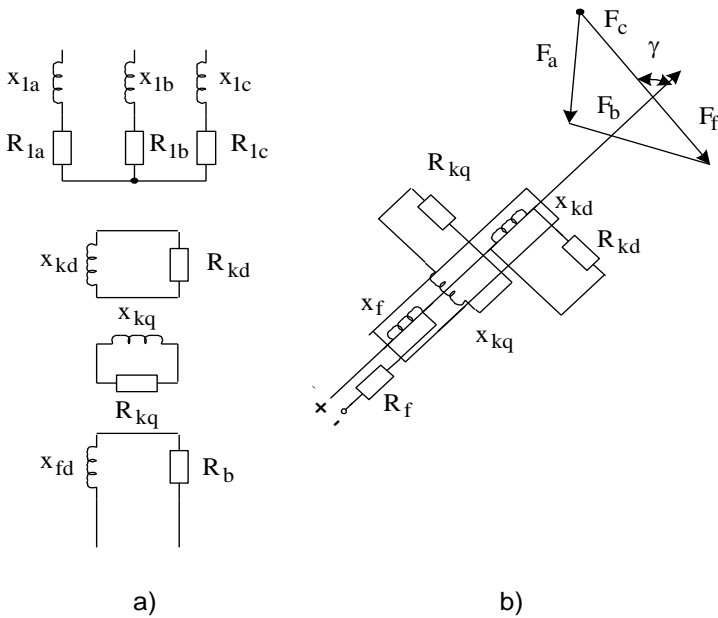
Figure 2.22 – A design circuit of a synchronous motor' stator and rotor windings:
Winding circuit; MMF relative position

When the rotor is locked, the electromagnetic system of a synchronous motor is an equivalent of a transformer with primary, secondary windings, and with shorted loops. Their relative position determines the magnitude and sign of the electromotive force (EMF) induced in the system of the windings, when one of them is excited.

a)   b)
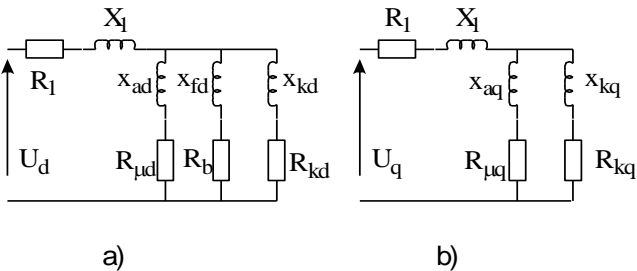
Figure 2.23 – Direct-axis (a) and quadrature-axis (b) equivalent circuits of a synchronous motor.

As follows from Fig. 2.22, b, depending on the relative position of the stator field and the rotor windings, we can obtain various magnetic-field couplings. Thus, if the stator MMF F_Σ and the field winding MMF are located at an angle $\gamma = \pi/2$, in case of alternating MMF F_Σ EMF will be induced only in the quadrature winding. If the angle $\gamma = 0$, EMF will be induced in the field winding and in the longitudinal short-circuited winding. We will obtain different modes with the discontinued winding R_f or a dead shorted winding or the one shorted to (resistance, inductive reactance, capacitive reactance). A change of the angle γ can be achieved by changing the rotor position (smoothly) or discretely in various combinations of stator phases connection to alternating voltage. Quite peculiar modes are obtained by applying an alternating voltage to the field winding: EMF will be induced in the longitudinal short-circuited winding and in the stator windings (various in magnitude in phases, depending on the relative position of the field windings and the corresponding phase windings). During experiments the stator windings can be open or closed. It means that there exist great opportunities to create various test modes by changing the relative position of the stator and rotor windings, as well as by applying a test voltage to the stator windings or to the field winding. The test voltage means the level and harmonic composition of the voltage, which allow us to obtain the expected diagnostic signs. The voltage can be sine-wave, alternating, constant, or polyharmonic. This issue deserves special attention, since its solution by various methods of implementation allows us to obtain different volumes of initial data, i.e. diagnostic signs [38].

The schematic 'a' shows all the windings included in the equivalent circuit. In this case, the rotor winding can be shorted to resistance R_∂ or operate during the experiment without current load (switch B1 is open). By the voltage induced at the output of the field winding, we can judge the relative position of the equivalent magnetic stator system. Thus, if the primary windings *a* and *b* are connected through the thyristor controllers T_a and T_b, and at the output of the field winding we get a voltage equal to zero, then the excitation winding is located at an angle $\pi/2$ to the direction of the total MDS of the winding system of the phases 'a' and 'b' of the stator.

It means that in the given position EMF is induced and the current passes only in the short-circuited winding of the rotor quadrature axis. It corresponds to the equivalent circuit (Fig. 2.23 b), which includes mutual inductance loop with resistances x_{aq} and $R_{\mu q}$. resistance $R_{\mu q} = R_{\mu q0} \cdot \nu^\varphi$, where φ - nonzero index of power.

The analysis shows that the quadrature-axis equivalent circuit is identical to the corresponding circuit of an induction motor in slid $s = 1.0$ [94]. Justification of the concept of 'the possibility of branches separation', performed in [94,96], shows that inductive-active circuits connected in parallel can be separated, i.e. the parameters of these branches can be determined only if the index of power φ, which characterizes the dependence of losses on the frequency of the iron reversal magnetization, is nonzero one; i.e. when it is basically impossible to perform the operation of IM parameters determining using the method of polyharmonic power supply. In this case we can use a symmetrical single-phase thyristor voltage controller (TVC) or a frequency converter as a generator of polyharmonic power.

The capabilities of such a technical solution are well known [165, 166]. In case of the significant impact of limitations associated with decrease of information signals with increasing frequency (for high-order voltage harmonics), we can use the field-proven ways for such studies: by powering the windings from a frequency converter (thus obtaining a polyharmonic supply voltage) or by modulating the current delay angles (their variation in time) during the use of TVC, which leads to a significant increase in the number of harmonic amplitudes, or rather, the number of harmonics as well as their amplitudes.

Schematics in Fig. allow us to receive all possible connection circuits for the synchronous motor parameters determination. If we slightly change the winding system of phases 'a' and 'b' by altering the connection sequence of one of the windings (interchanging the input and the end of the windings), we will get the rotation of the resultant MMF to $\pi/2$. It is well illustrated in Fig. 2.24.
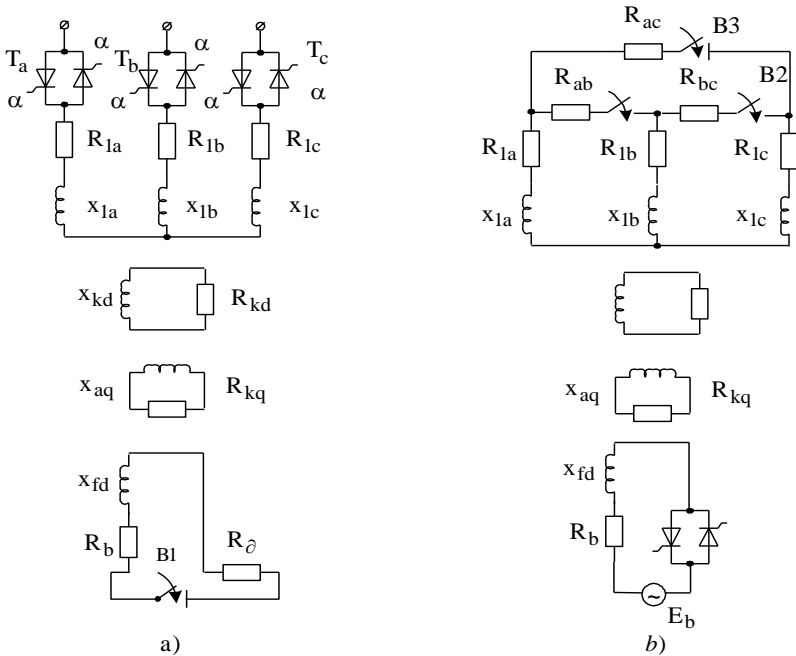
Figure 2.24 – Schematics of motor windings connection to determine the SM parameters:

a – primary power supply schematic; b – secondary power supply schematic

Thus, if the current in the phase 'a' passes from the input of the winding to its end, and in the winding 'b' - from the end to the input, the total MMF will correspond to the vector diagram in Fig. 2.26, a. If the voltage at the output of the field winding is zero, the direction $F_{ab\Sigma}$ coincides with the axis of the quadrature winding of the rotor. If you change the input and end of the winding 'b', the direction of MMF will coincide with the axis of the field winding. Thus, applying one technique of windings connection, we obtain the experiment in determining the quadrature-axis equivalent circuit, and applying the second technique - the direct-axis equivalent circuit. As unknown values we have the resistance of two stator windings $X_{1\Sigma}$; direct-axis resistance of mutual inductance x_{ad}, direct-axis iron resistance $R_{\mu d}$, parameters of a direct-axis shorted loopset x_{kd} and R_{kd}, and the corresponding quadrature-axis parameters.
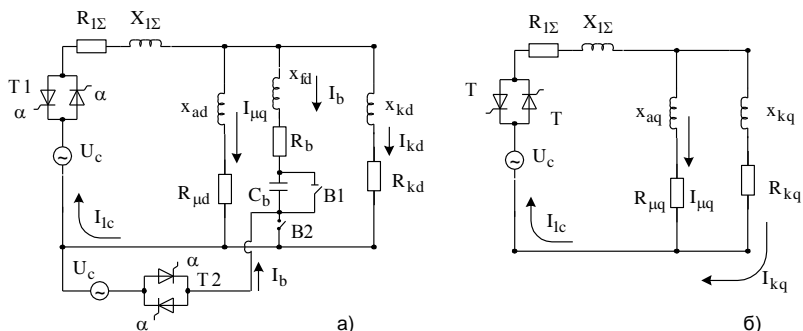
Figure 2.25 – Direct-axis (a) and quadrature-axis (b) equivalent circuits of a synchronous motor, powered by a thyristor controller.
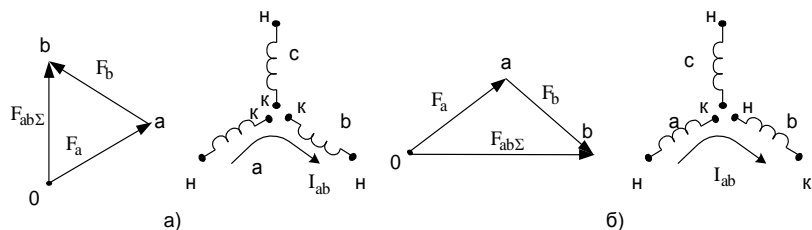
Figure 2.26 – Vector diagrams of two windings total MMF: a - traditional connection layout; b – winding b reverse connection.

It should be emphasized that the use of the analyzed method developed for induction motors is possible with such interpretations of the obtained results [40]:

− values $R_{\mu d}$ and $R_{\mu q}$, and the same values of total leakage reactance $X_{1\Sigma}$;

− use the dependencies for the direct and quadrature axes assuming the equality $R_{\mu d} + R_{\mu q} = R_{\mu c}$, previously determined in the no-load test. Simultaneous solution of two systems allows us to obtain the value $X_{1\Sigma}$ coincident with physical processes occurring during the diagnostics of a synchronous motor' parameters.

Such an interpretation, however, has a certain drawback, which probability and evaluation can be done when assessing the efficacy of working diagnostic models. It's a fair assumption to say that the losses obtained at synchronous speed include only the stator iron losses, because the rotor iron is not remagnetized at synchronous rotation speed. Therefore,

the iron losses defined according to the foregoing equivalent circuits, are based on the assumed closure the stator windings' flow through the gap with the rotor windings and the rotor iron. The above mentioned flow is of pulsating, alternating-sign nature, which determines to a greater extent one of the losses components – eddy current losses. In this regard, when evaluating iron losses, we should be be sufficiently careful, since the losses to be determined may differ from those occurring during the operation of an electrical machine at synchronous speed.

The power supply of the motor with polyharmonic voltage, which fully corresponds to the case under consideration, has its own specific features in the part of the energy processes occurring in the system. In the analysis, the equations of electrical equilibrium are compiled for each separate harmonic, independently of all the others [94, 166]. Equations of energy balance have their own particularities, namely: the energy balance equations for characteristic harmonics include distortion power components, which are present as the power from different frequency currents and voltages.

This issue requires attention at the stage of precision improvement of the computation results, since the neglect of the different frequency components is equivalent to exclusion of the distortion power from the analysis. Its value in relative units typically does not exceed 0.10; i.e. it is at the level of admissible errors of the electrical machines parameters diagnostics.

The analysis of circuit design solutions related to the process of synchronous motors parameters' determination with the influence of a primary polyharmonic stress shows that, having determined the parameters, we can solve the problem of determining the inductive reactance of the field winding as well. Let's use the direct-axis equivalent circuit of the machine (Fig. 2.25, a). The thyristor controller T2 is closed, the switches B1 and B2 are on that corresponds to the short-circuited field winding. Since the resistance R_b is known, and other parameters of the equivalent circuit are known or determined during the diagnostic procedure, then the required parameter is defined from the known values of the currents of harmonics x_{fd} [41].

As follows from the analysis, other connection layouts are possible, for example, inclusion of resistance, capacitive reactance, capacitive reactance-resistance in the rotor circuit. Thus, it is possible to obtain a system of four equations even in case of applying sine-wave voltage to the stator winding [42]:
- equations for the discontinued circuit of the field winding;
- equations for the shorted field winding;

- equations for capacitance connected;
- equations for capacitance connected to field terminals.

Until now, we have analyzed the diagnostic schemes for the parameters of synchronous motors with the primary impact (from the stator side). It is remarkable that while carrying out these experiments it is advisable to 'choose' the required position of the rotor, excluding from consideration the direct-axis machine parameters in one position of the rotor and quadrature-axis parameters of the machine in the other position of the rotor.

In the case of a secondary impact (from the rotor side), a quadrature-axis equivalent circuit is excluded from the analysis. It gives rise to the problem of creating the conditions under which the current in the field winding is at a level close to the rated one. The field winding is powered by the mains voltage source through the thyristor converter T2; the converter T1 must be closed. In the open state of T1, we get a more complicated version of simultaneous feeding of the stator and rotor windings from two sources of polyharmonic voltage. The capabilities of this circuit are not obvious; we can only state that it allows us to abandon the solution of the problem of selection the required rotor position when determining the quadrature-axis parameters. In other words, such type of an equivalent circuit basically allows us to combine both equivalent circuits in axes d and q.
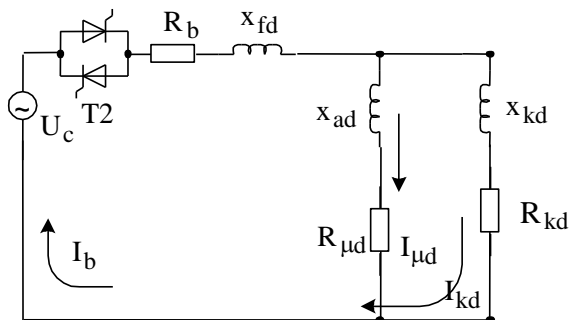
Figure 2.27 – SM equivalent circuit powered by field winding (stator windings are discontinued).

Analyzing the equivalent circuit with the T1 controller switched-off or closed, we obtain a simplified equivalent circuit (Figure 2.27).

The analysis of the equivalent circuit represented in the figure shows that it is also possible in this case to use the traditional approach to parameters determination developed by the authors for a squirrel cage

induction motor. It definitely shows the great advantage of the analyzed options over previously known ones. In our case, as it follows from the analysis, the same equipment is used to determine the parameters of synchronous motors and in testing and diagnostic schemes for asynchronous machines.

2.3 Parameters determination for thyristor converter-fed d.c. motors

Currently, the vast majority of electric drives are equipped with AC motors. But thyristor and transistor d.c. drives are applied in technical processes requiring high control performance parameters in static and dynamic modes and are still subject to extensive research [40-50] The development of the control theory gave rise to the creation of complex control systems using modal controllers, state observers, etc., the synthesis of which requires data on the parameters of the motor and the electric drive. The problem of knowing a motor parameters becomes particularly acute for machines after repair. In this case, the parameters of the windings will differ from the catalogued ones [44] and this will require the adjustment of the coefficients of the control systems. It should also be stated that during coefficients computation it the shape of the rectified voltage is assumed to be perfectly smoothed and the pulsations are neglected. In fact, the rectified voltage has a complicated shape, approaching a saw-tooth one with increasing delay angles, which must be taken into consideration for electric drives with a large control range.

Seeming simplicity of the d.c. machines diagnostics led to the emergence of a large number of technical solutions [17], which allow us to some extent to solve this problem, but are typically difficult for wide practical use. Therefore, in practice, simple approximate expressions are used to calculate the d.c. motor parameters according to the catalogued data [8]: for the armature circuit resistance - $R_{ac} = \alpha \dfrac{U_{\text{н}}}{I_{\text{н}}}\left(1 - \eta_{\text{н}}\right)$ and applying the Umanskiy formula for the armature circuit inductance - $L_{ac} = k \dfrac{U_{\text{н}}}{I_{\text{н}}} \dfrac{1}{p\omega_{\text{н}}}$. All this proves that the issue of creating an efficient, easily realizable, reliable method for determining the parameters of d.c. machines is still underway. This is especially true for direct current motors with the series-excited motorized wheels for heavy duty dump trucks, electric locomotives, city electric transport, etc.

Under the condition that the parameters of the electric machine are of quasistationary nature, the problem comes to an estimate of the

coefficients of the power balance equation written via the instantaneous values of the currents and voltages in the circuits of the electrical machine under consideration. It is of fundamental importance that the identification of the parameters of the electric machine is possible by the results of direct measurements using sensorsof electrical values (voltages and currents), which allows us to use the method for post-repair certification and monitoring of electrical machines state during their operation. Therefore, the choice of methods and procedures for identifying the parameters of the machine mainly depends on the field of application of the energy diagnostics system. Let's consider some aspects of the problem through the example of a separately excited d. c. motor (DCM SE).

2.3.1 Energy method of d.c. motor parameters determination

The fundamental concept of the method is that the parameters of the electrical machine under consideration are determined based on the condition of equality of the instantaneous values of the total power components (this total power being fed from the mains and dissipated on the elements, that form the physical entity of the electric machine (resistance, inductance, dynamic capacitance).

The equation of instantaneous power balance for a separately excited d. c. motor via electric variables can be written in the form:

$$U(t)I(t) = I^2(t)R_a + L_a I(t)\frac{dI(t)}{dt} + k\Phi(t)I(t)\int \frac{k\Phi(t)}{J}I(t)dt - I(t)\int \frac{I_C(t)}{J}k\Phi^2(t)d\,t, \quad (2.38)$$

where $U(t), I(t)$ - are the instantaneous values of the motor armature voltage and current respectively, $I_C(t)$ – is the static component of the armature current, R_A, L_A - armature circuit resistance and inductance, J – moment of inertia, $k\Phi (t)$ – flux coefficient.

The simplest way to carry out the procedure of identifying the parameters of DCM SE is to control the voltage of the armature motor at $k\Phi (t)=const$ and selectthe measurement interval [0,T] to assure $I_C(t)=const$. In this case, equation (2.38) is transformed to the form

$$U(t)I(t) = I^2(t)R_a + LI(t)\frac{I(t)}{dt} + \frac{k\Phi^2}{J}I(t)\int_0^T I(t)dt - \frac{k\Phi^2}{J}I_C TI(t) \quad (2.39).$$

Equation (2.39) is linear with respect to the variables:

$$x_1(t) = I(t)T,$$

$$x_2(t) = I^2(t),$$

$$x_3(t) = I(t)\frac{I(t)}{dt}, \tag{2.40}$$

$$x_4(t) = I(t)\int_0^T I(t)dt.$$

Having denoted $y(t) = U(t)I(t)$ can be written:

$$y(t) = \alpha_1 x_1(t) + \alpha_2 x_2(t) + \alpha_3 x_3(t) + \alpha_4 x_4(t). \tag{2.41}$$

where

$$\alpha_1 = \frac{k\Phi^2}{J}I_C; \; \alpha_2 = R_a; \; \alpha_3 = L_a; \; \alpha_4 = \frac{k\Phi^2}{J}. \tag{2.42}$$

Since the variables (2.40) in equation (2.41) are linearly independent, which follows from its physical meaning, any of the known identification methods can be used to determine the unknown parameters a_1, a_2, a_3, a_4. In this case, the resistance and inductance of DCM armature circuit are determined directly as a result of evaluation of the parameters of equation (2.41), and the dynamic capacitance of the electric drive $c = J/k\Phi^2$ and static current I_C are calculated as $c = 1/\alpha_4$; $I_C = \alpha_1/\alpha_4$.

Certain difficulties arise when calculating the values of the variables by expressions (2.40), which include, besides the instantaneous value of the current obtained by direct measurements, also the values of the current derivative and its integral. Due to this, a question arises as to the selection of the procedure of their estimation by the measured values of $I(t)$. To solve this problem, known methods of interpolation or approximation of functions are applicable. The choice of a particular method is basically determined by its computational complexity, provided that acceptable accuracy of estimates is obtained. Let's consider in more detail the possible procedures for obtaining estimates of the derivative and the integral of the function $I(t)$.

Let the estimation interval [0, T] is chosen in such a way that the function $I(t)$inside this interval is continuous and differentiable, and we obtained $N+1$ of discrete measurements I_i $i=0,1,2..N$ in the known points of time $t_i=i\Delta t$, where $\Delta t=T/(N+1)$. The simplest way to obtain the estimation of the value of the function derivative $I(t)$ is by the values of first divided differences in points t_i $\Delta I_i = I(t_{i+1}) - I(t_i)$, while the integral estimation $\int_0^{t_i} I(t)dt$ - by the value of the sum $\sum_i I(t_i)$, that corresponds to the piecewise

linear interpolation of the function $I(t)$. However, the low accuracy of the results makes unacceptable its practical use. The results of computational experiments on the interpolation of the curve segment, which represents variation of the instantaneous value of the thyristor converter current on the interval of thyristor conduction, showed that for a small number of measurements ($N<15$) the satisfactory accuracy of the derivative estimates is obtained by polynomial interpolation of the function $I(t)$ by a polynomial of degree N in the Newton form. For longer measurement arrays, polynomial interpolation becomes unacceptable, since we need the representation of polynomials in a special form (the use of the Chebyshev or other types of orthogonal decompositions) to achieve the required accuracy. As a result, the computational complexity of interpolation algorithms increases and becomes comparable with piecewise-polynomial interpolation. Calculations have shown that the most effective of all the methods we have tested is the interpolation of the function $I(t)$ by cubic splines.

To obtain the estimation of the coefficients of the polynomial approximant of degree m of the function $I(t)$ let's represent $I(t_i)=I(t_N-\tau_i)$, where $\tau_i=t_N-\tau_i$. In the neighbourhood of the point t_N expand this function $I(t_i)$ in a Taylor series

$$I(t_i)=I(t_N)-\ \dot{I}(t_N)\tau_i +\frac{1}{2}\ddot{I}(t_N)\tau_i^2 +...+\frac{(-1)^{m-1}}{(m-1)!}I^{(m-1)}(t_N)\tau_i^{m-1}. \quad (2.43)$$

Let's introduce two m-dimensional vectors

$$\mathbf{f_i}=(1,-\ \tau_i\ ,0.5\ \tau_i^2\ ,....,\frac{(-1)^{m-1}}{(m-1)!}\tau_i^{m-1})^{\text{T;}}\quad \mathbf{A}=(I(t_N),\dot{I}(t_N),...,I^{(m-1)}(t_N))\ ,$$

the first of which is known, and the second one should be calculated Then the expression (2.43) in vector form has the form $I_i = \mathbf{A f_i^T}$ [51].

Vector estimation $\mathbf{A}$ by the least square method can be obtained by the algorithm

$$\hat{\mathbf{A}} = (\mathbf{F}\mathbf{F}^{\mathbf{T}})^{-1}\mathbf{F}^{\mathbf{T}}\mathbf{I}, \quad\quad\quad (2.44)$$

where $\mathbf{F}$ - rectangular $(N+1)$ x m matrix, whose rows are row-vectors $\mathbf{f_i^T}$, $i=0,...,N;$ $\mathbf{I}=(I_0,I_1,...,I_N)^{\mathbf{T}}$ - column-vector of measured values of current. As follows from (2.42), estimation of the derivative $\hat{\dot{I}}(t_N)$ can be obtained directly from the expression

$$\hat{\dot{I}}(t_N)=\mathbf{H}^{\mathbf{T}}\mathbf{A}, \quad\quad\quad (2.45)$$

where $\mathbf{H}^{\mathbf{T}}=(0,1,...0)$.

with $\mathbf{H^T} = \int\limits_0^{t_N}[1,-(t_N-t),0.5(t_N-t)^2,....(-1)^{m-1}(t_N-t)^{m-1}/(m-1)!]dt$, using

the expression (4.75) we can obtain the estimation $\int\limits_0^{t_N}I(t)dt$.

In the general case, the algorithm for estimating the parameters of a separately excited d. c. motor, which operates in an electric drive of a thyristor converter-motor, is as follows [52].

1. Measured at discrete instants of time t_i, $i=0,...,N$ of the observation interval, the values of $I(t_i)$ and $U(t_i)$) are stored in the corresponding observation arrays.

2. Having completed the formation of observation arrays, we use one of the abovementioned methods to calculate the coefficients of the polynomial approximant of the current function, the estimation of the derivative and the integral of the function at time instants, and to form arrays of model variables (2.41).

3. The coefficients of the model (2.41) are estimated by one of the known methods (for example, by the least square method), and the motor parameters are calculated.

4. On the basis of measurements, as well as estimates of the values of electrical variables and machine parameters, we calculate the loss components on the observation interval.

Computations can be repeated many times with a specified frequency, the choice of which, due to the large amount of computations for points 2 and 3 of the above algorithm, is determined by the speed of the computer tools used. In this case, as computational experiments have shown, in order to obtain stable estimates of a motor parameters, 10-15 values of current and voltage must be measured at each observation interval, which corresponds to the measurement discreteness (for a six-pulse thyristor converter) $\Delta T \approx 0.00016$ s, and therefore the technical implementation of the monitoring presents no technical difficulties.

2.3.2. D.c. motor parameters determination by the discrete-time continuous function of armature current

Let's consider the problem of finding the parameters of the DCM equivalent circuit from the measured input (armature voltage $U_d(t_i)$) and output (armature current $I_d(t_i)$) signals at discrete instants of time when a d.c. motor is powered by the thyristor converter (Fig. 2.29). The current and voltage signals are registered using a computer-based measuring and diagnostic complex [49].
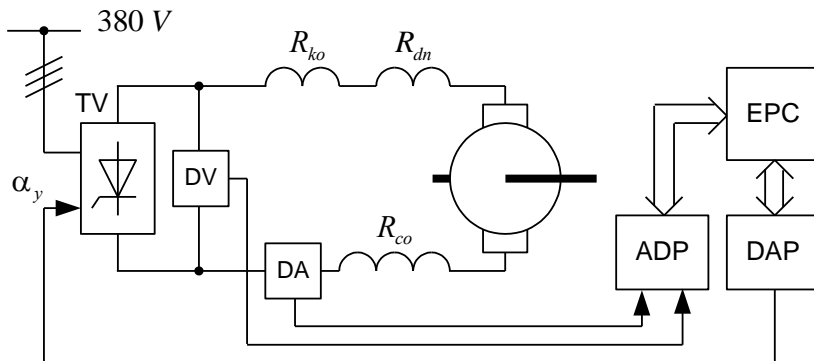
Figure 4.28 – Simplified schematic diagram of the measuring complex for determining the DCM parameters.

The simplest way is to determine the parameters at a lower voltage, which is insufficient to overcome the moment of no-load resistant torque, i.e. when the motor armature does not rotate.

Such a mode can be easily obtained at delay angles of the converter close to $90^0.$ Subsequently, the DCM equivalent circuit will have the form shown in Fig. 4.29.

For the above equivalent circuit, the operator equation for the armature circuit is:

$$\left(R_{ac} + pL_{ac}\right)i_d\left(p\right) = U_d\left(p\right). \qquad (2.46)$$
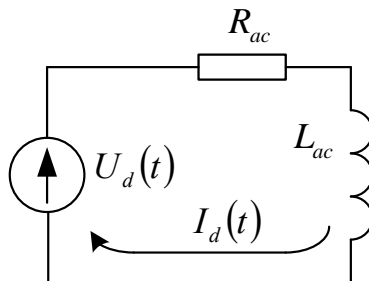
Figure 4.29 – DCM equivalent circuit with stationary armature.

When powering the DCM armature from a thyristor converter with control angles close to 90^0 (Fig.2.30), the voltage has the form of a linearly varying function $U_d(t) = U_{m1} - k \cdot t$, where U_{m1} - the maximum value of the

voltage when the thyristor is switched on, $k = \dfrac{1}{\Delta t \cdot N}\left(U_{d\,m1} - U_{d\,m2}\right)$,

$U_{d\,m2}$ - the voltage value when the thyristor is being closed, Δt - discreteness, N - the quantity of samples in the thyristor conducting interval.
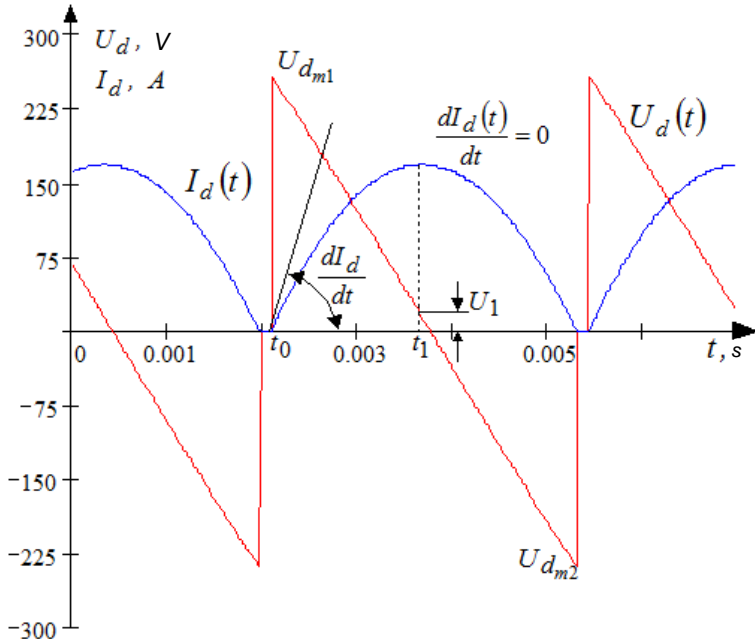
Figure 4.30 – The instantaneous values of armature voltage $U_d(t_i)$ and current $I_d(t_i)$ (current scale 1:2)

Let's write the operator equation for voltage in the form $U(p) = U_{d\,m1} - \dfrac{k}{p}$ and use in the equation (2.46). Thus we obtain the equation for the armature current in the form

$$i_d(p) = \frac{(p + \alpha)}{\left(p^2 + \dfrac{1}{T}p\right)} \frac{U_{d_{m1}}}{L_{ac}}, \tag{2.47}$$

where $T = \dfrac{L_{ac}}{R_{ac}}$, $\alpha = -\dfrac{k}{U_{d_{m1}}}$.

The original equation (2.47) [142]:

$$I_d(t) = \frac{U_{d_{m1}}}{L_{ac}} \left[T^2 \left(\alpha - \frac{1}{T} \right) e^{-\frac{t}{T}} + \alpha Tt + T^2 \left(\frac{1}{T} - \alpha \right) \right]$$

or

$$I_d(t) = \frac{U_{d_{m1}}}{L_{ac}} \left[\left(\frac{L_{ac}}{R_{ac}} \right)^2 \left(\alpha - \frac{R_{ac}}{L_{ac}} \right) e^{-t\frac{R_{ac}}{L_{ac}}} + \alpha \frac{L_{ac}}{R_{ac}} t + \left(\frac{L_{ac}}{R_{ac}} \right)^2 \left(\frac{L_{ac}}{R_{ac}} - \alpha \right) \right] \quad (2.48)$$

Now the problem of parameters determining can be reduced to finding the equation (2.48) by the discrete values of armature current $I_d(t_i)$ measured in t_i time points.

The numerical solution of the equation (2.48), also belongs to the class of mathematical problems, which solutions are unstable to minor changes of the source data [43].

One of the ways to improve the sustainability of finding the approximate solution is to use the principle of possible solutions selection using additional information i.e. quasisolution.

Such additional information may be obtained as a result of finding specific solutions in "special" curve points of the armature current $i_1(t)$.

1. At the moment of a thyristor connection $t = t_0 = t(0) = 0$, when $i_d(t_0) = 0$, $\dfrac{di_d(0_+)}{dt} \neq 0$.

we differentiate (2.48):

$$\frac{di_d(t)}{dt} = \frac{U_{dm1}}{L_{ac}} \left[-T \left(\alpha - \frac{1}{T} \right) + \alpha T \right]. \quad (2.49)$$

For $t = 0$ we obtain the value of armature circuit inductance

$$L_{ac} = \frac{U_{dm1}}{\dfrac{di_d(0_+)}{dt}}. \quad (2.50)$$

Numerical differentiation can be performed with the known discrete current values $i_1(t)$ by backward differentiation using the expression [48].

2. At the moment $t = t_1$, when $\dfrac{di_d(t_1)}{dt} = 0$, $i_d(t_1) \neq 0$.

For $t = t_1$ we obtain the value of armature circuit resistance:

$$R_{ac} = \frac{U_d(t_1)}{i_d(t_1)}.$$ (2.51)

Now the determination of the parameters can be reduced to solving the problem of their numerical determination by the methods of direct minimization, where we take for the function (2.48) its grid approximation $I_i = I_d(t_i)$, $i = 1,2,...n$, i.e. finding minimum of the function n of variables:

$$\sum_{i=1}^{n}[I_d(t_i) - i_d(t_i)]^2 = 0.$$ (2.52)

Taking into account the fact that DCM parameters' computation applying the proposed method requires knowing both the exact instantaneous values of the current signal $I(t_i)$, and its first derivative $\frac{dI(t_i)}{dt}$ in various points, taking into consideration the error in measuring instantaneous values of current, it is advisable to approximate the experimental set of measured values of current by regression analysis methods [44]. For example, the polynomial dependence of the degree n:

$$\tilde{i}(t) = A_0 + A_1 t + A_2 t^2 + A_3 t^3 + A_4 t^4 + A_5 t^5.$$ (2.53)

To improve the accuracy of the solution of the system of equations (2.52), it is appropriate to apply not the measured values of current instantaneous values $I(t_i)$, but the values $\tilde{i}(t)$ to the right parts. Thereupon the system of equations (2.52) takes the form:

$$\sum_{i=1}^{N}[\tilde{i}(t_i) - i(t_i)]^2 = 0,$$ (2.54)

where N - the quantity of discretes (samples) in the thyristor conducting interval.

Figure 4.32 shows the results of calculations to determine the DCM parameters, on the basis of which we obtained the dependence of the armature current: 1 - experimental one, 2 - for the parameters calculated applying the present calculation technique using the system of equations (8).
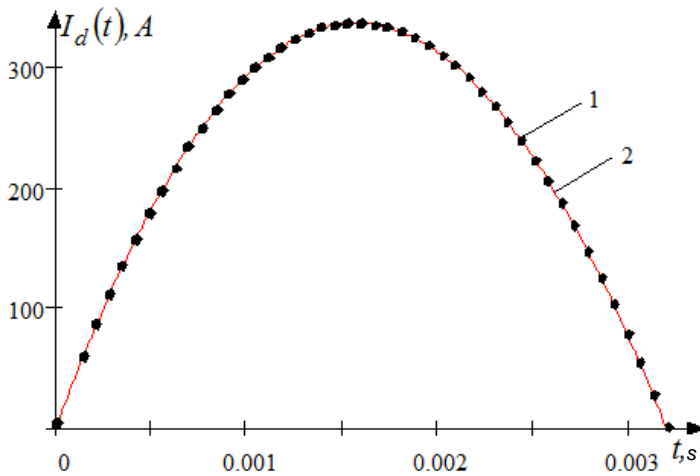
Figure 2.31 – Characteristic curve of the armature current:
1 – experimental $I_d(t_i)$; 2 – design $\tilde{I}_d(t_i)$.

The d.c. motor of the BELaZ (Belarusian Autoworks) dump truck was an object of study; its nameplate data are given in Table 2.1.

The efficiency criterion for the obtained solution is the compliance of the instantaneous values (design and experimental ones) of the armature current. The measure of compliance can be estimated by the value of determination coefficient:

$$R^2 = \frac{\sum\limits_{i=1}^{N}\left[\tilde{I}_d(t_i) - I_{d\,cp}\right]^2}{\sum\limits_{i=1}^{N}\left[I_d(t_i) - I_{d\,cp}\right]^2},$$

where $I_{d\,cp} = \dfrac{1}{N}\sum\limits_{i=1}^{N} I_d(t_i)$ - mean value of the armature current in the thyristor conducting interval, obtained on the basis of experiment data; $\tilde{I}_d(t_i)$ - the value of armature current obtained by solving the equation (2.38) when the parameters R_{ac} and L_{ac} found from (2.54) are plugged in the equation [45-56].

92

Table 2.1 – Catalogued data of ДК-722-А

Parameter	Value
Rated power capacity, kWn	360
Rated voltage, V	750
Rated current, A	520
Rated speed, rpm	1040
Armature resistance, Ohm	0.0159
Compensation winding resistance, Ohm	0.0125
Intermediate poles resistance, Ohm	0.00348
Intermediate poles resistance, Ohm	0.011
Armature circuit inductance, H	0.0006
Transformer phase inductance, H	0.00015

Table 2.2 – Assessment of experimental and design data compliance

Parameter	Precise value	By the procedure [12]	Percentage error, %	By the system of equations	Percentage error, %
Armature resistance, Ohm	0.04288	0.08329	94.3	0.04056	5.4
Armature circuit inductance, H	0.0006	0.00132	120.7	0.00058	3.3
Determination coefficient				0.990909	

LIST OF REFERENCES FOR CHAPTER 2

1. Goldberg O. D. Scientific basis of induction motors diagnostics and quality management// Electricity, №1, 1986. - pp. 20-22.
2. Kopylov I. P. Electrical machines. - Moscow: Energoizdat Publ., 1986. - p. 360
3. Stolyarov I. M., Sinelnikov G. A., Litvinov N. I. The method of parameters' indirect estimation and the induction motor coordinates locator //News of Higher Educational Institutions, Mining Journal - 1984. - №10. - p. 102-105
4. Kvynke Mifoslaw. Computational and experimental method for determining electromagnetic parameters of an induction motor with a deep bar rotor //"Zesz. Nauk. Plodz. Elek." - 1985. - №78. - pp. 5-16(tot.)
5. Deleroi W. Determining parameters of induction machines based on the results of the on-load testing //Etz. Arch. -1985. -7. - №10. - pp. 329-336 (Germ.).
6. Pavlina V. F., Semenova S. V. The technique of experimental determination of the a.c. electrical machines parameters //Technical electrodynamics -1986. №5. - pp. 62-66.

7. Eschin E. K., Tynkevich M. A., Novoselov V. V. Determination of the induction motors' parameters in an automated test system// Automation and electrification of mining enterprises equipped with Automatic Control System. – Kemerovo, 1985. - pp.62-66.

8. Vodovozov A. M., Elyukov A. S. Interference-free algorithms for parametric identification of electromechanical systems // News of Higher Educational Institutions. Instrument engineering. – 2009. – Edition 12. - pp. 40-43

9. Stephan J., Bodson M., Chiasson J. Real-Time Estimation of the Parameters and Fluxes of Induction Motors // IEEE Trans. Ind. Appl., vol. 30, No.3, 1994, – pp. 746-758

10. Kovarsky E. M., Yanko Yu. I. Electrical machines testing. – Moscow: Energoatomizdat Publ., 1990. – 317с.

11. Barkov, Barkova N. A., Mitchell J. S. Condition Assessment and Life Prediction of Rolling Element Bearings // Sound and Vibration. – June, 1995. –Part 1. – pp. 10-17., – September, 1995. – Part 2. – pp. 27-31

12. Barkov A. V., Tulugurov V. V. Vibration diagnostics in the paper industry // Paper, cardboard, cellulose. – 1999. – №4.

13. Cherniy A. P. Specific features of arrangement and engineering support of the monitoring of the motors in the industrial electric drives// Bulletin of Kharkov State Polytechnic University. Electric drive problems. Theory and practice. – Kharkov: Kharkov State Polytechnic University. – 1998. – Special issue - pp. 353-358

14. Rodkin D. I., Cherniy A. P., Martynenko V. A. Rationale for criteria of energy conversion quality in electromechanical systems // Bulletin of Kremenchug State Polytechnic University. – Kremenchug Kremenchug State Polytechnic University – 2002. – Edit.1. -pp. 81-85

15. Lugovoi A. V., Cherniy A. P. Issues of practical energy saving on industrial enterprises // Problems of new machinery and technologies (Kremenchug State Polytechnic Institute): Collected volume of scientific papers. – 1998. – Edit.1 (4). - pp. 5-15

16. Shidlovsky A. K. Some features of the circuits construction of balancing units. - Converting Devices, 1961, Edit.1, pp. 287-291.

17. Cherniy A. P. Figures of energy conversion quality while monitoring the electromechanical equipment // Bulletin of Kremenchug State Polytechnic University. – Kremenchug: Kremenchug State Polytechnic University, – 2003. –Edit.2, Vol. 1 (19). – pp. 149-151.

18. Cherniy A. P., Lugovoy A. V. Rationale for the principles and solutions of the energy efficiency enhancement for the industrial electric drives. Zeszyty naukowe NR 112, Elektryka 16, wydawnictwo politechniki Zielonogorskiej, Zielona Gora, 1997. pp. 101-107

19. Syromyatnikov I. A. Induction and synchronous motors operation modes / in L. G. Mamikonyants (Ed.), 4-th Ed. Revised and Extended – Moscow: Energoatomizdat Publ., 1984. – 240 с.

20. Vibration of electrical machines. Reference book. In PhD (Eng.), Prof. Grygoriyev N. V. (Ed.) – Leningrad: Mechanical engineering, Leningrad dev., 1974. – 464 с.

21. Boiko V. S., Lashko Yu. V., Cherniy A. P., Zhivora V. F. Velasco H. A. On levels and ways of improving the high voltage synchronous motors protection. // Bulletin of Kremenchug State Polytechnic University. – Kremenchug: Kremenchug State Polytechnic University, – 2003. – Edit.2, Vol. 2 (19). -pp. 205-210

22. Rodkin D. I., Cherniy A. P., Kalinov A. P., Barvinok D. V., Kharadjyan A. A., Zdor I. E. Nikitin A. V., Zhivora V. F., Velichko T. V. Facilities for instant diagnostics of a.c. motors. // Collection of scientific papers of National Mining University. – Dnepropetrovsk: OP National Mining University, – 2003. – Vol. 2, №17. - pp. 110-121

23. Aktira Nabal Toshihko Tanaka. A New Definition of Instantaneous Active – Reactive Current and Power Based on Instantaneous Space Vectors on Polar Coordinates in Three-Phase Circuits // IEEE Transactions on Power Delivery. – 1996. – 11, № 3. – pp. 1238-1244

24. Gzarnecki L. Comments on Active Power Flow and Energy Accounts In Electrical Systems With Non-sinusoidal Waveforms and Asymmetry // IEEE Transaction on Power Delivery. – 1996. – 11, № 3. – pp. 1244-1250

25. Senko V. I., Yurchenko N. N. et al. Mathematical model of an induction motor fed by an autonomous inverter. Automated electric drive problems. Theory and practice // Bulletin of Kharkov State Polytechnic University. Special issue. - Kharkov: Kharkov State Polytechnic University – 1998. – 400.pp.

26. Cherniy A. P., Rodkin D. I., Lugovoy A. V. et al. Modelling of electromechanical systems. High school manual. – Kremenchug, 2001. – 376 pp.

27. Cherniy A. P., Sisyuk G. Yu., Rodkin D. I. Diagnostics of induction motors with rotor unbalance // Problems of new machinery and technologies (Kremenchug State Polytechnic Institute) – Kremenchug: Kremenchug State Polytechnic Institute – 1999. – Edit.1 (6). - pp. 102-106

28. Rodkin D. I., Kurowski T. Elementy teorii układów dynamicznego obciążenia w stanowiskach diagnostycznych maszyn elektrycznych. // Zeszyty Naukowe. Elektryka 16. – Zielona Góra. -1997. –Nr 112. - pp. -6.

29. Heming R. V. Numerical methods for scientists and engineers. – Moscow: "Nauka" (Science) Publishing House, 1972. – 400pp.
30. Voloshchenko A. V., Rodkin D. I., Cherniy A. P., Lashko Yu. V. Principles of constructing the systems for speed of an induction motor drive. // Bulletin of Kremenchug State Polytechnic University – Kremenchug: Kremenchug State Polytechnic University – 2001. – Edit.2 (11). - pp. 44-45
31. Stephan Jennifer, Bodson Marc. Real-time estimation of the parameters and fluxes of induction motors // IEEE Transactions on Industrial Applications. – 1994, May/June. – Vol. 30, N 3. – pp. 746-759
32. Iwasaky T., Kataoka T. Application of an extended Kalman filter to parameter identification of an induction motor // IEEE, Industry Application Society Annual Meeting. – 1989. – Vol.1. – pp. 248-253
33. Marino R., Peresada S., Tomei P. On-line stator and rotor resistance estimation for induction motors // IEEE, Transaction on control system technology. – 2000. – Vol. 8. – pp. 248-253
34. Bilate A., Grottstollem H. Parameter identification of inverter fed induction motor at standstill with correlation method, proc. of 5th European Conference on Power Electronics and Applications. – 1993. – vol.5. – pp. 97-102
35. Rodkin D. I., Zdor I. E., Cherniy A. P. Engineering methods for induction motors' parameters determination // Problems of new machinery and technologies (Kremenchug State Polytechnic Institute) – Kremenchug: Kremenchug State Polytechnic Institute – 1999. – Edit.1. - pp. 16-22
36. Zdor I. E., Mospan V. A. Analysis of the diagnostic methods for squirrel-cage induction motors. // Problems of new machinery and technologies (Kremenchug State Polytechnic Institute): Collected volume of scientific papers. – 1998. – Edit.2.
37. Sokolov M. M., Masandilov L. B., Grasevich V. N. Technique of experimental determination of an induction motor parameters // Electrical Engineering. – 1973. №5. – pp. 15-29.
38. Lerner L. G., Sidelnikov A. V. Synthesis of the equivalent schematics for calculation of a number of transient and steady-state processes in synchronous and induction machines // Electrical Engineering. – 1975. – №9. - pp. -35.
39. Rogozin G. G., Pyatlina N. G. Induction machine identification means based on experimental data of its dynamic mode // Electricity. – 1981. – №. 8 pp. - 15-21
40. Rodkin D. I., Cherniy A. P., Zdor I. E. Tasks and technical means for the parameters diagnostics of induction motors // Bulletin of Kharkov

State Polytechnic University. – Kharkov: Kharkov State Polytechnic University – 1999. – Edit. 61. - pp. - 123-128

41. Declaration patent № 50115 A / Induction motor diagnostic technique and the diagnostic device // Rodkin D. Y., Chornyi O. P., Gladir A. I., Voloshchenko O. M., Golovko O. S., Lashko Yu. V. / № 2001096286. Filing date 12.09.2001; publication date 15.10.2002. Bulletin № 10.

42. Declaration patent № 49334 A / Diagnostic device for squirrel-cage induction motors // Rodkin D. Y., Barvinok D. V., Panchenko MV, Chornyi O. P., Ogar O. S. / № 2001117657. Filing date 08.11.2001; publication date 16.09.2002. Bulletin № 9.

43. Declaration patent № 36060 A / Technique of parameters diagnostics of squirrel-cage induction motor and the diagnostic device // Rodkin D. Y., Lugovoy A. V., Chornyi O. P., Sisyuk G. Yu., Dobretsov V. V., Pasmursky O. O., Dolzhenko V. V., Voshun O. M. / №99105901. Filing date 28.10.1999; publication date 16.04.2001. Bulletin № 3.

44. Rodkin D. I., Cherniy A. P., Kalinov A. P. Modern circuit design solutions for diagnostics of synchronous motors parameters // Bulletin of Kremenchug State Polytechnic University – Kremenchug: Kremenchug State Polytechnic University, – 2003.– Edit.1. -pp. 120-126

45. Declaration patent № 50115 A / Synchronous motor diagnostic technique and the diagnostic device // Rodkin D. Y., Chornyi O. P., Kalinov A. P., Zhyvora V. F., Amirov A. M. / № 2003042860. Filing date 02.04.2003; publication date 15.04.2004. Bulletin № 4.

46. Declaration patent № 64083 A / Induction motors diagnostic technique and the diagnostic device // Rodkin D. Y., Chornyi O. P., Barvinok D. V., Ogar O.S. / № 2002108608. Filing date 12.03.2003; publication date 16.02.2004. Bulletin № 2.

47. Akimov L. V. et al. Control systems of d.c. electric drives with condition observers. – Kharkov: Kharkov State Technical University, 1998. – 117 pp.

48. Sadovoy A. V., Sukhinin B. V., Sohina Yu. V. Systems of optimal control of precision electric drives: In A. V. Sadovoy (Ed.) – Kyiv: ISIMO Publishers, 1996. – 298 pp.

49. Rodkin D. I., Velichko T. V., Bakhmetiev Y. A. Method of energy diagnostics of d.c. machines // Problems of new machinery and technologies (Kremenchug State Polytechnic Institute): Collected volume of scientific papers. – 1998. – Edit.1. - pp. 94-100

50. Rodkin D. I., Harajyan A. A., Mikhailov S. V. Diagnostics of d.c. motor parameters during testing // Problems of new machinery and technologies (Kremenchug State Polytechnic Institute) – Kremenchug: Kremenchug State Polytechnic Institute – 1999. – Edit.1. - pp. 40-42

51. Beshta A. S. Using the discrete model of the power ring current in the electric drive with the separately excited d.c. machine to identify electromagnetic and electromechanical time constants // Mining electromechanics and automation: Collected volume of scientific papers. - 2000. - №64. - C. 54-56.
52. Sen P. Thyristor d.c. electric drives: Transl. from Engl. – Moscow: Energoatomizdat Publ., 1985. – 232 pp.
53. Birger I. A. Technical diagnostics. Moscow: "Mashynostroyeniye" (Manufacturing industry) Publishing House, 1978. – 240 pp.
54. Birger I. A. Determination of symptoms diagnostic value // Cybernetics. – 1968. №3. - pp. 80-85
55. Gemke R. G. Electrical machines faults. In R. B.Umantsev 9-th Edition Revised and Extended – Leningrad: Energoatomizdat Publishers, Leningrad dev., 1989. – 336 pp.
56. Bessonov L. A. Theoretical Basics of Electrical Engineering: Electrical circuits: Electrical Engineering, Power Engineering Instrument Engineering Manual for high school students – 8-th Edition Revised and Extended – Moscow: Higher School Publishers, 1984. – 559 pp.

CHAPTER 3
DIAGNOSTICS OF STORAGE BATTERIES PARAMETERS

3.1 Features of storage batteries as components of electric power systems

(Sinchuk I. O., Boiko S. M., Shmeleva T. F., Shmelev Yu. M.)

It is well known that the efficiency of traction batteries' functioning and their applicability as sources of autonomous power supply of traction electrotechnical systems in biaxial locomotives are determined by the operational properties and price indices of the types of batteries that are projected to be used [1]. The research works of professor Sinchuk O. M. and associate professor Shokareva D. A. Provide efficiency estimate of different types of modern storage batteries with regard to the conditions of types of trolley-battery locomotives used in mines with traction electrotechnical system structures: IGBT converter-traction induction motors [2]. The named scientists identified the real facts and prospects of the use of certain types of storage batteries as sources of autonomous power for newly created domestic types of mine trolley-battery locomotives. However, it is shown and emphasized that, in its turn, the traction types of storage batteries have a wide scatter of electrical and design parameters and represent a complex system of chemical, operational and other external random factors that simultaneously influence the battery properties and affect each other. At the same time, it is emphasized, in its turn, that each battery, besides the general properties, has its particular inherent properties, which are determined by the features of the design, the physical condition of the secondary cells and their operation mode. Therefore, to perform a reliable analysis of the operational properties of each particular type of traction batteries, we need to have at our disposal the appropriate amount of statistical material collected by methods of passive and active-passive experiments. In this case, there is a natural manifestation of the patterns of charge and discharge processes in the traction batteries, which are of interest to the researcher; it is very important when creating new technical means and evaluating the effectiveness of a certain type of traction electrotechnical system and the traction batteries efficiency.

As is known [3], the basic parameters of traction batteries, being time functions, are simultaneously functions of many other factors, which are stochastic in nature in particular situations. In the operational conditions such factors are: the discharge rate, which is determined by the specific features of the technological process and the functioning of corresponding equipment; charging rate, which depends on the technique and the type of charger; the latter determines the quality of adjustment of the storage battery main electrical parameters (current or voltage), the shape of the

rectified current curve, the physical condition of the battery, characterized by the initial (weight of the electrodes active mass), the design parameters of the batteries, the state of electrodes and electrolyte, number of charge-discharge cycles (expired service life), etc.

Thus, the dependencies which express the variation of traction batteries parameters in time during their operation, should be considered as random functions; and the efficiency traction batteries operation should be evaluated with the help of possible characteristics. The performance criterion should characterize the system under consideration as a whole, it should provide an opportunity to obtain a quantitative estimate of its dependence on the prescribed factors with the required accuracy, have clearly defined boundaries of its variation area [4].

Evaluation of the chosen performance criterion for certain conditions in the course of in-situ tests is done on the basis of expert estimations of the parameters and characteristics of traction batteries taking into account the influence of the main production factors.

Taking into account the complexity and duration of the traction batteries field tests, and what is the most important in the given type of research - when the operation of trolley-battery locomotives in mines is not paid, we can accept experimental-theoretical method as the method of efficiency evaluation [5]. The basis of this method is:

− content description of the problem, specification of the degree and nature of the performance criterion dependence on the characteristics of individual processes of traction batteries operation and external conditions, setting the generalized parameters of the traction batteries operations, defining the requirements for the accuracy and reliability of the required estimates: selection of relevant factors according to a priori data;

− definition of test conditions by means of factor planning and the selection of appropriate methods for evaluating the required characteristics on the basis of an in-situ experiment and mathematical modelling (simulation);

− rationale and selection of rational composition and structure of mathematical models;

− planning and organization of in-situ experiments and rationale for their scope;

− testing and calibration of mathematical models based on the results of in-situ experiments;

− evaluation of performance criteria of the particular traction battery type.

Experimental-theoretical method, being conducted in real-life conditions with the entire complex of components, allows you to evaluate

both the individual characteristics of objects in the system and the characteristics of the entire system in the form of a performance criterion within its entire variation range. In the given method, the number of points in the factorial space, parameters and characteristics of the significant factors are chosen to obtain or confirm a priori selected required dependence; it involves the use of the factorial planning apparatus.

The most important task that arises when creating new technical means of the traction batteries operation, which include charge and charge-discharge devices, monitoring means, means of control and protection against inadmissible operating conditions of the mine locomotives' traction electrotechnical systems, is the study and mathematical description of the main operational (electric, power and reliability) characteristics of storage batteries. This will ensure that we obtain sufficiently universal, demonstrable and simple mathematical models that allow us to evaluate the operational properties and operating modes of storage batteries, monitor the state of the parameters, forecast these parameters in different industrial situations, characterized by a multitude of possible states.

In the process of operational charge and discharge cycling of traction batteries, basing on the characteristics that express the time dependence of voltage $U = f_1(t)$ and current $I = f_2(t)$, we can mark two distinctive modes: 1) switching mode; 2) actual charge-discharge. The switching mode occurs at the moments of the batteries connection (disconnection) to the load or the charger, as well as during the pulse sequence of charging and discharging current, pauses during a discrete charging method, and actual discharge. Transient processes occurring in this case are characterized by a rapid increase of the currents and voltages drops. The second mode in the passive version corresponds to the presence of the load with constant magnitude in the external closed circuit of the traction battery, this load provided by the discharge device, or the presence of the rectified voltage source (discharging device). In this case, transient processes in the traction battery run slowly, they are characterized by large time constants and can be considered as quasi-stationary ones [6].

During the operation of the traction batteries in the active mode of operational discharge, there are typically random interchanges of transient processes that run quickly and slowly. The realization of full-scale charge processes in the actual operation of such traction batteries comprises areas with smoothly varying parameters, for example, steady-speed moving of a mine locomotive, and areas with parameters of rapidly varying processes, for example, shunting operations of the locomotives in question. In the case under consideration, the discharge mode is generally characterized by complex dependencies of the traction batteries' electric and energy

parameters on the characteristics of the route, the characteristics of the electric stock, the type of locomotive electric drive, the human factor - the individual qualities of the driver, etc. The indicated dependencies are random in nature, therefore it is appropriate to distinguish significative feature, which characterizes the process of operational discharge to the full extent. Such a generalized characteristic can be 'conditional – operational discharge mode', which refers to the calculated mode of the traction battery discharge, equivalent by its current loads, and the magnitude of the discharge capacity, statistically defined for different conditions of the actual discharge modes.

Within the framework of the reduced task of analyzing the traction battery properties, to simplify the mathematical description of the traction battery operational properties, it is advisable to divide the task into the stages, on which the following partial mathematical models are obtained [6]:

− models characterizing storage battery properties on a section, limited by the time of polarization processes' occurrence in secondary cells $1s \leq t \leq 300s,$ for synthesis of discrete monitoring subsystems;

− models of a storage battery as an object of control, which describes the behavior of a storage battery in a traction electrotechnical system on a section, limited by the time of modes regulation when using pulse converters $0 \leq t \leq 1s$, for the synthesis of continuous charge-discharge cycling subsystems;

− models of a storage battery in the time interval from 0 to $t_3(t_p)$ at a prescribed range of charge-discharge currents (voltage) variations for synthesis of the equivalent circuit;

− models describing the electric and energy characteristics of a storage battery during operational charges and discharges in order to create the electric circuits for their evaluation and forecast;

− models describing their reliability characteristics and functions of the running operation time, taking into account the process of natural ageing, for evaluation and forecast of the batteries technical condition and the residual operation time.

3.2 Properties of battery power supply sources

It is well-known that [7] theoretical research, parameters synthesis and configuration for systems containing storage batteries, are simplified in their mathematical model. In general, the mathematical model of a storage battery should reproduce dynamic characteristics in a wide range of external conditions changes with prescribed accuracy, and at the same time provide

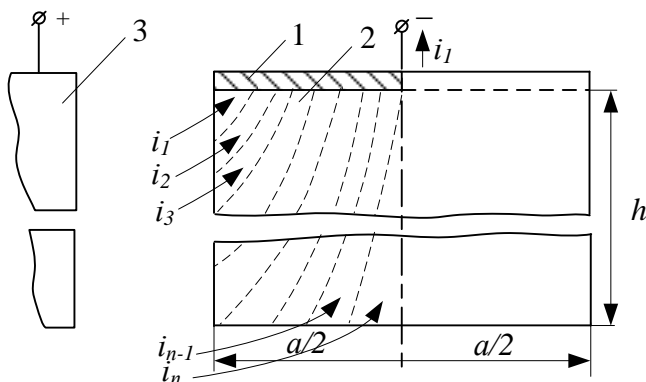significant information on simulated physical and chemical processes, at least at the level of analogies.

Figure 3.1 – Equivalent circuit of a cell plate

The real shape of the characteristic curve showing dependence of current or EMF on time in the range *1s* $\leq t \leq$ *300 s* significantly differs from the exponential [8]. At the beginning of the transient process, it is steeper than the exponential curve, and then it is gradually 'flattened out', till at a certain point of time it becomes more flat than any exponential curve with a predetermined time constant. Such characteristic curves, typical for diffusion processes, are described in the equation of the form:

$$Y = A / \sqrt{t},$$
(3.1)

where Y – the parameter under study (voltage or current); A – constant coefficient; t – current value of time.

However, the expression (3.1) does not reflect the physical nature of the processes, and the coefficient A can be expressed analytically only for a smooth electrode with a strictly constant phase composition, it can not be done for a real multicomponent charge. Besides, this model, being a solution to the known differential equation of diffusion, gives distorted results at small values of time *t*. For example, the initial moment of charge, discharge or pause, when *t = 0*, the value of the output parameter (current, voltage) always has a finite value that contradicts (3.1).

One of the options for obtaining an acceptable mathematical model of a storage battery can be the consideration of processes that occur during charge or discharge on one electrode plate (Fig. 6.1), which is represented as a bulk element with distributed electrical parameters: specific impedance ρ and specific capacitance q. Parameter ρ characterizes the processes

associated with the conversion of charge-discharge electric energy into heat, while parameter q simulates oxidation-reduction reactions that change the electric potential.

The charge-discharge processes in the surface layers of the porous electrode proceed more actively than in the depths, which have greater electrical resistance. The irregularity of the distribution of potential and current fields in the depth and height of the porous electrode is confirmed by experiments [9], therefore the resulting current i passing through the plate under study will be equal to the infinite sum of infinitesimal elementary currents $i_1, i_2, \ldots, i_n$, passing through particular layers.

In the mathematical description of a storage battery as an element of the traction electrotechnical system' control, the dependences of the resulting values of current and voltage on the time are of particular interest, while the distribution of these parameters in the bulk of the electrode is not significant. Therefore, the infinite sum of infinitesimal currents, without introducing a noticeable error, can be replaced by the finite sum of finite currents occurring in layers of electrodes of finite thickness, and the interconnection between the layers can be considered as eventual coincidences.

An equivalent circuit of a secondary cell can be obtained by presenting the process of potential accumulation as a charge of a capacitor that imitates the corresponding electrode layer (Fig. 3.1), and the connection between the layers as a resistive connection (Fig. 3.2). Resistors $R_{01} - R_{cn}$ simulate internal (interlayer) resistance of the storage battery, resistors $R_{11} - R_{1n}$ – external leakage and cells' self discharge. The charge of capacitors during voltage supply U proceeds at velocities, which are inversely proportional to their capacitances $C_1 - C_n$ and resistances of the corresponding resistors.
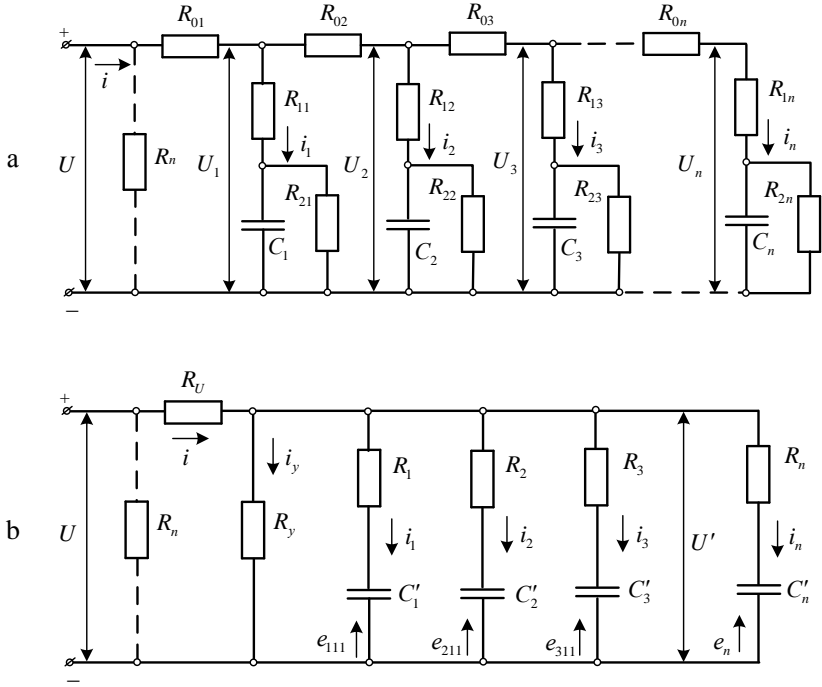
Figure 3.2 – Equivalent circuits of traction batteries

After the storage battery has been disconnected from the voltage U voltage grading commences on the capacities of the elements layers $C_1 - C_n$ similarly to the grading of the potential field on the electrode. The traction battery discharge mode is simulated by the connection instead of U the external load resistance, which is indicated by the dotted line in Fig. 3.3.

To obtain an equivalent circuit consisting of n circuits of identical shape, which correspond to the design element layers of the storage battery, in the charge mode we can compose n pair of equations having the form:

$$U_k(p) = U(p) - R_{01} \sum_{i=1}^{n} i_i(p) - R_{02} \sum_{i=1}^{n} i_i - \ldots \qquad (3.2)$$

$$i_\kappa(p) = U_\kappa(p) \frac{T_\kappa p + 1}{\alpha_\kappa (K_\kappa T_\kappa p + 1)} \qquad (3.3)$$

105

as well as the equation

$$i(p) = \sum_{i=1}^{n} i_i(p),$$

(3.4)

where U – charge voltage, V; i – resultant charging current, A; $U_{\hat{e}}$, $i_{\hat{e}}$ – voltage and current on the random к-th circuit; $T_{\kappa} = R_{\kappa} C_{\kappa}$ – time constant of the к-th circuit, s; $\alpha_{\kappa} = R_{1\kappa} + R_{2\kappa}$ – ohmic resistance of the к-th circuit, Ohm; $K_{\kappa} = R_{1\kappa} / R_{1\kappa} + R_{2\kappa}$ – transfer factor of the к-th circuit.

As a result of the simultaneous solution of *2n+1* equations (3.2) - (3.4) we obtain a transfer function:

$$W(p) = i(p)/U(p) = a_0 + a_1 p + a_2 p^2 + ... + a_n p^n$$

(3.5)

The expression (3.5), whose coefficients are determined basing on the known parameters of the equivalent circuit, is an operator representation of the storage battery electrical conductance.

However, the transfer function (3.5) can be obtained using a simpler equivalent circuit (Fig. 6.2), for which the system of basic equations will be as follows:

$$W(p) = U'(p) \cdot T_k p / R_k (T_k p - 1)$$

(3.6)

$$i_y(p) = U'(p) / R_y$$

(3.7)

$$i(p) = i_y(p) + \sum_{i=1}^{n} i_k(p)$$

(3.8)

$$U'(p) = U(p) - R \cdot i(p),$$

(3.9)

where U' – voltage on parallel circuits, V; R_k – resistance of *k*-th circuit, Ohm; $T_k = R_k C'_k$ – time constant, s; R_y – resistance of leakage and self-discharge circuit, Ohm; i_y – leakage current, A.

During the capacitors charging $C'_1, C'_2, ..., C'_n$ voltages on them from non-zero initial values equal to $e_{1N}, e_{2N}, ..., e_{nN}$ increase exponentially to the levels $e_1, e_2, ..., e_n$. Moreover, in the circuits with a smaller time constant, the increase happens faster and attains a higher level. Therefore, at the moment of ending of the charging pulse, the indicated voltages have equal value [10].

During the pause when U is disconnecter, the current i immediately becomes equal to zero, and $U = U'$. Capacitors $C_1', C_2', ..., C_n'$ begin to discharge by R_y, there is also a redistribution of their charge via $R_1 - R_i$, and their voltages attempt to grade. In this case, it is possible to approximate the sum of the exponentials by changing the battery voltage, these exponentials having the time constants $T_1, T_2, ..., T_n$, which includes both polarization components and components of the oxidation-reducing reactions. The battery self-discharge is much slower than the decrease of polarization voltage, that's why the progress of depolarization, when U is disconnected, is perceived (in the exponential) as a voltage drop not to zero, but to a level corresponding to the actual battery charge at the moment of the charge cease.

The considered consisted patterns allow us to present the equivalent structure of the cell in charge and pause modes, which corresponds to the equivalent circuit (Fig. 6.2, b) by the schematics shown in Fig. 6.3.

Thus, in the general case when the battery is switched to the charge or discharge, the current and the voltage at its terminals in the pause mode can be approximated by the sum of exponential curves with different initial values and time constants. This allows us to expand experimental dependencies $U = f(t)$ and $i = f(t)$ in the exponential components and determine the parameters of the traction battery mathematical model.
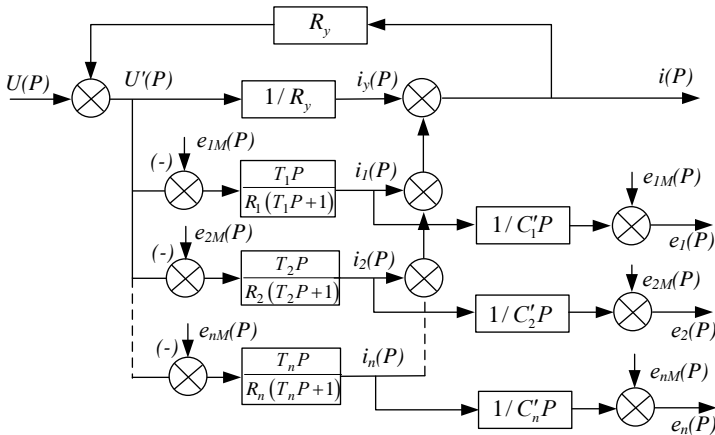

Figure 3.3 – Cell structure in charge-discharge mode

In accordance with the chosen design and the corresponding operation mode of mine trolley-battery locomotives, the operation mode, that is, the power supply of a traction induction motor from the batteries, is short-term, i.e. only during the load handling operations; whereas during the power supply from the traction contact network there is a time-limited process of its charge, where the battery behavior in a limited period of time is of particular interest. We may assume that the parameters of individual cells and the entire battery, which are the object of control in the above mentioned traction electrotechnical systems, remain essentially constant for specific levels of charge-discharge current of the battery state of charge during the transition process caused by the input of single or step impact [11].

The basis of the formulation of the mathematical model of a storage battery is the equivalent circuit of cells (Fig. 6.4), shown in [12]. The storage battery (secondary cell) is considered to be fully charged (charge level C = 100%) if it is charged with a capacity of 1,5 $C_н$ ($C_н$ – rated capacity). The charge level is C = 0%, if the analog-digital converter is discharged with a current of five-hour mode to the voltage equal to 1V for a cell.

The electrical processes in the cell equivalent circuit can be described by a system of equations:

$$u_3 = L_0 di_3 / dt + r_0 i_3 + u_c,$$

$$u_c = E_0 + 1 / C_n \cdot \int_0^t i_c dt$$

$$i_n = (u_c - E_0) / r_n,$$

$$i_3 = i_n + i_c, \tag{3.10}$$

where u_3 – charge voltage; L_0, r_0 – inductance and resistance of the cell; i_3, i_c, i_n – the currents of the charge and the internal circuit in the capacitor circuits and the EMF respectively; u_c – voltage on the internal circuit of the cell; E_0 – EMF of the cell (open circuit battery voltage) at the moment of its connection to the charge; C_n, r_n – capacitance and resistance of the cell electrodes polarization.
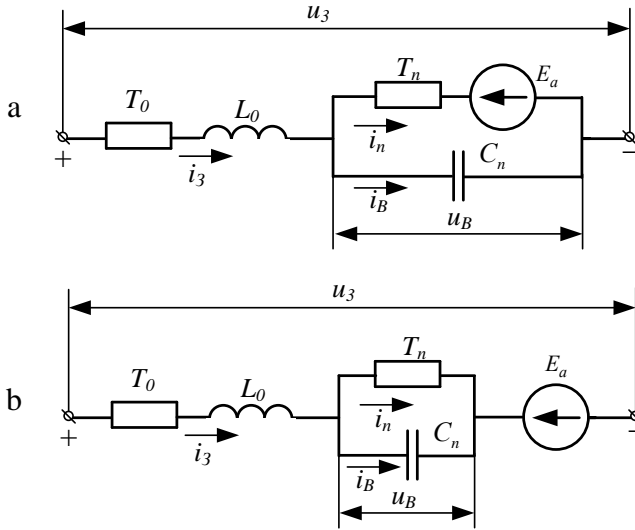
Figure 3.4 – Traction battery equivalent circuit

The solution of the system (3.10) in operator notation will have the form:

$$U_3(p) = \left[(T_0 p + 1) r_0 + r_n / (T_n p + 1) \right] I(p) + E_0(p) \tag{3.11}$$

where U_3 – voltage and current of the charge; $T_0 = L_0 / r_0$ – time constant, conditioned by cell inductance; $T_n = r_n C_n$ – polarization time constant.

The transfer function of the traction battery based on (6.5) will be written

$$W_a(p) = \frac{I_3(p)}{\Delta U_a(p)} = \frac{K_a(T_n p + 1)}{T'^2 p^2 + Tp + 1}, \tag{3.12}$$

where $\Delta U_a(p) = U_3(p) - E_0(p)$; $K_a = 1/(r_o + r_n)$ – transfer factor of a secondary cell;

$$T = \frac{r_0}{r_0 + r_n}(T_0 + T_n), \ T' = \sqrt{\frac{r_0}{r_0 + r_n} T_0 \cdot T_n}$$

– secondary cell time constants.

The equation (3.12) with the same assumptions is used for another version of the equivalent circuit, shown in Fig. 6.4, b.

The block diagrams of a secondary cell for the charge/discharge cycle service, that correspond to the model (3.12), are shown in Fig. 6.5.

Applying the obtained structures, we can synthesize a mathematical model of a battery consisting of an arbitrary number of n of cells having different parameters r_{ol}, L_{ol}, C_{ni}, r_{il}, E_{oi}. In case of the most common series connection of the cell, the input of the first cell is the voltage and its output - the current, which is common to other cells and is supplied to their input. Therefore, on the basis of (3.12) the cell block diagram can be illustrated by Fig. 3.6, and the generalized transfer function can be expressed by the equation [13]:

$$W_B(p) = \frac{I_3(p)}{U_B(p)} = \frac{K_B \prod_{i=1}^{n}(T_{ni}p+1)}{1/\sum_{i=1}^{n}\prod_{\substack{k=1 \\ k \neq 1}}^{n}\cdot\sum_{i=1}^{n}\left[\left(T'^2 p^2 + T_i p + 1\right)\prod_{k=1}^{n}(T_{nk}p+1)K_{ak}\right]}, \quad (3.13)$$

where $K_B = 1/\sum_{i=1}^{n}(r_{ol}+r_{ni}) = 1/(R_0 + R_n)$ – transfer factor of a battery;

$R_0 = \sum_{i=1}^{n} r_{ol}, R_n = \sum_{i=1}^{n} r_{n1}$ – ohmic and polarization resistance of a battery;

$\Delta U_5(p) = U_3(p) - \sum_{i=1}^{n} E_{ol}(p); \sum_{i=1}^{n} E_{ol}(p) = E_3(p)$ – increment of voltage and EMF on a secondary cell.
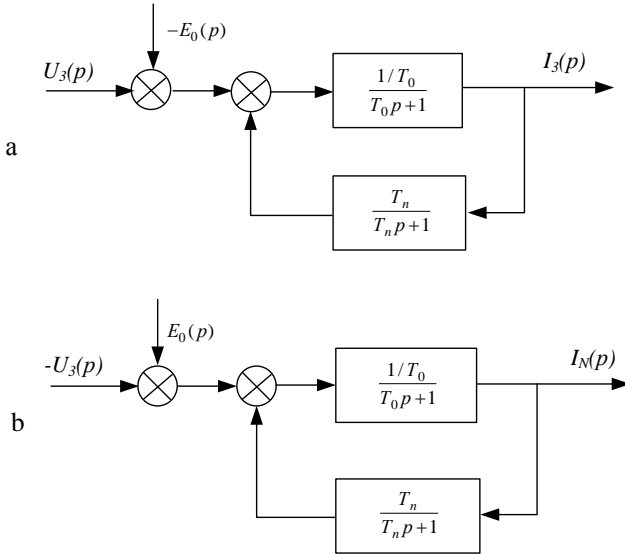
Figure 3.5 – Block diagrams of a traction battery in charge-discharge mode

A generalized model (3.13) can be used for studying the processes occurring in a battery under consideration, taking into account the individual characteristics of particular batteries. Taking into account that during the synthesis of charge-discharge modes, the transient processes in the entire battery are of particular interest, it is advisable to simplify its mathematical model. With this objective in view, the battery should be considered as a system of cells with equal, average parameters, that is, as an ideal one. Then (3.13) can be represented by the expression [14]:

$$W_B(p) = \frac{I_3(p)}{\Delta U_B(p)} = \frac{K_B(T_n p + 1)}{T'^2 p^2 + T p + 1} \quad , \qquad (3.14)$$

where $K_B = K_a / n$, and time constants T', T, T_n – are equal to the corresponding time constants of one averaged cell.
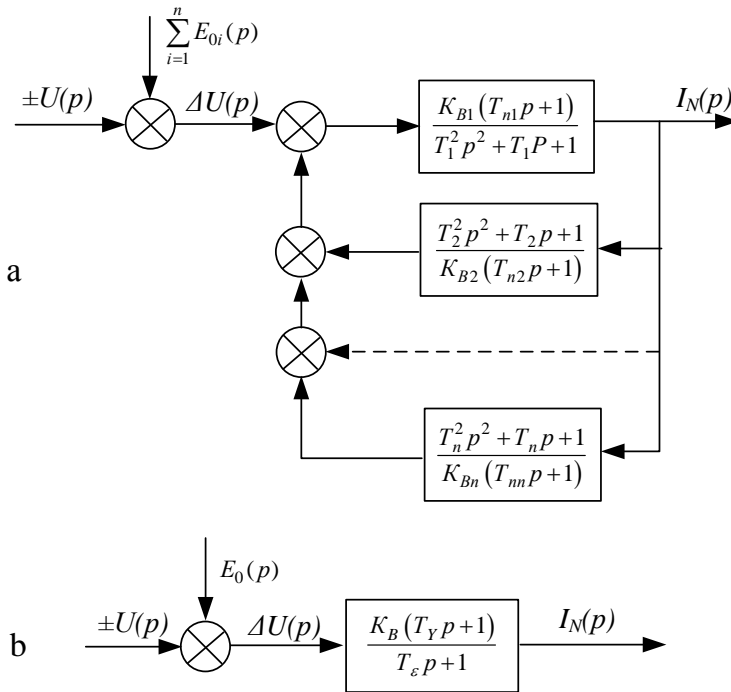
Figure 3.6 – Block diagram of the storage battery

Similarly, it can be proved that during the battery discharge on a pulse converter, which operates in inverter mode, the generalized and simplified models of the battery it will be identical to the corresponding models in charge mode (3.13) and (3.14). Consequently, in the expressions of transfer functions instead – $E_B, +U_{CH}$ while charging should be substituted by $+ E_B, - U_n$ (voltage at the inverter input) while discharging.

Model (3.13) can be reduced to a simpler expression if the inductance of traction batteries is neglected, which is known to be $(0,7+0,3) \cdot 10^{-6}$ H for the capacity range from 100 to 500 AHr [15]:

$$W_B(p) = K_B(T_n p + 1)/(T_B 3 + 1) \qquad (3.15)$$

or

$$W_B(p) = K_B(\alpha_B T_B p + 1)/(T_B p + 1), \qquad (3.16)$$

where $\quad K_B = 1/(R_0 + R_n) \quad$ – transfer factor of a battery;

$T_i = R_n C_n, T_B = \dfrac{R_0}{R_0 + R_n} T_n = \dfrac{T_n}{\alpha_B}$ – time constants of a polarization circuit

and a battery' transient process; R_o, R_n – ohmic and polarization resistance

of a battery; $\alpha_B = \dfrac{T_n}{T_B} = \dfrac{R_0 + R_n}{R_0}$ – divisibility factor of time constants,

characterizing the degree of differentiation of input influence by the storage battery [16].

The block diagram of a simplified battery model is shown in Fig. 3.6, b. The primary function (3.15) or (3.16) has a corresponding transient function of a battery

$$i_B(t) = \Delta U_B K_B \left[1 + (\alpha_B - 1)\exp(-t/T_B)\right] \qquad (3.17)$$

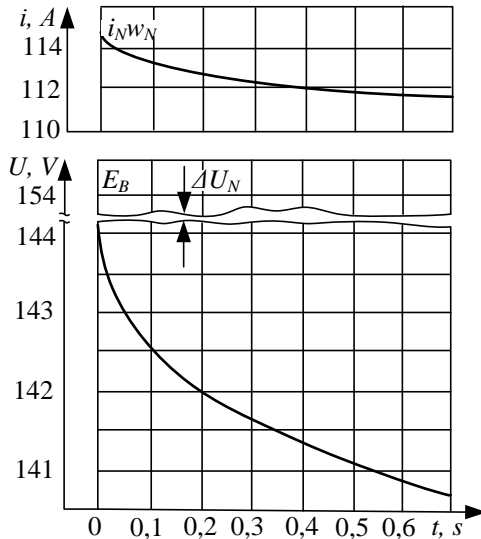Figure 3.7 – Diagram of processes of current flow $i_n(t)$ and voltage flow $U_n(t)$ for a traction battery

Thus, a specific traction battery under certain initial conditions at a given interval of time (up to 1 s) is approximated by the first order link of the general form of the differentiating action with constant parameters. At the same time, under different initial conditions, the parameters of the

model (3.17) are determined by the nature of the internal resistance variation of the battery. The initial condition refers to the degree of the traction battery charge level, the quantity, type and technical state of the secondary cells, which is characterized by the number of operational charge-discharge cycles, the electrolyte quality, internal resistance, temperature and other factors [17].

The differentiation effect of this object is determined by the fact that there is inequality

$$T_n \succ T_B \text{ Tn>Tor } \alpha_B \succ 1, \tag{3.18}$$

according to this formula, when the step impact is applied to the traction battery input, current step occurs at the initial moment of time

$$i_n(0) = K_B \alpha_B \Delta U_B \tag{3.19}$$

and then it gradually decreases with a time constant T_B to the value

$$T_B(\infty) = i_{B \text{ st}} = K_B \Delta U_B \ . \tag{3.20}$$

The processes of current $i_n(t)$ flow and voltage $U_n(t)$ flow, an example of which for a particular battery is shown in Fig. 3.7, have specific features that distinguish the traction battery as an object from the well-known ones. In particular, at the time $t = 0$, that is, when the battery is connected to the load R_n, the discharge current reaches its maximum value, changing almost immediately from 0 to $i_n = i_{n\max} = i_n(0)$, respectively, the voltage on the osmic resistance of a storage battery decreases in a step from the E_B to $U_n(0_m)$, proving that we can replace the model (3.13) with a simplified one (3.16).

Further variation of the current and voltage results from the transient process in the loop E, r_n, C_n (Fig. 3.7) and the battery size.

In order to increase the accuracy of oscillograms processing, the curves of the battery voltage variation are assumed to be the basic ones, which simplifies the implementation of the measuring circuit (since only the voltage increment is recorded, and it allows us to increase the scale of the oscillogram in Y-direction). In this case, the reference voltage source, which compensates the E_B before the test, and the precision instrument for measuring the open circuit battery voltage (EMF), are introduced in the measuring circuit.

The transient resonse curves, which are experimentally obtained, are processed by approximation on the prescribed time interval applying the calculation curves, which present timing characteristics of the equivalent system "battery-load", the block diagram of which (Fig. 3.8) constitute two series links (battery and load), connected by singular negative feedback [18].
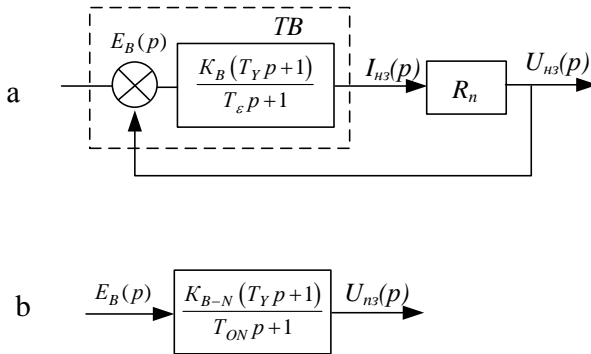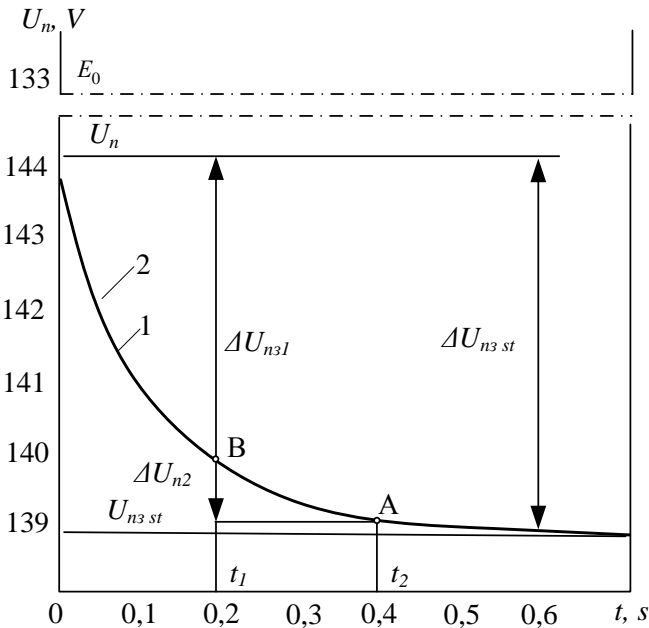
Figure 3.8 – Storage battery block diagram

Figure 3.9 – Voltage and current experimental curves of a storage battery in charge cycle

The transfer function, which corresponds to the structure (Fig.3.8), is determined by the expression

$$W_{B-H}(p) = \frac{U_N(p)}{E_B(p)} = \frac{K_B R_N (T_n p + 1)/(T_B p + 1)}{i + K_B R_N (Tp + 1)/(T_B p + 1)} =$$
$$= \frac{K_B R_N (T_n p + 1)/(1 + K R_n)}{\dfrac{K_B R_N T_n + T_B}{1 + K_B R_N} p + 1} = \frac{K_{B-N}(T_n p + 1)}{T_{ON} p + 1}$$

(3.21)

or

$$W_{B-N}(p) = K_{B-N} \frac{\alpha T_{ON} p + 1}{T_{ON} p + 1} , \qquad (3.22)$$

where $U_{ES}(p)$ – an operation description of the load voltage of the equivalent system; $K_{B-N} = \dfrac{K_B R_N}{1 + K_B R_N} = \dfrac{U_{ES\,ST}}{E_B}$ the equivalent system transfer factor; $U_{ES\,ST}$ – the value of the steady voltage of the equivalent system;

$$\alpha = \frac{T_n}{T_{ON}} = \frac{U_N(0_+)}{U_{ES\,ST}} - \text{forcing coefficient;}$$

$$T_{ON} = \frac{K_B R_N T_n + T_B}{1 + K_B R_N} - \text{the time constant of the system transient}$$

process;

Taking into account (3.21) and (3.22) we can write:

$$K_{B-N} = \frac{R_N}{R_0 + R_N + R_B}, \quad T_{ON} = \frac{R_0 + R_n}{R_0 + R_N + R_n} T_n = \frac{T_n}{\alpha}, \quad \alpha = \frac{R_0 + R_N + R_n}{R_0 + R_N} \quad (3.23)$$

The transfer function (3.21) has a corresponding structure shown in Fig. 6.8. The transient process in the system under study, according to (3.23), will be described by the equation

$$u_{ES}(t) = K_{B-N} E_c \left[1 + (\alpha - 1) \exp(-t/T_{ON}) \right]. \quad (3.24)$$

Thus, the voltage on the battery of the equivalent system will be determined:

$$u_{EB}(t) = \begin{cases} E_B & \text{at } t \prec 0 \\ u_{ES}(t) & \text{at } t \geq 0 \end{cases}, \; . \qquad (3.25)$$

Comparing the correlations of equations (3.23), (3.24) with (3.25), we obtain the expression to determine the parameters via the equivalent system parameters [19]:

$$K_B = \frac{K_{B-N}}{R_N \left(1 - K_{B-N}\right)}, \ \alpha_B = \alpha + \frac{R_N}{R_0}(\alpha - 1), \ T_B = \frac{\alpha}{\alpha_B} T_{ON}, \quad (3.26)$$

$$T_n = \alpha T_{ON} = \alpha_B T_B$$

In case under consideration only the initial section of the transient process' curve is of particular interest, based on the conditions of limiting the chage/discharge cyle time within 0,3+0,5 s.

Results of studines of the traction batteries, in which the maximum deviation of parameters of the current function from their mean values does not exceed for K_B 2%, for T_B, T_n 7%, show that with the increase of the number of secondary cells the influence of the current value on the value of the battery parameters reduces. It can be explained by the fact that the batteries under question present a quite large set of cells, which characteristics are random values, that are subject to the normal distribution law. Therefore an entire battery can be presented as sets of averaged secondary cells or as a particular abstract secondary cell with average electric parameters, which vary at a considered time interval and almost do not depend on the value of current [20].

The parameters values of the batteries under study as monitoring object are determined to some extent by their charge level and technical condition. Dependence of parameters T_B, T_n on the charge level has more predictable pattern than K_6, which value varies on a few percents in certain cases, and 2 times and more in othe rcases. The given parameters for the charged battery show a trend toward increasing as compared to the discharged batteries; it is especially true for batteries the had the greater number of operating charge-discharge cycles. Parameter α_6 for the charged storage battery has a smaller value, than for the discharged one.

The transfer factor value depends significantly on the number of secondary cells within the battery, while the dependence of the time constants T_B, T_n and α_B on this factor is less defined. In all cases the polarization time constant is bigger that the battery time constant ($T_B < T_n$), that indicates the presence of the differentiation effect by the object of incoming disturbances.

On the basis of the above stated, we can conclude again, that any type or kind of the traction battery contitutes a complex dynamic system with variable parameters, however, as a monitoring object on the prescribed time interval it can be approximated by the first-order link of general form of differentiation action, which has constant parameters determined by the charge level, level of current, type, number and technical condition of secondary cells. Dependence of the parameters under study on the current

decreases with the increase of the secondary cells quantity; and is almost absent for the traction batteries installed on mine locomotives [21].

3.3 Analysis of schematic-based design solutions of monitoring subsystems for storage batteries condition

As it was stated in section 1 of this monograph, modern traction systems and industrial complexes, and especially mine types of electric locomotives must combine software and hardware that can significantly reduce the number of components of the traction electrotechnical systems. In the given monitoring and control system, the hardware part acts as an executive unit, while the software loaded into the control system's microcontrollers is responsible for measuring, processing and analyzing incoming information.

On the basis of received and processed data, a decision is made to change the operation mode of the traction battery.

The main components of the monitoring subsystem of the traction batteries components are [22]:

- monitoring of the voltage level on the components;
- monitoring the current value of the power circuit.

Measurement of the voltage of secondary cells in the lithium-ion battery should be carried out with an accuracy of at least $\pm$ 0,5% of the range. There is a number of circuit design solutions that allow us to measure the voltage of the series circuit. The fundamental difference between these design solutions is the accuracy of the voltages measuring, secondary cells, the technique and complexity of the circuit design.

Method of the resistance dividers circuit. The inputs of analog-digital converters in microcontroller structures are multiplexed and do not have a galvanic isolation, that is, voltage measurements in all channels are performed relative to the general grounding terminal. The reference voltage of the analog-digital converter of the microcontroller typically does not exceed 5 V. Thus, to calculate the voltage of the secondary cells, connected in series in the battery (provided that galvanic isolation is absent), we need to reduce the voltage at the secondary cells' terminals to the voltage U_n, which does not exceed the reference value (Fig. 3.10), otherwise the measurement result will be incorrect

or will cause the measuring equipment failure. The applied voltage Un, let's call it "the reduced voltage of the cell".
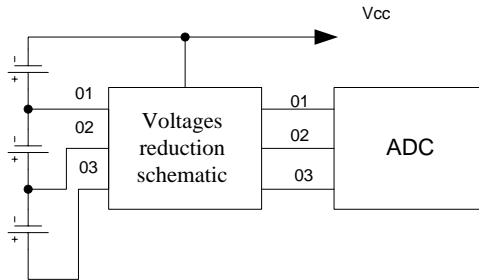
Figure 3.10 – Structure of the cells voltage measurement complex by applying the method of voltages reduction.

The measuring method of secondary cells' voltage in the battery under study consisits in composing such a dividing circuit so that the voltage at the positive terminal of the n-th cell relative to the general output terminal is calculated as the product of the voltage, measured on the corresponding terminal of the divider and the battery number:

$$U_{ANn}^{gen} = n \cdot U_{ANn}, \qquad (3.27)$$

where U_{ANn}^{gen} - voltage on the positive terminal of the n-th cell relative to the general output terminal Vcc; n – the secondary cell number; U_{ANn} - voltage value on the corresponding terminal of the divider.

Schematic implementation of the divider is shown in Fig. 3.11.
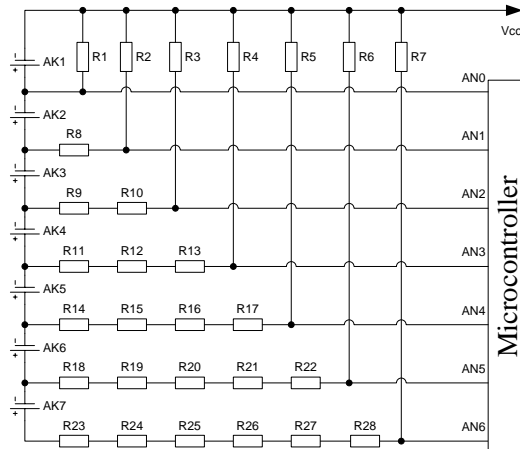
Figure 3.11 – Schematic of voltage divider

The resistances of R1-R28 resistors are equal. The accuracy of the real voltage computation on the secondary cell depends on the resistors' accuracy. Based on the dividing circuit structure (Fig.3.11), each cell voltage is calculated according to the formula [23]:

$$U_{akn} = n \cdot U_{ann} - (n-1)U_{ann-1}, \tag{3.28}$$

where U_{akn} - calculated voltage of the secondary cell; n - the secondary cell, which voltage is calculated, number; U_{ann} – measured reduced voltage at the analogue input of the secondary cell, which voltage is calculated; n-1- the previous cell number; U_{ann-1} - measured reduced voltage at the analogue input of the previous secondary cell.

Below there is an algorithm for calculating the voltage during the realization of the measurement circuit by the method of resistance dividers:

– measurement of the reduced voltage of the secondary cell U_{ann} is carried out according to the algorithm of voltages calculation [21];

– the calculated reduced voltage is multiplied by the secondary cell number: $U_{Sak} = n \cdot U_{ann}$;

– the action is carried out: $U_{akn} = U_{Sak} - U_{Sak-1}$, де $U_{Sak-1} = (n-1)U_{ann-1}$. The voltage is the calculated voltage of the secondary cell number n.

In practice, resistances of the divider's resistors vary in their parameters, so this circuit design introduces an error in the calculation of the secondary cells' voltage.

As the formula (3.28) shows, the value of the secondary cell calculated voltage depends on the dividers' error of secondary cell, which are less time in operation. Thus, in the diagram shown in Fig. 3.11, during the voltage calculation the biggest error will be on the *Ak7* cell, the smallest error – on the *Ak1* cell.

Table 3.1 – Functions of variation patterns

№ Ак Cell	Condition	Voltage variation function	
		Measured by instrument	Calculated value
7	Charge	y=0.0005x+4.0019	y=0.0006x+4.0424
4	Charge	y=0.0005x+3.975	y=0.0005x+4.0083
1	Charge	y=0.0006x+3.9934	y=0.006x+3.9781
7	Discharge	y=0.001x+3.6859	y=0.0011x+3.7242
4	Discharge	y=-0001x+3.6840	y=0.0011x+3.6653
1	Discharge	y=0.001x+3.6013	y=0.001x+3.5957

As Table 3.1 shows, the difference between the slopes of the measured and calculated functions cures of the corresponding cells is negligible,which makes it possible to assume that the difference between

the absolute terms of the measured and calculated functions is the mean error of the voltage calculation within the whole measurment range.

Table 3.2 shows the error of voltage calculation for each secondary cell.

As Table 3.2 shows, the voltage calculation error for *Ak7* is the biggest one, it accounts for 40,5mV when charging, and 38,3mV when discharging.

Adjusting factors are introduced to reduce the error for each calculated voltage of the secondary cell. The value of these factors is individual for each set of resistors.

<u>Method of the cell' measuring terminals commutation.</u> This principle of the circuit design for the voltages measurement of series secondary cells is based on commutation of the voltage meter terminals to the measuring terminals of the secondary cells. Here, the measuring terminal of the microcontroller's analog-digital converter is switched to the positive terminal of the secondary cell, and the general terminal is switched to the negative terminal. Such voltage commutation eliminates the mutual influence of the measuring circuit components on the calculation of each cell voltage in the system. Such a solution requires the galvanic isolation between the general output terminal of the voltage meter and the general output terminal of the traction battery installed in the electric vehicle.

Table 3.2. – Voltage calculation error

№Ак/Cell	Condition	Calculation error, $\Delta\varepsilon_R$,mV
7	Charge	40.5
4	Charge	33.3
1	Charge	15.3
7	Discharge	38.3
4	Discharge	18.7
1	Discharge	5.6

The block diagram of the hardware realization, presented in Fig. 3.12, provides the galvanic isolation for the measuring part of the electrical circuit from the general output terminal of the traction battery [22].
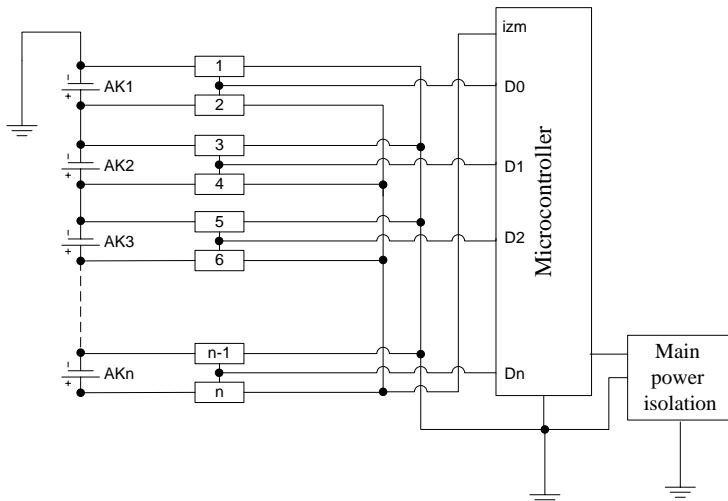
Figure 3.12 – Block diagram of the galvanic isolation of the voltage
measurement

Here K_{OMo}-K_{OMn} – are optolectronic switches, that change their state under the influence of a control signal D_o- D_n and assure sequential connection of each cell' measuring circuits to the microcontroller. K_{OM} elements are commuted paiwise (K_{OM0}–K_{OM1}, K_{OM2}-K_{OM3}, K_{OM4}-K_{OM5}, K_{OMn-1} - K_{OMn}). K_{OM} electronic switch, connected to the negative terminal of a secondary cell, on which the voltage will be measured, is commuted to the logic ground of the galvanically isolated system; while K_{OM}, electronic switch connected to the positive terminal of a secondary cell - to the measuring terminal of the microcontroller's analogue-digital converter. In the process of the measurement algorithm operation, only one pair of electronic switches K_{OM} can be closed; otherwise, the current, with value near to that of the short-circuit current, will pass through the system.

The equivalent circuit for the secondary cell connection to the the battery to the measuring input terminal of the analogue-digital converter (ADC) is shown in Fig. 3.13.

Figure 3.13 – Equivalent circuit of the measuring channel commutation to the analogue-digital converter input

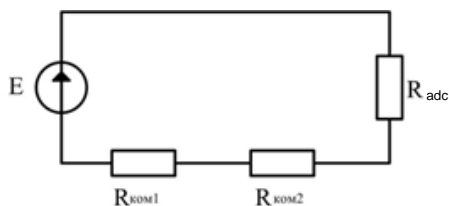Since the resistance of the switches R_{KOM1} and R_{KOM2} is much less that the resistence of the ADC measuring input, the voltage drop on R_{KOM1} and R_{KOM2} can be neglected (R_{KOM1}, $R_{KOM2,} << R_{adc}$).

The voltage meter is based on the galvanic isolation, designed on the basis of microprocessing logic, it ensures data transmission and logging in the computer via RS-232 interface. Specialized software installed on the computer decrypts the received data packet and displays values for each measurement channel on the screen in digital decimal and graphic form. The protocol of the measurement results allows us to compare the values of the calculated voltages of the secondary cells with the voltages measured by the voltmeter. Measuring of the potential difference with the help of the test voltmeter B7-34A and the measurement device are carried out directly on the plates of each cell in an electrochemical energy storage device. The electrochemical energy storage device is a storage battery consisting of 8 Li-ion cells having capacitance of 10AHr and connected in a series circuit. Since the measurements are carried out in the conditions of charge or discharge, to ensure the obtained data compliance, we need to simultaneously record the measured voltage with the help of a voltmeter and the calculated voltage, which is displayed on the screen of the personal computer. To construct the voltage variation pattern, 6 measurements with a discrete interval of 10 minutes were performed [22].

The compliance of the voltage values measured with the help of the test voltmeter B7-34A (measured value) and with the help of the microprocessing measurement system (calculated value) in cycling service are given in Table 6.3 and Table 3.4, respectively.

Table 3.3 – Charging mode

Voltage measurement with the voltmeter B7-34A								Voltage measurement with the microprocessing measurement system (computer data protocol)							
Measur. №	U AK 1	U AK 2	U AK 3	U AK 4	U AK 5	U AK 6	U AK 7	U AK 8	U AK 1	U AK 2	U AK 3	U AK 4	U AK 5	U AK 6	U AK 7	U AK 8
1	3.922	3.902	3.905	3.904	3.906	3.906	3.909	3.931	3.920	3.900	3.905	3.905	3.905	3.905	3.910	3.930
2	3.952	3.930	3.932	3.931	3.932	3.930	3.936	3.955	3.949	3.930	3.930	3.930	3.930	3.930	3.935	3.954
3	3.972	3.951	3.953	3.952	3.953	3.949	3.958	3.976	3.969	3.949	3.954	3.949	3.949	3.949	3.954	3.978
4	3.991	3.967	3.970	3.969	3.970	3.965	3.975	3.992	3.988	3.969	3.969	3.969	3.969	3.964	3.974	3.988
5	4.007	3.980	3.983	3.982	3.983	3.978	3.988	4.005	4.008	3.978	3.983	3.983	3.983	3.978	3.988	4.003
6	4.019	3.991	3.994	3.993	3.994	3.988	3.999	4.016	4.018	3.988	3.993	3.993	3.993	3.988	3.998	4.018

As Table 3.5 shows, the difference between the slopes of the corresponding curves for each secondary cell is negligible (infinitesimal), which allows us to assume that the difference between the absolute terms of the corresponding approximated curves is constant throughout the whole time interval of measurements. Voltage calculation error for each cell is summarized in Table 3.6.

Table 3.4 – Discharge mode

Voltage measurement with the voltmeter B7-34A								Voltage measurement with the microprocessing measurement system (computer data protocol)							
Measur. №	U AK 1	U AK2	U AK 3	U AK 4	U AK 5	U AK 6	U AK 7	U AK 8	U AK 1	U AK 2	U AK 3	U AK 4	U AK 5	U AK 6	U AK 7	U AK 8
1	3.895	3.928	3.928	3.928	3.924	3.920	3.926	3.889	3.895	3.925	3.925	3.925	3.925	3.920	3.925	3.891
2	3.867	3.902	3.903	3.904	3.900	3.897	3.902	3.866	3.866	3.905	3.905	3.905	3.900	3.900	3.905	3.866
3	3.846	3.882	3.882	3.884	3.879	3.878	3.882	3.846	3.847	3.881	3.881	3.886	3.871	3.876	3.881	3.847
4	3.829	3.863	3.863	3.865	3.860	3.861	3.863	3.829	3.827	3.866	3.866	3.866	3.861	3.861	3.861	3.827
5	3.813	3.846	3.845	3.847	3.842	3.845	3.845	3.812	3.812	3.847	3.847	3.847	3.842	3.847	3.847	3.812
6	3.795	3.828	3.827	3.829	3.824	3.828	3.827	3.794	3.793	3.827	3.827	3.827	3.822	3.827	3.827	3.793

Charge curves equations, obtained by linear approximation are summarized in Table 3.5.

Table 3.5. – Functions of variation patterns

№	Condition	Voltage variation function	
		Measured value	Calculated value
Ak7	Charge	y=0.0191x+3.9103	y=0.0196x+3.9067
Ak4	Charge	y=0.0176x+3.8937	y=0.0177x+3.8929
Ak1	Charge	y=0.0178x+3.8985	y=0.0177x+3.8979
Ak7	Discharge	y=-0.0196x+3.9427	y=-0.0195x+3.9427
Ak4	Discharge	y=-0.0196x+3.9447	y=-0.0195x+3.9444
Ak1	Discharge	y=-0.0194x+3.9087	y=-0.0198x+3.9092

The table shows that the maximum mean voltage calculation error relative to the measurement by the test device B7-34A comprises 3.6 mV for the charging mode and max. 0.5 mV for the discharge mode. Higher

mean calculation error in the charging mode is caused by the disturbances from the pulsating currrect supply.

To choose the circuit design solution for the voltages measurement, we need to compare the obtained experimental data and consider the advantages as well as disadvantages of both methods.

Table 3.6. – Voltage calculation error

№Ak/Cell	Condition	Calculation error, $\Delta\varepsilon_R$, mV
7	Charge	3.6
4	Charge	0.8
1	Charge	0.6
7	Discharge	0
4	Discharge	0.3
1	Discharge	0.5

Table 3.7a – Mean measurement error comparison (charge)

№ Ak/Cell	Mesurement circuit based on the voltage divider (mean voltage calculation error, $\Delta\varepsilon_R$, mV)	Mesurement circuit based on the galvanic isolation (mean voltage calculation error, $\Delta\varepsilon_{gal}$, mV)
Ak1	15.3	0.6
Ak4	33.3	0.8
Ak7	40.5	3.6

Let's compare the mean measurement error obtained during charging and discharging in the voltage measurement circuits with the voltage divider and commutation of the cell measuring terminals (Table 3.7 a, b).

Table 3.7b – Mean measurement error comparison (discharge)

	Mesurement circuit based on the voltage divider (mean voltage calculation error, $\Delta\varepsilon_R$, mV)	Mesurement circuit based on the galvanic isolation (mean voltage calculation error, $\Delta\varepsilon_{gal}$, mV)
Ak1	5.6	0.5
Ak4	18.7	0.3
Ak7	38.3	0

Maximum mean calculation error $max\Delta\varepsilon_R$ during the charge and discharge in the circuit based on the voltage divider is observed for the Ak7 secondary cell (Tabl.6.7a), since the voltage calculation of the given cell depends on the calculated voltage on the previous cells [23]:

$$\Delta\varepsilon_{Rn} = U_{AKn} - U_{AKn\,MEAS}, \tag{3.29}$$

where $\Delta\varepsilon_{Rn}$ – voltage calculation error on the secondary cell with the sequence number n; U_{AKn} – cell voltage, calculated by the formula (6.28); $U_{AKn\,MEAS}$ - cell voltage, measured by a test device.

In the circuit with output terminals commutation the calculation error $\Delta\varepsilon_{tot}$ does not depend on the calculated voltage on the previous cells, since in this case voltage measurement is performed directly on the potential terminal of the cells without pre-adapting circuits.

Let's compare the maximum mean voltage calculation error for a circuit with a voltage divider and outputs commutation ($_{max}\Delta\varepsilon_R = 40,5$ mV, $_{max}\Delta\varepsilon_{tot} = 3,6$ mV) during charge and discharge according to the formula:

$$k = \frac{_{\max}\Delta\varepsilon_R}{_{\max}\Delta\varepsilon_z} \ , \tag{3.30}$$

where k – maximum mean voltage errors ratio; $_{max}\Delta\varepsilon_R$ - maximum mean measurement error in a circuit with a voltage divider; $_{max}\Delta\varepsilon_{tot}$ - maximum mean calculation error in a circuit with measuring outputs' commutation.

Applying the mean measurement errors in the above formula (3.29), we get [21]:

- during the charging the maximum mean voltage calculation error in a circuit with a voltage divider exceeds the calculation error in a circuit with measuring outputs' commutation by $k = 11,25$ times;

- during the discharge the maximum mean voltage calculation error in a circuit with a voltage divider exceeds the calculation error in a circuit with measuring outputs' commutation by $k = 76,6$ times.

While designing the voltage measurement circuit based on a voltage divider, we need to introduce individual calibration constants for each product in order to compensate the constant component of the divider calculation error. We cannot attain high accuracy of measurement with the given circuit design solution to the full extent, even with the precision resistance elements. Serial production applying a circuit with a voltage divider is complicated due to the natural spread of the resistors parameters. Still, the proposed circuit solution, though relatively simple to implement and instructive for understanding, does not ensure the required accuracy of the voltage measurement ($\pm$ 0.5%).

The circuit with the battery cells' measuring outputs commutation ensures the prescribed accuracy of voltage calculation in 0.5%, but its cuircuit realization is more complicated, since it requires an additional sorce of voltage with galvanicallu isolated power supply and switching optoelectronic elements. As far as the software implenetation is concerned, voltage calculation algorithm is simplified as compared to the algorithm of

a circuit with a voltage divider, since it does not require additional computation operations. In this case, the calculation of the voltage of each cell is reduced to the algorithm described in section 6.

Basing on this comparative analysis we can draw a conclusion that, despite the possibility of simpler realization of a circuit with a voltage divider and its demonstrative simplicity, it can not ensure the required accuracy of measurement. As a result of the low accuracy of voltage measurement, when cells are overcharged, the life of lithium-ion batteries may be significantly reduced, since the intermittent overvoltage of the battery leads to the inevitable release of metallic lithium, which is highly reagent to the electrolyte. In case of undercharging and insufficient discharging, the battery does not provide you the required amount of energy. Obviously, in the latter case, the function of the batteries voltage leveling has no sense.

Notwithstanding more expensive and complex circuit design solution, the method of voltage measurement by commutation of measuring terminals has no drawbacks, which may lead to overcharge, undercharge or insufficient discharge of a battery.

The above mentioned determines the reasons for which the given method of voltage measurement is recommended for use in the monitoring and control system of the lithium- ion storage battery installed in the traction drive.

Let's compare the advantages and disadvantages of both current measurement methods [10-20].

1. Inductive sensor of current.

1.1. Advantages:

− galvanic isolation of power and measurement circuits;

− voltage measurement on the load resistor Rm by the internal analogue-digital converter of the microcontroller;

− higher operational temperature range as compared to a shunt;

− reseponse time to signal measurement 1 µs. max.

1.2. Disadvantages:

− the source of dual supply voltage is required.

2. Shunt measurement.

2.1. Advantages:

− easy maintenance;

− easy installation.

2.2. Disadvantages:

− an external analogue-digital converter is required to measure the voltage drop on the shunt;

−it requires synchronizing of commutation of the microcontroller's analogue-digital converter for measuring of the cells' voltages with the external microcontroller's analogue-digital converter for measuring the voltage drop on the shunt;

−the conversion result time 2 μs. max.;

−more complex software is required for the microcontroller in order to provide data exchange with the external analogue-digital converter via SPI interface;

−operational temperature range as compared to an inductive sensor of current.

As is evident from the above stated advantages and disadvantages of both methods, shunt operation complicates software-hardware realization of the monitoring system, dispite its easy maintenance and lower cost. But the combination of additional software and hardware means required to ensure the shunt operation in the control and monitoring system significantly increases the design cost. The disadvantageous need for dual power for the inductive current sensor is compensated by cuircuit organizing of the very control and monitoring system. The monitoring and control system has its own power supply (DC/DC converter) with galvanic isolation from the general output of the storage battery power circuit. A wide range of DC/DC converters allows us to select the source of dual supply voltage.

The useof inductive current sensors is preferred in the operation of the monitoring and control system of the locomotive traction battery. But the current shunt is recommended to install in the power circuit of the battery to ensure input control during setting and testing of the monitoring and control system of the locomotive traction drive battery [23].

LIST OF REFERENCES FOR CHAPTER 3

1. Sinchuk O. N. Control and protection sampled-data systems in mine electric locomotive transport / Sinchuk O. N., Chumak V. V., Erzhov O. V. – Kyiv: «ADEF – Ukraine» Publishers, 1998, – 280 pp.
2. Pougachev Ye. V. Systems of mine electrical equipment with storage battery power supply. Study guide/ Kouzbass Polytechnic Institute – Novokuznetsk, 1966. – 90 pp.
3. Stepanenko V. P., Vantslaff V., Dayneko R. Design and testing of mine battery-trolley locomotives // Ugol' (Coal) Publ. – 1986. – №12. - pp. 32-33
4. Sinchuk O. N. Mine battery-trolley locomotive / O. N. Sinchuk, E. S. Guzov, P. K. Savorskiy, N. N. Dolhiy // Mining Journal. – 1988. – №6. - pp. 22-25

5. Sinchuk O. N., Guzov E. S., Mine haulage with battery-trolley locomotives with multi-unit control system. News of Higher Educational Institutions Mining Journal. №7, 1980. – pp. 104.-106.

6. Lane White. New haulage lever at Kiruna, Sweden, has massive capacity. – Mining Journal. – 1978, vol. 119, N6, 112 p.

7. Sinchuk O. N. Synergistic system of an induction motor drive in a biaxial battery-trolley locomotive. / D. A. Shokarev, I. O. Sinchuk. Sci-tech digest "Electromechanical and energy-conserving systems"

8. Sinchuk O.N. Combinatorics of voltage converters in modern traction electric drives on board of mine electric locomotives / O. N. Sinchuk, I. O. Sinchuk, N. N. Yurchenko, A. A. Chernyshov, O. A. Udovenko, O. V. Pasko, E. S. Guzov. Scientific publication. – Kyiv: IEDNANU Publishers, 2006. – 252 pp.

9. Sinolitsy A. F. Pilot model of energy-efficient traction electric drive: KTU, - 2005. Issue. 88. - P. 120-125 IGBT-converter - IM for mine electric locomotives. Ore mining. / A. F. Sinolitsy, O. V. Pasko, V. I. Kolotilo, S. V. Lebedkin // Bulletin of Krivoy Rog Technical University. – Kryvyi Rih: Kryvyi Rih Technical University, – 2005. – Edition 88. - pp. 120-125

10. Sinchuk I. O. Semiconductor converters of electrical energy in the structures of electric drives. Circuitry and control principles / I. O. Sinchuk, A. A. Chernyshev, O. V. Pasko, I. I. Kiba, A. S. Klyuchka, O. E. Melnyk // Study guide. – Kremenchug: PE Shcherbatykh O. V. Publishing House, 2008. -pp. 88.

11. Pasko O. V. A.c. electric traction drive with adjustable structure intended for a mine electric locomotive. Synopsis of a Ph.D. thesis in Engineering Science Kharkov. – 2005. – p. 155

12. Hans-Natting Jochens Elektpische Grubenlogomotive EL 51 mit Pulsstellerantrieband Mikroprozessor kompoktstenepung. LEW – Nachrich-ten, 41. – 1989. – P. 10-11.

13. Shultz L., Van Wyk D., Dunford W.S., Pzest R.B., Landy C.F. An inverter and induction motor traction drive underground mining's Locomotives. // Elek. Bahnen. – 1990. – 88. №3. – P. 145-148.

14. Brunnecker. Drehstromtechnik fur Stadt - und Strassentriebwagenan Beispiel des Stadtbahnwagens M der Verkehrsbetriebe Mulheim/Ruhr // Stadtverkehr. – 1979. – Bd 24. – N 2. – S. 80 – 83.

15. Ciebow G., Steller G. Betriebserprobung des Drehstromzuges der Berliner Verkehrs – Betriebe (BVG) // Tech. Mitt. AEG. Telefunken 67. – 1977. – N 7. – S. 311 – 316.

16. Moser R. Vergleichende Studieuber die verschied enenelektrischenTraktions – motore. Typen in ihremspezifischen

Anwendungsbereich // Brown Boveri Mitt. – 1978. – Bd 65. – N 12. –
pp. 795 – 810.

17. EGL 160. Batterielokomotiven Typ EGL 160 2 "System Milles" der
firma Diema. (ETR: Eisenbahntechn. Rgsch). –1983, 32, №12,
863-864 pp.

18. Hahn. Karl; Verfahrenzur Regelung der Antrieba – order Bremskraftan
der Haftreibungsgrense der Rader. Licentua Patent-Verwaltungs-GmbH.
MKU B60, L 3/10, B61 c 15/00.

19. Syntchouk I.O. Traction variable-frequency induction motor drive for
mine trolley-electric locomotives. Synopsis of a Ph.D. thesis in
Engineering Science Kharkov. – 2009.

20. Rosenberg S. A., Dewan S. B. An inventer/cycloconventor system for
variable frequency, variable voltage, ac power supplies // IEEE / IAS
Intern. Semiconductor power Convertor Conf. Lake. Buena Vista, Fla,
1977. – New York, 2003. – pp. 247 – 255.

21. Shidlovsky A. K. Energy efficiency and power electronics in electric
power engineering / A. K. Shidlovsky, V. B. Pavlov // Techn.
Electrodynamics. Special issue Power Electronics and Energy
Efficiency. - Kyiv: Institute of Electrodynamics of the National
Academy of Sciences of Ukraine – 2006. – Part 1. - pp. 3-8

22. Klepikov V. B. To the development of an electric drive for an electric
vehicle / V. B. Klepikov, A. S. Gonchar, E. I. Makhnonosov //
Electrotechnical and computer systems. Scientific and technical journal.
Special issue. Automated electric drive problems. Theory and practice. -
Kyiv: Engineering - pp. 128-130

23. Khechinashvily A. V. Monitoring and control system of the energy
source of an electric vehicle traction drive /Synopsis of a Ph.D. thesis in
Engineering Science – Moscow 2006, p. 19

Golovenskyy Volodymyr Vasyliovych
Chief of Kremenchuk Flight College of
National Aviation University. The
Honoured Worker of Transport Industry
of Ukraine.

Shmeleva Tetyana Fedoryvna, DSc.
(Engineering), Prof., Head of Department
of Aeronautic Systems, National
Aviation University.

Shmelev Yurii Mykolayovich, PhD
(Engineering), Deputy Chief, the head of
Academic Training Department,
Kremenchuk Flight College of National
Aviation University.

Sinchuk Ihor Olehovych
PhD (Engineering), Assoc. Prof.,
Doctoral Candidate of the Department of
Automated Electrical-Mechanical
Systems in Industry and Transport, the
SIHE "Kryvyi Rih National University".

Boiko Serhii Mykolaiovych
PhD (Engineering), lecturer of the
Department of Energy supply and control
systems, Kremenchuk Flight College of
National Aviation University.

Smenova Lydia Vitalyevna, Senior
lecturer of Ukrainian State University of
Railway Transport.

SCIENTIFIC PUBLICATION

Golovenskyy Volodymyr Vasyliovych
Shmeleva Tetyana Fedoryvna
Shmelev Yurii Mykolayovich
Sinchuk Ihor Olehovych
Boiko Serhii Mykolaiovych
Smenova Lydia Vitalyevna

**ASPECTS OF TECHNICAL DIAGNOSTICS OF ELECTRICAL
EQUIPMENT IN MODERN ELECTRIC POWER SYSTEMS**
Science Editor DSc. (Engineering), Prof. T. F. Shmeleva

Multi-authored monograph